UNIVERSIDAD EUROPEA DE MADRID

ESCUELA DE ARQUITECTURA, INGENIERÍA Y DISEÑO

MASTER UNIVERSITARIO EN INGENIERÍA AERONÁUTICA

FINAL PROJECT REPORT

SIMULATION OF METAL ROLLING PROCESS

Miguel Domínguez García

SUPERVISOR: Alan Domínguez Montero

YEAR 2022-2023

TITLE: SIMULATION OF METAL ROLLING PROCESS

AUTHOR:

Miguel Domínguez García

SUPERVISOR:

Alan Domínguez Montero

DEGREE OR COURSE: 2nd

DATE: 10/01/2023

"Engineering is not only study of 45 subjects but it is moral studies of intellectual life."

(Prakhar Srivastav)

ABSTRACT

The goal of this project is to carry out a simulation of sheet metal rolling manufacturing process. This is a very common process in the aeronautical industry, performed to obtain sheet metal plates for the subsequent manufacture of elements used in aeronautical structures such as aluminum supports or stiffeners.

Sheet metal rolling is a metal forming process where the plate is deformed by a roller to obtain the desired thickness. However, during the process there is friction between the roller and the plate that generates heat, producing an increase in temperature both in the roller and in the plate. Therefore, it is necessary to carry out a mechanical and thermal analysis of the physical phenomena that occur during the process.

Throughout this project physical factors occurred during the process are detailed, as well as the equations that describe the process and the numerical model used to solve the problem.
In this project, a parametric analysis is carried out to study the behavior of the process at different speeds. Due to the high non-linearity of the problem and the importance of studying the thermal behavior, a dynamic-explicit finite element numerical model with thermal coupling is carried out using the SIMULIA Abaqus Explicit software.

Keywords:
Metal rolling
Roller
Plate
Thermal coupling
Abaqus
FEM

RESUMEN

El objetivo principal de este proyecto es realizar una simulación del proceso de fabricación de laminado de chapa. Se trata de un proceso muy habitual en la industria aeronáutica, por el cual se obtiene láminas de metal de un espesor deseado para la posterior fabricación de elementos utilizados en estructuras aeronáuticas como soportes o rigidizadores de aluminio.

Durante el proceso, además de producirse una deformación en el grosor de la placa de metal, se produce un rozamiento entre el rodillo y la placa que genera calor, produciéndose un aumento de temperatura tanto en el rodillo como en la chapa. Por lo tanto, es necesario realizar un análisis mecánico y térmico de los fenómenos físicos que ocurren durante el laminado. A lo largo de este proyecto se detallan estos factores físicos, así como las ecuaciones que describen el proceso y el modelo numérico utilizado para resolver el problema.

En este proyecto se realiza un análisis paramétrico para estudiar el comportamiento del proceso a distintas velocidades lineales de placa y de rotación del rodillo. Debido a la alta no linealidad del problema y la importancia de estudiar el comportamiento térmico, se realiza un modelo numérico de elementos finitos dinámico-explícito con acoplamiento térmico mediante el software SIMULIA Abaqus Explicit.

Palabras clave:
Laminación
Rodillo
Placa
Acoplamiento térmico
Abaqus
FEM

AGRADECIMIENTOS

Quiero agradecer en primer lugar a mi tutor Alan Domínguez, cuyo conocimiento, implicación y apoyo han hecho posible la realización de este proyecto. Él me ha guiado y motivado durante todo este proceso, ayudándome a encontrar la mejor solución a cada problema y transmitiéndome energía positiva en todo momento.

También quiero agradecer a todos mis profesores, cada uno de ellos me han aportado un gran valor durante esta etapa. Agradecimientos también a la Universidad Europea, por poner a disposición todos los medios posibles durante mis estudios de grado y máster, y por formarme para ejercer la profesión que siempre quise ejercer.

Gracias a las personas más cercanas a mí, que me han dado el apoyo necesario durante mi camino como estudiante.

Contents

Chapter 1. OBJECTIVES AND MOTIVATION

1.1 Objective

The objective of this project is to simulate metal rolling processes using a finite element scheme. Also deepening into the physics behind the problem and parametrizing the properties of the workpiece and the tooling in order to extract conclusions from the results obtained from the finite element solution.

In the rolling process, a metal ingot is passed between one or more pairs of rollers in order to reduce thickness. This process is mainly focused on the cross-section of the metal ingot to be pressed which aid the reduction of the workpiece thickness. Rolling processes increases the length and decreases the thickness while the width of the material remains almost constant.

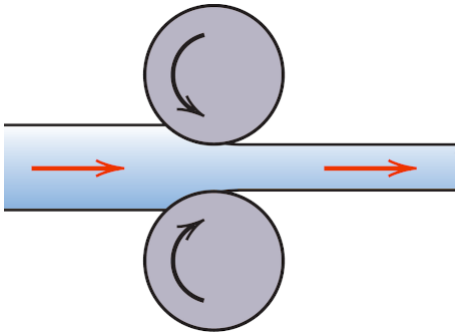

Figure 1. Conceptual scheme of Rolling manufacturing process [1]

This project can be considered as a continuation of my final degree project, where a sheet metal bending process was simulated using a finite element scheme. The process studied during this master's thesis is, in fact, the preceding process to the one studied in my final degree project. Rolling metal process consists on obtaining a metal plate with the required thickness for later, by means of sheet metal bending processes, get elements like L, U and V-shaped profiles (as shown in the figure below), which can be used as supports, stiffeners or fittings. In the aeronautical industry, these pieces can be shown for example in typical frame to skin joints, structural elements of aircraft.

The development of metallurgical processes has resulted in the improvement and refinement of manufacturing technologies. New methods and designs are constantly being tested in an effort to produce more efficient, cost-effective products. Nowadays, manufacturing techniques are being explored to produce complex metal components with optimal mechanical properties and minimal waste. However, the design freedom offered by these techniques comes at the cost of added complexity in the simulation process. The importance of developing reliable simulation methods for these processes cannot be overstated. This is especially relevant when applied to aerospace industry, where any failure could be extraordinarily catastrophic and costly.

In this project, a method for simulating metal rolling processes is developed using an finite element analysis software package. Simulia Abaqus provides the ability of representing in an accurate way metal forming processes where a the heat generation is relevant. An Explicit FEM provides a more accurate representation of high temperature processes than previous methods based on the Generalized Lagrangian-Eulerian approach used in implicit finite element methods.

Throughout this project, simulations of FEM numerical models will be carried out using Dassault SIMULIA Abaqus FEA software, explaining the physics behind this manufacturing process, obtaining parameters that determine the set up of the Rolling mills, and analysing how results obtained can be extrapolated to a real model. Many experimental approaches have been nowadays replaced by FEM analysis

due to the complexity of the process. In this case, plastic deformation, friction or thermo-mechanical coupling among other physical phenomena need to be studied [2]**.** The development of realistic mathematical models for production processes also encourages the improvement of these manufacturing processes, since they are helpful for understanding the physics behind them. This optimization of processes implies an improvement in efficiency and effectiveness, which is reflected into economic savings and an step forward in the quality of the final product.

For this case study, an explicit coupled thermal-displacement model is used, since during this process the temperature plays a relevant role in how the material deforms. During rolling, there is a generation of heat due to the friction of the roller with the plate and due to its deformation. Models with one roller and with two rollers will be carried out to study a process with more than one rolling phase. Different models will be created, varying the friction and the initial temperature of the plate, with the aim of studying how these parameters affect the necessary force that the rollers must exert for a given deformation.

During this project, a parametric study of different process conditions is performed and results are discussed and compared. In addition, some possible applications of this method are discussed along with suggestions for further development and testing.

1.2 Motivation

The motivation of this project lies on the necessity of developing manufacturing processes for metal parts for the aeronautical sector in a period of increasing use of composite materials in the aeronautical industry. Metal is widely used for the construction of airplane parts, wings, fuselage or tail sections. The most commmon materials used in the construction of airplanes are still aluminum, titanium, and stainless steel. Aluminum is the most popular due to its light weight and its high resistance to corrosion.

Today, manufacturers' requirements have increasing standards of precision and optimization, as tighter engineering tolerances are imposed, resulting in higher costs that can only be dampened by improved tools and production processes. For this purpose, it is necessary to create patterns or methodologies that make it possible to have this precision with the greatest possible speed and energy and material cost. It is important that the type of manufacturing engineering conforms to the requirements specified in the offer, so that in case of a part with new specifications is requested from the design office, it is not necessary to go through an experimental phase to manufacture the piece precisely.

Together with this, the ease of manufacturing is a point to take into account when selecting the material for each component of an aircraft, since this usually implies reducing manufacturing time, which translates into economic savings.

Rolling is commonly used in aerospace industry, and these manufacturing methods require machinery and calibrated processes to obtain desired thicknesses on workpieces. This calibration was initially done using test pieces, which entailed a certain expense of time, personnel, material, energy and, therefore, money. Nowadays, all these tests are carried out using software capable of parameterizing all possible variables, through iterative processes that help to optimize manufacturing processes faster and cheaper.

Currently, through the use of software tools, the most important factors involved in these processes can me parametrized, to carry out experimental simulations that replace a large number of laboratory tests. In this project, the aim is to simulate metal rolling processes using a calibrated model, that can be very useful to set up the manufacturing process and predict its behaviour.

1.2.1 Use of metal in the aerospace industry

The use of composite materials offers advantages such as weight reduction and improved mechanical properties. However, it has some disadvantages among which its high cost stands out, in addition to involving higher recurring and non-recurring costs. In addition, impact damage is not as easy to be detected in visual checks as it is in metals, together with the more time-consuming, higher complexity and cost required for this materials to be repaired. Moreover, these materials need to be isolated to be integrated into structures where the pieces are adjacent to aluminum pieces in order to avoid galvanic corrosion.

Figure 2. Metallic fuselage on commercial aircraft [3]

Since the Wright brothers first flew their Flyer in 1903, metal parts have been an integral part of aircraft. For many years, aluminum was considered to be the optimum material for aircraft construction. It was lighter than other metals and had excellent mechanical properties and electrical conductivity. However, aluminium does not perform very well in the presence of chemicals or high temperatures, and it can easily be damaged by strong impact forces. In recent years, there have been great advances in the science of metallurgy, and materials scientists are now able to develop much stronger alloys than those that were possible in the past.

First passenger aircraft like Boeing 707 only contained 2% composite materials in its structure, which were different types of fiberglass. The composition of the Boeing 707 contrasts with the one of the 787, with 80% of composite in volume and 50% of composite in weight. In this aircraft, aluminum takes 20% of the weight, titanium 15% and steel 10% [4]. An example of the use of a structure with moderate use of composites is the Airbus A380, which was manufactured with 25% of the structural weight in composites [5].

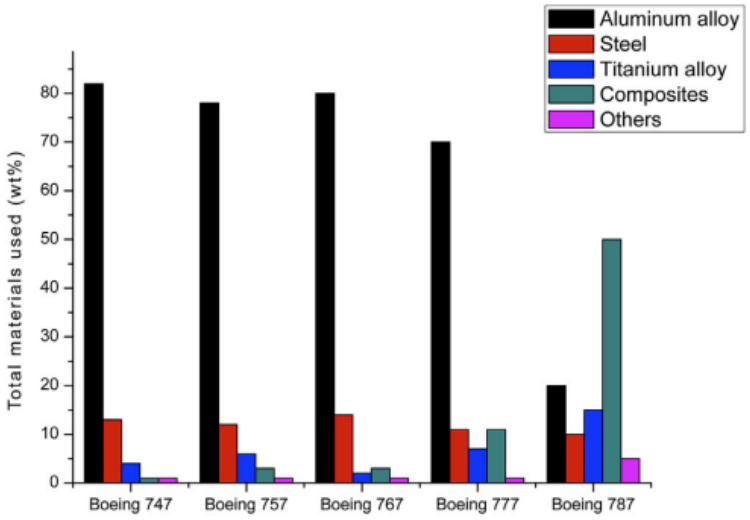

Figure 3. Materials used in Boeing aircraft [6]

The typical characteristics of metals to be used for aircraft components are those having good mechanical properties such as high strength, ductility, and toughness. They also provide some degree of protection against electromagnetic interference, which is a major problem for electrical components on aircraft. Mechanical properties are those which describe the ability of a material to withstand physical deformation without breaking or being permanently damaged. A metal's mechanical properties are mainly determined by factors such as the amount of carbon present in its structure, the nature of its shape and the size and/or composition of the grains present within its structure. In addition, the manner in which the metal has been processed may also have an effect on its mechanical properties.

Common materials used to form these parts include aluminum alloys which are strong and lightweight materials with high strength-to-weight ratios that. Alloys are created combining one or more metals together through a chemical process. The most common elements in aluminum alloys are magnesium, copper, zinc, silicon, and tin. Mechanical properties of aluminum alloys vary with the composition of the alloy and can be altered to achieve different properties as required for specific applications. These properties are important in determining the type of application in which the metal will be used as well as the physical properties exhibited by the final product after it has been manufactured.

Between the most used aluminum alloys are the aluminum–copper (2XXX series) and aluminum–zinc (7XXX series) alloys. Therefore, it is important to keep developing efficient manufacturing processes for metallic components [7].

1.2.2 Metal components in aircraft structures

Aircraft metallic structure components are critically important in order to maintain the integrity of the aircraft and its passengers. The metal parts that make up an aircraft are designed to withstand the stress and strain caused by aerodynamic forces and gravity. For example, the wings of a plane must be strong enough to resist the forces of lift and drag, while the fuselage of the plane must be strong enough to withstand the pressure of the air traveling at high speeds around the body of the plane at high altitudes. Airplanes also rely on a strong fuselage to keep stability during flight.

Metal rolling is used to produce structural shapes, plates or sheets, and bars or rods. Either finished or semi-finished products can be produced, which serve as a starting point for other processes. Components of an aircraft made of sheet metal and therefore produced using metal rolling include the following:

1.2.2.1 Fuselage

Airframe materials are designed to provide long-term (60000 flight hours) support for both the static weight of aircraft and additional load subjected from service. This concept requires airframe materials to possess acceptable densities for the weight reduction and appropriate mechanical properties for the intended use. It also requires materials to provide suitable damage tolerance for the purpose of long-term use in extreme temperature conditions (-30-370ºC), moisture (both extreme humidity and desert environment), and ultra-violet radiation [6]. The skins of most commercial airliners are made from aluminum because of its low corrosion potential and good resistance to heat.

The conventional structure of the fuselage is the shown in the image below. Moreover, these lamination processes is used to manufacture structural profiles. The main application on aircraft industry is the frames of the fuselage. These frames are supporting all pressure loads from the cabin, and transmit the shear loads from the fuselage skin.

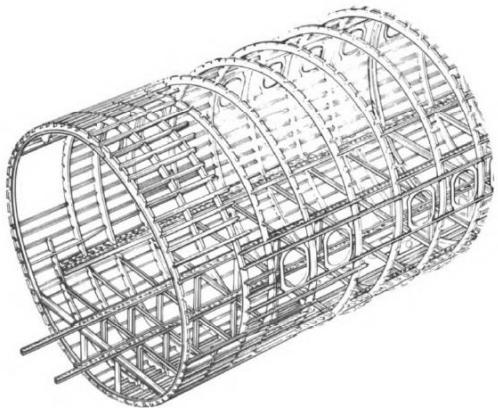

Figure 4. Conventional fuselage structure - De Havilland Canada - Dash 7 [8]

1.2.2.2 Wings, horizontal and vertical stabilizers

The skins of the aircraft carry out an important structural role. When the aircraft flies, the wings are deflecting air downwards, and as stated in Newton's third law, the action-reaction principle occurs generating a force upwards better known as lift that sustain the aircraft flight. These forces are transmitted to the air through the aircraft structure ultimately by means of the wing skin. Moreover, the ribs and spars of the wings are usually sheet metal beams. Wing spars run the length of the wings and attach the wings to the rest of the airplane's structure.

Figure 5. Wing skin panels [9]

Figure 6. Aircraft ribs [10]

1.2.2.3 Control surfaces

Flaps and control surfaces are usualliy made of sheet metal skins.

Figure 7. Flaps and slats of A320 aircraft [11]

1.2.2.4 Structural supports and brackets

In the same way as metal rolling is part of the process of these engine fittings, it is used for other structural components such us supports, stiffeners and brackets. Supports hold up other structures in an aircraft, such as the main wings or the tail fins. Stiffeners are elements that add stiffness and strength to other parts of the aircraft, such as the frame of a fuselage or the landing gear of an airplane. In the figure below, sheet metal brackets manufactured by Godrej Aerospace are shown. These are titanium, inconel, steel or aluminum brackets used for aircraft structure. These parts are manufactured from sheet metal,

which is cut with laser, it is bended with a press brake, finally are provided with heat and chemical processes and welded to get the final product:

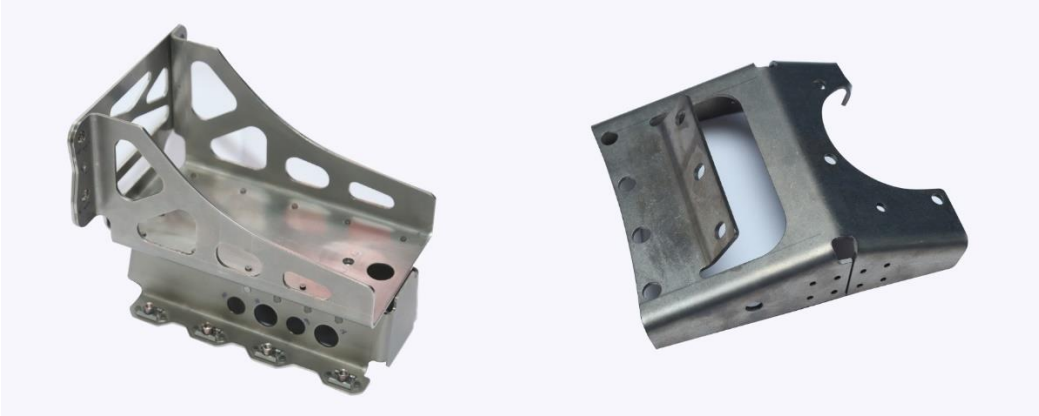

Figure 8. Sheet metal brackets [12]

The performance of these structural elements directly affects safety and airworthiness of aircraft. In addition, the optimization of these elements has a great impact on the performance of the aircraft itself, since reducing the weight and efficiency of each of these parts can be translated to fuel consumption savings.

1.2.3 Use of FEM to simulate metal forming processes

In the manufacturing industries, the design and analysis of metal forming processes are among the most challenging tasks faced by engineers today. This is because these processes involve highly complex interactions between different physical phenomena and they require extensive experimental validation before they can be implemented in actual production systems. In addition, machinery is extremely susceptible to mechanical degradation and mechanical failure. In order to overcome these challenges and ensure their safe and reliable operation, it is essential for the manufacturers to have access to fast and reliable simulation methods that are capable of accurately predicting the behavior of these systems under a wide range of operating conditions.

However, in most cases, the complexity of the processes involved makes the development of such methods a very difficult and time-consuming task. This is especially true when the process in question involves complex deformation mechanisms such as thermo-mechanical coupling or thermal softening. In such cases, it is often necessary to resort to relatively complicated numerical methods and long computation times in order to obtain reliable results. Despite these limitations, however, simulation methods are indispensable because they can be used to optimize the design of new processes and isolate and eliminate sources of error before real production systems are deployed. As a result, there is a trend towards the increased use of simulation techniques in the design and optimization of metal forming processes in order to improve the overall quality and efficiency of these products and reduce the costs associated with their manufacture.

Metal rolling is an industrial process that involves plastic deformation and heat generation. This makes it especially challenging to design and implement an effective control strategy to minimize scrap losses and also reduce energy consumption. In order to fully represent these processes, heat generation has to be taken into account as well as mechanical behaviour. In response to this need, this project uses a Dynamic Explicit Coupled Temperature-Displacement Method to address metal rolling production process simulation by means of Dassault Simulia Abaqus/explicit solver.

1.3 Structure of the project

1.3.1 Chapter 2

In this chapter it will be detailed the rolling process which are applicable to the aerospace industry. It is described the physical behaviour of the manufacturing process analyzed in this project, breaking down the possible types of rolling. A theoretical approach of the main parameters calculation is made for later comparison with the numerical results. The machinery and tooling required for rolling and the steps to carry out these processes are also explained along the chapter.

1.3.2 Chapter 3

The numerical model is analyzed in this chapter, explaining how an explicit scheme of FEM works. This chapter details what calculations the software performs for the solver configuration that will be used in this project. It is detailed how displacements and the temperature fields are calculated.

1.3.3 Chapter 4

In this chapter the characteristics of the models to be simulated are established. The geometry of each of the elements is described, in this case, the plate and the roller. The material used is also defined, as well as its main properties and its stress strain curve. In addition, the assumptions, the boundary conditions of the model, the meshing and the loads are configured. The set up of the solver is also specified in this chapter, indicating the main features of the time steps used.

1.3.4 Chapter 5

In this chapter a study of the results obtained is performed. First, a mesh convergence study is carried out to determine the optimum mesh thickness for the models. A parametric study to analysis the behaviour of the process at different velocities is made running models for different linear plate velocity and different roller rotation velocity. The precision and reliability of the results obtained are also discussed.

Chapter 2. INTRODUCTION TO METAL ROLLING MANUFACTURING PROCESSES

2.1 Introduction

Rolling is a process of resizing a piece of metal. Obtaining a sheet of the desired thickness starting from a thicker sheet. This process is carried out using pairs of rollers that rotate in the opposite direction, through which the piece is passed to which compression forces are applied in order to reduce its transverse thickness. This process can be carried out hot or cold. In either case, it is important to perform a thermal analysis of the process. Each rolling process is defined by a target thickness and torque and force values that the roller must exert on the part to obtain said thickness.

This process can be carried out continuously, where the piece passes through several rolling stands in one direction, or discontinuously, when the piece goes back to make more than one pass through the different rolling stands of the line. This project will focus on explaining what happens in one of these passes, independently of the rest of the product manufacturing process.

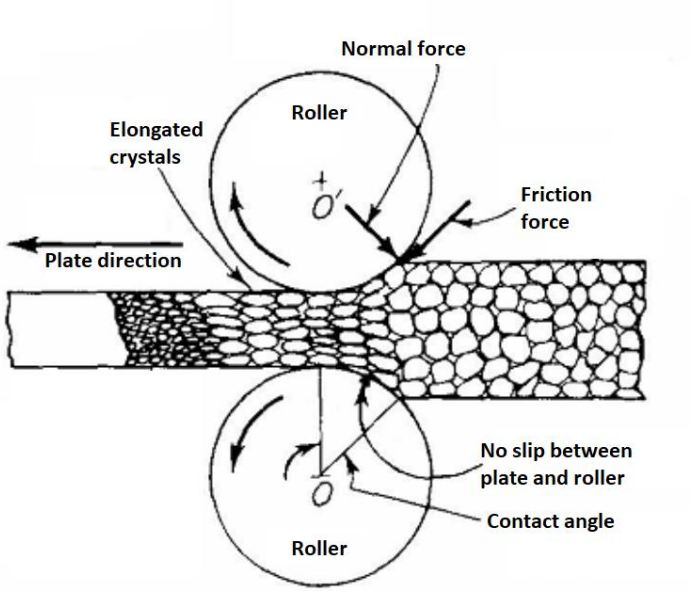

Figure 9. behavior of the plate's crystals during rolling [13]

The thickness reduction depends on the friction force of the roller with the part. The greater the friction force, the greater the thickness reduction that can be achieved, there being a thickness reduction limit for a given friction value.

Metal rolling is combined with other processes to produce parts. Metalworking is the process of working metal to obtain an product with predetermined shape and physical properties. Typically, metalworking involves the removal of unwanted material from a piece of metal to obtain the required shape and dimensions. Some of the following metalworking methods are used independently or combined after metal rolling to finish the desired part production:

- Stretch forming is a method of shaping metal parts that where a strip of metal is wrapped around a tool called a die to form the shape of the die. As the strip is wrapped tightly around the die, it stretches until the part achieves the desired shape. This process is typically followed by heat treatment to ensure that the surface of the part is properly hardened.

- Stamping operations are used to manufacture parts made of ferrous and nonferrous metals, as well as parts made from plastics and composite materials. Stamping operations are classified into two main categories based on their application: primary and secondary stamping operations. Primary stamping operations are used to fabricate basic shapes such as rectangles, circles, and squares from a sheet of metal. In contrast, secondary stamping operations are used to develop and refine the basic shapes created by the primary stamping operations. Secondary stamping operations include flanging, coining, piercing, embossing, blanking, punching, and other processes that allow manufacturers to further refine the shapes of formed parts by creating features such as holes, indentations, ridges, etc.

- Other metalworking processes typically used include cutting, drilling, milling, turning, bending, riveting, screwing, hammering, swaging, filing, grinding, boring, drawing and sawing. Some of these processes involves the removal of unwanted material from a piece of metal to obtain the required shape and dimensions.

2.2 Types of rolling according to the process temperature

The rolling process is classified according to whether it is done cold or hot. In cold, it is carried out at a temperature below the recrystallization temperature of the metal, while in hot it is carried out at a temperature above the aforementioned recrystallization temperature.

2.2.1 Hot rolling

As stated, the working principle of rolling is to apply pressure to a metal sheet or slab in order to deform it into the desired shape. Hot rolling is one of the most common types of rolling used for steel and aluminum parts production. In hot rolling, the metal is heated to a high temperature above its recrystallization temperature and then it is pressed between two rollers to reduce the thickness and increase the length. This increases the yield strength of the metal and provides it with increased ductility.

In this process, the metal sheet is heated to very high temperatures (typically above 1,000 °C) before it is passed through a series of rollers that exert pressure on the metal. This high pressure causes the metal to deform and thus assumes the desired shape. This process is usually followed by heat treatment in order to further harden the surface of the metal.

In the case of steel, hot rolling must be done at a temperature above 926 degrees Celsius. When the temperature is higher than the recrystallization temperature, the metal becomes a much more ductile material, so a considerably lower tonnage is necessary to achieve a reduction in thickness, just as in a cold rolling process. In other words, the higher the temperature, the lower its elastic limit, requiring less force to plastically deform it. Also, heating the material gives it a greater ability to plastically deform without breaking. In this way, it is possible to give the piece a greater variety of shapes, maintaining the integrity of the material. Which is why it is commonly used to make structural elements.

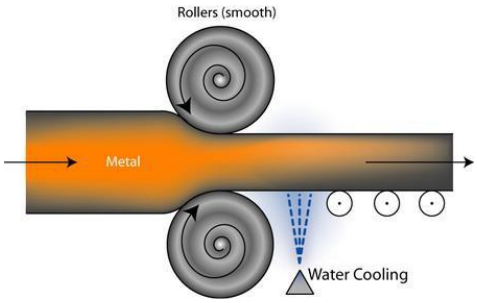

Figure 10. Hot rolling with cooling [14]

One of the drawbacks to take into account is that the volume of the piece varies when it cools down. For this reason, the cooling process must be controlled, observing how this volume varies depending on the temperature curve.

One effect of hot working with the rolling operation is grain refinement caused by recrystallization. Hot rolling is applied to the initial shaping of large ingots (currently it is also part of the product of continuous casting), in which the considerable deformations that they suffer are only possible with the concurrence of mechanical and thermal energy at high volumes of production. The most common products are plates, bars, rods, structural profiles, etc. Hot rolled products have slightly rough surfaces covered with oxide known as scale or calamine. Dimensional tolerances are between 2 and 5%.

There are two stages in hot rolling:

- Heating and rough rolling of the ingots obtained in the casting in the mold to transform them into blooms or slabs.
- New heating followed by forging and finishing rolling of the blooms and slabs obtained in the previous step or in a continuous casting machine to obtain, respectively, long or flat.

In hot rolling, the ductility of steel is used, that is, its deformation capacity, which is greater as the temperature increases.

2.2.2 Cold rolling

The process is carried out at room temperature. This forming process is performed at room temperature, allowing it to recrystallize. Since the steel is made at a much lower temperature, there is no need to worry about the change in volume and shape of the material, as is the case with hot rolled steel, suitable for uses where precise shapes and forms are not required.

Cold rolling increases the strength and hardness of steel and decreases its ductility (i.e. its ability to sustainably deform plastically without breaking), thus requiring it to undergo a process called annealing. That's why cold rolling is basically hot rolling that has gone through an additional forming process.

This process is applied in the case of producing deformations with a small field of tolerances (greater dimensional precision), when it is desired to obtain characteristics of these treatments in the material (better mechanical properties), as well as to achieve a finer surface finish. . Examples are sheets, stringers, rods, etc.

Cold strain hardening is the phenomenon by which a ductile metal becomes harder and stronger as it is plastically deformed. The strength of the material increases with increasing percentage of cold work, however the ductility of the material decreases.

Manufacturing is usually done in 5 steps:

- Pickling: carried out together with a cleaning process and a bath in diluted sulfuric acid.
- Rolling of the workpiece.
- The degreasing of the metal plate already reduced to the final thickness is carried out using silicate of soda activated by electrolysis.
- Annealing: using furnaces heated by gas or fuel-oil in a neutral atmosphere to avoid oxidation caused by direct flame.
- Hardening: a surface tempering that gives it a set of mechanical properties.

A rolling mill for cold rolling comprises:

- Support devices on the reel.
- Drive device formed by three parallel small diameter rollers.

Characteristics of cold rolling:

- Cold rolling produces smooth surfaces and better dimensional tolerances (between 0.5 and 1%).
- Improves strength, machinability.
- Hardening during deformation.
- Low cost method for the production of small parts.
- Anisotropic behavior and residual stresses can be generated.

2.3 Rolling forming process

The steps followed during rolling forming process are:

1. The workpiece is placed on the rolling milling machine and the ingots are fed into the machine. Depending on the material being formed, these ingots may be preheated.

2. The ingots are held in place while the milling head rotates around them, forming the ingots into a thinner piece. This process continues until the part has the desired thickness.

3. The completed parts are removed from the milling machine and transferred to a storage area for further processing.

The thickness reduction depends on the friction force of the roller with the part. The greater the friction force, the greater the thickness reduction that can be achieved, there being a thickness reduction limit for a given friction value. To obtain a laminated product, several operations are usually needed in which the thickness is reduced step by step.

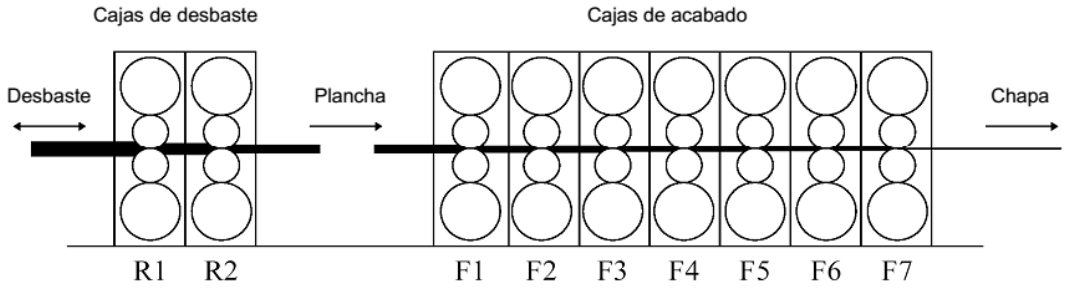

Figure 11. Rolling mill [15]

The cylinders are grouped in boxes or frames. The set of boxes forms the rolling train. There are different frame configurations (two, three, four or more rollers). The cylinders are usually made of forged steel (normally) or cast iron.

Rolling is a forming process by plastic deformation in which the material flows continuously and in a preferred direction by means of compression forces, exerted when the metal passes between cylinders, and shear forces, caused by friction between the cylinders and the metal. Essentially, rolling consists on passing the metal between two rollers separated by a gap smaller than the thickness of the incoming metal, that rotates in the opposite direction.

The rolling process can be defined as the combination of two processes. First, the translation movement of the workpiece towards the space between the rollers. Then, the rolling process in which the rollers act on the plate.

The rollers roll without slip in the plane in which the plate moves. During the process, a deformation may occur in the roller that displaces the center of the rolling axis, but in the study case presented in this project, this deformation will not be taken into account due to the limitation of computational resources, since this deformation is very low specially in cold rolling processes [16].

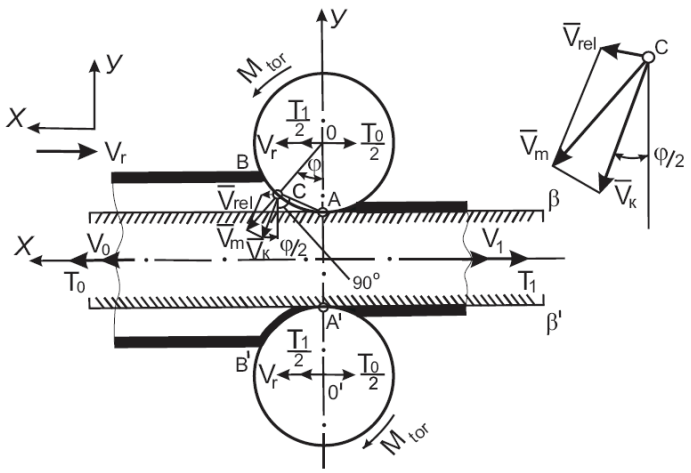

Figure 12. Diagram of the rolling process in the absolutely 'rigid' rolls, represented [16]

Rolling process is defined as an elastoplastic process, when the roller enters into contact with a certain section of the plate, there is a region at which it deforms elastically. In order to reduce the thickness of the workpiece, it is necessary to exceed the elastic limit, forcing it to deform plastically, not allowing the material to recover its original shape.

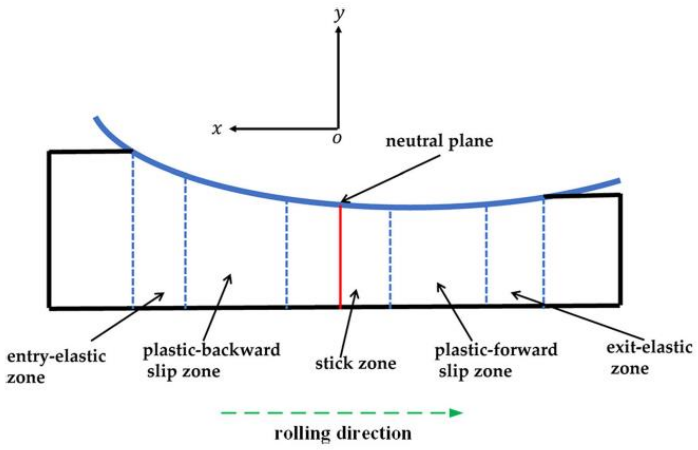

Figure 13. Elastic-plastic zones during rolling [17]

2.4 Rolling mill

Rolling mills used in the rolling process are adapted according to its dimensions and purpose. Its main parts are described below:

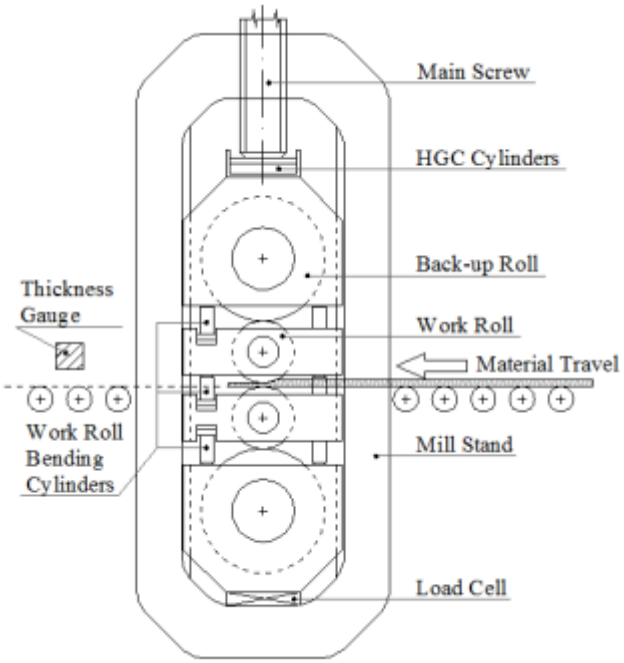

Figure 14. Typical structure of a rolling cell. In this case, hydraulic gap control us used with the purpose of increasing process accuracy [18]

- Hearth: It consists of a bed in which metal is placed before being poured onto the rolls to receive the required thermal treatment. It is sloped to allow the molten metal to flow easily to the rolls. A door-like structure is used to keep the metal inside the hearth when the machine is in operation.

- Guide: Leads the slabs onto the rollers.

- Rollers: are composed of a cylindrical sleeve, or shell and a cylinder, called the "core." The core is the heart of the roll and provides the strength necessary to support the weight of the product being rolled on the rolls. For each cell there are at least 4 rollers, the upper and lower work rollers and their respective back up roller.

- Stands: These are the vertical pillars that support the machinery of the mill. Each stand has a group of four rolls mounted on it. Each roll supports its own group or series of rolls above it. The main frame of the mill consists of a group of these stands connected together and used to support the rolling process. Additional support is provided for the machine by cross-bracing or tie rods located between the main frame and the bolsters.

2.5 Rolling forming process main parameters

This process consists on reducing the cross sectional area of the metal piece. Reducing the thickness while the with remains almost constant. As a consequence, the length of the plate tends to increase.

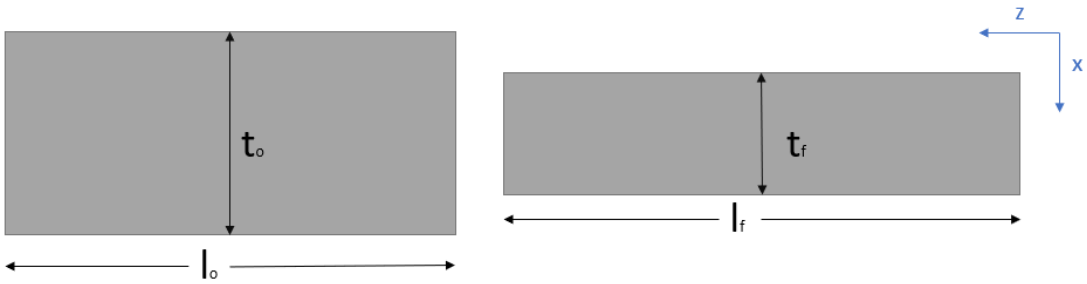

Figure 15. Initial and final plate geometry

Where:

- l_0 *is the initial length of the plate.*
- t_0 *is the initial thickness of the plate.*
- l_f *is the final length of the plate.*
- t_f *is the final thickness of the plate.*

The angle of the bite (θ) determines the thickness reduction that takes place. This parameter depends on:

- Temperature of the process. For cold rolling θ is usually between 3 and 4 degrees and for hot rolling 24º-32º.
- Surface roughness of the roller. For smooth surfaces, low angle of the bite is required while for rough surfaces high angle of the bite is required.
- Diameter of the roller. The larger the diameter, the less the angle of the bite would be.

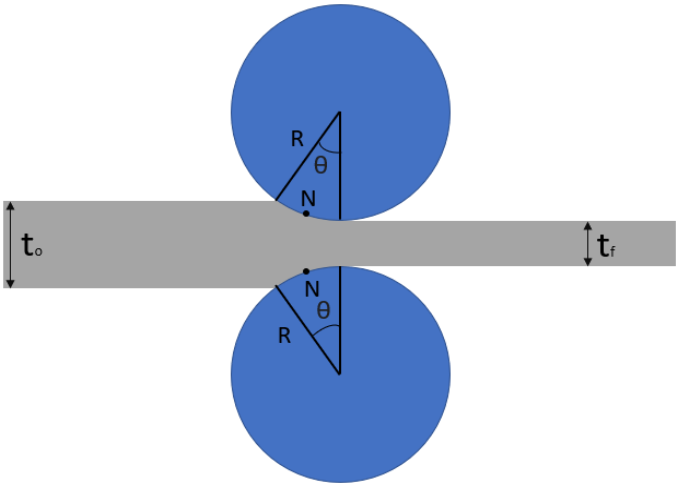

Figure 16. Rolling scheme

Draft is defined as the difference between initial and final plate thickness.

$$d = t_o - t_f$$

Thickness reduction ratio is:

$$r = \frac{d}{t_o}$$

Maximum draft determines the maximum deformation that can be achieved for a given roughness and radious of the roller:

$$d_{max} = \mu^2 \cdot R$$

Where:

- *μ: Friction coefficient of the roller*
- *R: Radious of the roller*

Friction coefficient depends if performing cold or hot working.

- μ ≈0.1 for cold working
- μ ≈0.2 for warm working.
- μ ≈0.4 – 1.0 for hot working

Due to the rotation of the roller, the friction between the roller and the plate pushes the plate in between the rollers. When the metal enters between the roller, the material is compressed leading the metal to deform plastically and therefore, to thickness reduction. Grain of the metal is elongated in the plate's linear movement direction, leading also to a length increment. As a consquence, the speed of the metal increases when passing through the rollers. The pressure exerted to the metal increases from the first contact point until the neutral plane, then it decreases until the plate exits the rolling section.

Then, at the entry, the velocity of the metal is lower than the surface velocity of the roller. At the exit of the contact between the rollers, the velocity of the plate metal is higher than the velocity of the roller surface. In the neutral plane, the velocity of the metal and the roller is equal.

True strain:

$$True\ strain = \ln \frac{t_o}{t_f}$$

Average flow stress:

$$\sigma_f = k \cdot \frac{\varepsilon^n}{1+n}$$

Where:

- *ε: strain*
- *k: stiffness*
- *n: strain-hardening exponent.*

During the process, the volume of the metal is conserved:

$$t_o w_o l_o = t_f w_f l_f$$

Contact length (L):

$$L = \sqrt{R(t_o - t_f)}$$

Rolling force (F):

$$F = \sigma_f \cdot L \cdot w$$

Where w is the width of the plate.

Torque (T):

$$T = 0.5 \cdot F \cdot L$$

Power (P):

$$P = 2\pi \cdot \omega \cdot F \cdot L$$

The main parameters that determine the performance of the process are:

- Material resistance to plastic deformation, which is a function temperature and strain rate.
- Friction.
- Roller diameter.
- Presence of a stress front in the plane of the plate.

Chapter 3. NUMERICAL METHOD

3.1 Introduction

The metal rolling process is an important step in the manufacturing of many products. In this process, a metal sheet is placed between two rolls and crushed into thin sheets. During rolling, a metal sheet is passed through a pair of opposing cylinders following an elastic deformation of the sheet metal into the space between rolls, the applied force is constant and the rolls apply a constant pressure to the sheet metal. The pressure is kept constant throughout the process, so no shearing forces are present. We can therefore treat this process as compression of a spring-like object.

3.2 Rolling process governing equations

3.2.1 Stress-strain analysis

To define the equilibrium equation of an infinitely flat plate, following assumptions are taken into account:

- Stress and strain along the two dimensions of the thin plate are constant in all the vertical sections of the deformated zone.
- Inertial force is neglected.

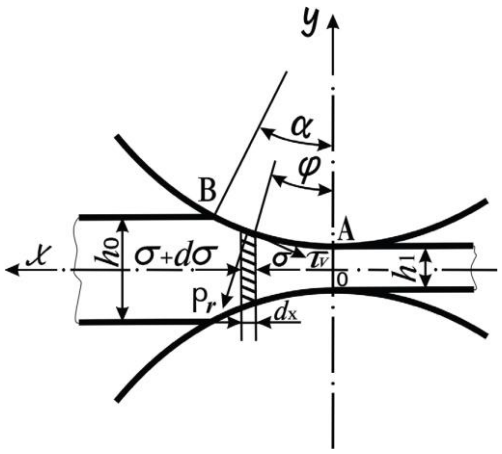

Figure 17. Deformation zone scheme [16]

The equilibrium differential equation can be defined as follows [16]:

$$\sigma \cdot h - (\sigma + d\sigma) \cdot (h + dh) + 2p_r \frac{dx}{cos\varphi} sin\varphi - 2\tau_v \frac{dx}{cos\varphi} cos\varphi = 0$$

Where:

σ: longitudinal stresses

p_r: contact normal stresses

τ_v: contact tangential stresses

h: height of the cross section

φ: central angle

Neglecting the negligible second order values:

$$d\sigma - (p_r - \sigma) + \frac{2tg\varphi}{h}dx + \frac{2\tau_V}{h}dx = 0$$

So, taking into account that the coordinate x can be put as a function of φ, to obtain the stresses it would be necessary to solve a differential equation of this type [16]:

$$\frac{d\sigma}{d\varphi} = f(\varphi, \sigma)$$

Once the stresses have been calculated, Abaqus uses Hooke's law for isotropic materials. The elastic deformation of materials is governed by the Hooke's law, which states that the strain (ε) is proportional to the elastic modulus (E) and inversely proportional to the Poisson's ratio σ/ε. For isotropic materials, E is the ratio of stress and strain while ε is the ratio of the change in the length to the change in the width. Therefore, E=σL. The Young's modulus is defined as the ratio of the stress to the strain in an elastic body. When the object is under a constant load, the increase in length is equal to the increase in tension.

From Hooke's Law, where the force acting on the metal piece is equal to its elastic constant times the displacement that the force causes, we have:

$$\varepsilon_x = \frac{1}{E}[\sigma_x - \nu(\sigma_y + \sigma_z)]$$

$$\varepsilon_y = \frac{1}{E}[\sigma_y - \nu(\sigma_z + \sigma_x)]$$

$$\varepsilon_z = \frac{1}{E}[\sigma_z - \nu(\sigma_y + \sigma_x)]$$

$$\gamma_{xy} = \frac{\sigma_{xy}}{G}$$

$$\gamma_{yz} = \frac{\sigma_{yz}}{G}$$

$$\gamma_{zx} = \frac{\sigma_{zx}}{G}$$

Where ν is the Poison's ratio, E is the Young modulus of the material, ε_x, ε_y and ε_z are the normal strains, σ_x, σ_y and σ_z are the normal stresses, G is the shear modulus of the material, γ_{xy} , γ_{yz} and γ_{zx} are the shear strains, and σ_{xy}, σ_{yz} and σ_{zx} are the shear stresses.

The elastic deformation corresponds to the phase in which the deformation and the tension the material is subjected to are proportional.

$$\begin{bmatrix} \varepsilon_{xx} \\ \varepsilon_{yy} \\ \varepsilon_{zz} \\ \varepsilon_{yz} \\ \varepsilon_{zx} \\ \varepsilon_{xy} \end{bmatrix} = \frac{1}{E}\begin{bmatrix} 1 & -\nu & -\nu & 0 & 0 & 0 \\ -\nu & 1 & -\nu & 0 & 0 & 0 \\ -\nu & -\nu & 1 & 0 & 0 & 0 \\ 0 & 0 & 0 & 1+\nu & 0 & 0 \\ 0 & 0 & 0 & 0 & 1+\nu & 0 \\ 0 & 0 & 0 & 0 & 0 & 1+\nu \end{bmatrix}\begin{bmatrix} \sigma_{xx} \\ \sigma_{yy} \\ \sigma_{zz} \\ \sigma_{yz} \\ \sigma_{zx} \\ \sigma_{xy} \end{bmatrix}$$

Solving this equation for [σ], Abaqus solves all normal and shear stresses in each of the components:

$$\begin{bmatrix}\sigma_{xx}\\ \sigma_{yy}\\ \sigma_{zz}\\ \sigma_{yz}\\ \sigma_{zx}\\ \sigma_{xy}\end{bmatrix} = \frac{E}{(1+\nu)(1-2\nu)}\begin{bmatrix}1-\nu & \nu & \nu & 0 & 0 & 0\\ \nu & 1-\nu & \nu & 0 & 0 & 0\\ \nu & \nu & 1-\nu & 0 & 0 & 0\\ 0 & 0 & 0 & 1-2\nu & 0 & 0\\ 0 & 0 & 0 & 0 & 1-2\nu & 0\\ 0 & 0 & 0 & 0 & 0 & 1-2\nu\end{bmatrix}\begin{bmatrix}\varepsilon_{xx}\\ \varepsilon_{yy}\\ \varepsilon_{zz}\\ \varepsilon_{yz}\\ \varepsilon_{zx}\\ \varepsilon_{xy}\end{bmatrix}$$

3.2.2 Thermal analysis

From the governing the diffusion of heat in a conductor, the equations to get the temperature distribution of the roller and the plate can be obtained:

$$\nabla^2 T + \frac{\dot{q}}{k} = \frac{1}{\alpha}\frac{\partial T}{\partial t}$$

$$\alpha = \frac{k}{\rho C_p}$$

Where

q	Heat (J)
k	Thermal conductivity $\left(\frac{W}{m\cdot K}\right)$
C_p	Specific heat $\left(\frac{J}{K\cdot kg}\right)$
ρ	Density $\left(\frac{kg}{m^3}\right)$
T	Temperature(K)

In the case of the roller, a cylinder whose mechanical and thermal properties are constant in the direction of the axis in which it rotates is considered, so that the temperature field remains constant in this axis. Also, steady state is assumed. The rotational speed of the roller is constant, and the heat flux distribution at the interface is uniform.

For a cylinder in cylindrical coordinates, the equation governing the diffusion of heat in a conductor can be expressed as:

$$\frac{\partial^2 T}{\partial r^2} + \frac{1}{r}\frac{\partial T}{\partial r} + \frac{1}{r^2}\frac{\partial^2 T}{\partial \theta^2} = \frac{\omega}{\alpha_r}\frac{\partial T}{\partial \theta}$$

For the plate, heat is generated by friction with the roller and the deformation energy of the plate itself. Using the governing equation of the heat diffusion in a conductor for cartesian coordinates, it is obtained the following expression for the temperature field:

$$\alpha_s\left(\frac{\partial^2 T}{\partial x^2} + \frac{\partial^2 T}{\partial y^2}\right) + \frac{q''\alpha_s}{k_s} = u\frac{\partial T}{\partial x} + v\frac{\partial T}{\partial y}$$

There are two main sources of heat generation in the process, which are the heat generated due to the deformation of the plate and the generated due do the friction between the roller and the plate. This heat can be calculated as follows [19]:

$$q_f'' = \tau \cdot V_{rel} = \mu P \left[\frac{2V_r R(cos\theta_n - cos\theta)}{y_0 + 2R(cos\theta_T - cos\theta)}\right]$$

$$q_d'' = \frac{KV_r y_n w}{y\Delta l}\left[\frac{2}{\sqrt{3}}\ln\left(\frac{y_0}{y_f}\right)\right]^{\eta+1}$$

Where:

q_f''	Heat flux due to friction, W/m^2
τ	frictional shear stress, MPa
V_{rel}	relative surface velocity, m/s
μ	coefficient of friction
P	roll pressure, MPa
V_r	roll surface velocity, m/s
θ_n	neutral point angle
θ	circumferential coordinate
y_0	initial strip height or thickness, m
R	roll radius, m
q_d''	Heat flux due to deformation, W/m^2
K	material strength coefficient, MPa
y_n	strip thickness at neutral point, m
w	strip width, m
y	y coordinate
y_f	final strip thickness, m
Δl	length of the bite region, m
η	strain hardening exponent

3.3 Numerical solution

Rolling process is a elastoplastic process, which corresponds to a nonlinear behaviour. Nonlinearity is a characteristic of many processes in nature. Mathematical models are used to understand the underlying physics of a system and identify important parameters that will affect the results. To study nonlinear systems, finite element methods (FEM) become even more important. A variety of different applications can be modeled using the FEM, including mechanical, thermal and fluid systems. Metal rolling processes are an example of highly non-linear systems.

Heat generation is another key challenge that must be taken into account when designing a control strategy for a metal rolling operation. Heat generation is inevitable during the process of bending and stretching the metal. The heat energy generated is distributed into the surrounding atmosphere and absorbed by the steel rollers. The resulting increase in the temperature of the metal can have a significant effect on its mechanical properties. This can lead to increased wear of the rolls and reduced quality of the rolled metal piece. As such, the steel rolling process an efficient thermal management system must be developed that can reduce the amount of energy required to maintain a stable operating temperature.

Along this project, Dynamic Explicit Coupled Temperature-Displacement is used to solve the heat diffusion problem associated with the heat transfer from the slabs to the rollers and to the environment. The purpose is to determine how the variation of the main operating parameters affect the results of the process. The expected outcome is a rolling process model that can be used as a design tool to optimize the performance and efficiency of the process.

Rolling involves both mechanical and chemical processes and is therefore a complex and dynamic process. It requires a high degree of control and synergy between the various elements involved to ensure high quality output with minimal waste. This is even more important in hot rolling. One of the main challenges in controlling the process is achieving and maintaining a stable operating temperature for the rollers and the workingpart. If the rollers become too hot, they will burn through the metal and cause cracks to develop in the rolled product. On the other hand, if the rollers are not hot enough, they will be unable to deform the metal properly and result in uneven thickness of the rolled product. In addition, if the rollers are heated unevenly they will also be unable to reach the target temperature at the same time and there will be a delay in reaching the target temperature. This can further increase the risk of damage to the product and create inconsistent product quality. It is therefore necessary to predict the operating conditions of the rollers as well as monitoring it in real time to be able to take corrective action when necessary in order to ensure consistent quality.

3.3.1 FEM: Dynamic Explicit Coupled Temperature-Displacement

To calculate stresses and strains, abaqus explicit uses finite element methods to perform the calculations. The finite element method is a numerical method for solving differential equations. Differential equations of real physical problems have a particular way of discretizing, dividing the domain into a finite number of elements. To solve the governing equations of the problem, which are ordinary differential equations, numerical methods are used to find numerical approximations to solutions of these ordinary differential equations (ODE). Its use is also known as numerical integration, although this term is sometimes taken to mean the calculation of an integration.

In differential analysis, the domain is discretized into a finite number of elements of infinitesimally small size. The FEM divides the domain into larger elements, these elements are joined by nodes. The main characteristics of finite element methods are described below:

- Nodes are associated with certain parameters that characterize their behavior. In this way, the complete system is an assembly of all these elements that form it, therefore, the solution follows the rules of discrete problems.
- The unknowns of the problem cease to be mathematical functions that describe the general behavior of the structure. The value of these functions in the nodes become functions themselves.
- The behavior inside the elements is defined from the behavior of the nodes by means of shape functions.

Static implicit solver works well with most of the metal forming processes. For this cases, static applied loads and boundary conditions are assumed for each node. Steady deformation of the roller is therefore also assumed. The legth of the analysis step (time period) plays no role in the outcome of the analysis, the solver will reach a steady-state by the end of the step.

Nevertheless, dynamic explicit model, is shown to be much more effective for highly non-linear problems which includes metal rolling processes. During cold rolling, metal has an elastoplastic behaviour, being a non-linear process itself. Additionally, heat generation is high, generating even more non-linearities. For this reason, dynamic explicit coupled temperature-displacement FEM is used. The applied loads, boundary conditions and the resulting temperature field can be defined as a function of time. So, the defined time period is interpreted as real time, the results at the end of the step correspond to the state of the modelled system at that instant. In Dynamic Explicit Coupled Temperature-Displacement, thermal load will be defined according to a calculation of dissipated kinetic energy .

Thermal diffusivity is the thermophysical property that defines the speed of heat propagation by conducion during changes of temperature. The higher the thermal diffusivity, the faster the heat propagation. The thermal diffusivity is related to the thermal conductivity, specific heat and density of the material.

3.3.2 Implementation of the Dynamic Explicit Coupled Temperature-Displacement FEM

This chapter will describe on the one hand the implementation of the method in terms of mechanical behavior, and on the other hand, in terms of thermal behavior.

3.3.2.1 Mechanical solution

Firstly, the domain or structure is divided into elements joined by nodes, having each of these elements their own geometric and physical-mechanical properties. The stiffness properties of the material are compiled into a single matrix equation that governs the internal behaviour of the structure:

$$\{f\} = [k] \cdot \{x\}$$

Where {f} is the vector of element nodal forces, [k] is the element stiffness matrix (normally square and symmetric), and {x} is the vector of unknown element nodal degrees of freedom or generalized displacements. The unknown data on the structure are the forces and displacements that can be determined by solving this equation.

The stiffness matrix conceptually relates the displacements of a series of nodes with the effective local stresses at those nodes. From an operational point of view, it relates the unknown displacements of a structure with the known external forces, which allows finding the reactions, internal stresses and stresses at any point of the structure.

The stiffness matrix, then, contains all the physical-mechanical and geometric properties of an element. These properties act on each other through the nodes. It is then, that all the elements of the structure connect with each other to form the complete structure to be analyzed. In the same way that the elements are connected to each other, mathematically, the individual stiffness matrices of each element connect with each other to form the global stiffness matrix [K].

In the study case of this project, a dynamic problem is faced, so the inertia of the system and its damping must be taken into account. The governing equation that Abaqus uses to solve a dynamic system is:

$$[M]\{x''\} + [C]\{x'\} + [K]\{x\} = \{f\}$$

This equation describes the behaviour of a general mechanical system. Where $[M]$ is the mass matrix, $[C]$ is the damping matrix and $[K]$ is the stiffness matrix. The $\{x\}$ is the position funcion and $\{f\}$ is the force, which is time dependent. Whether the analysis is considered static, dynamic or quasi static, depends on the excitation frequency of working frequency. Being ω_n^{min} the minimum natural frequency of the system [20]:

For dynamic analysis: $\omega_{\text{excitation}} > \frac{1}{3}\omega_n^{min}$

For quasi static analysis: $\omega_{\text{excitation}} < \frac{1}{3}\omega_n^{min}$

In a dynamic analysis, for such excitation frequency, the inertia is significant, so it cannot be neglected and the problem cannot be solved without considering the mass matrix. For quasi static analysis, the force is constant or nearly constant with respect to the time, which was the case of the punch acting over the plate on sheet metal bending processes [20].

In explicit analyses, nodal accelerations are solved directly without iterations, as the inverse of the diagonal mass matrix multiplied times the net nodal force vector while an implicit solver requires inverting the stiffness matrix, once or more than once. This matricial inversion is a complicated and time consuming operation. These operations are not required in explicit analyses, which manages the contact and material non linearities easier than the implicit solvers. In this case, diagonal or lumped element mass matrices are used, with the purpose of gaining relevant computational efficiency [21]:

$$\{x''\} = [M]^{-1} \cdot (\{f\} - [C]\{x'\} - [K]\{x\})$$

Below are shown the equations based on central-difference integration that describe the mechanical behavior in the explicit dynamic finite element scheme used [22]:

$$\dot{x}^{N}_{\left(i+\frac{1}{2}\right)} = \dot{x}^{N}_{\left(i-\frac{1}{2}\right)} + \frac{\Delta t_{(i+1)} + \Delta t_{(i)}}{2}\ddot{x}^{N}_{(i)};$$

$$x^{N}_{(i+1)} = x^{N}_{(i)} + \Delta t_{(i+1)}\dot{x}^{N}_{\left(i+\frac{1}{2}\right)};$$

where $x^{N}_{(i)}$ represents any degree of freedom and it can be either a displacement or a rotation component. Subscript i refers to the time step increment [22].

3.3.2.2 Thermal solution

To calculate the temperature field, equation of energy conservation law in explicit form is used to state each node's internal heat [17]:

$$Q^t_{i-1,j} + Q^t_{i+1,j} + Q^t_{i,j-1} + Q^t_{i,j+1} + Q^v_{i,j} = \Delta E^t_{i,j}$$

Where:

$\Delta E^t_{i,j}$ is the increasing amount of the internal energy in the control volume in unit time.

$Q^v_{i,j}$ heat of the internal heat source in the control volume in unit time

$Q^t_{i-1,j}$, $Q^t_{i+1,j}$, $Q^t_{i,j-1}$, $Q^t_{i,j+1}$ heat transferred from the surrounding nodes to P respectively (see Figure below)

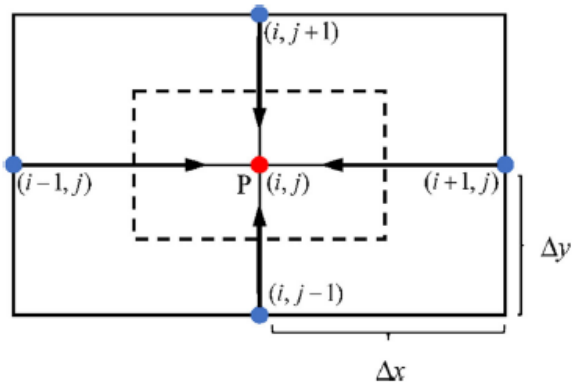

Figure 18. Heat transfer for internal node diagram [17]

According to Fourier's law of heat conduction, $Q^t_{i-1,j}$, $Q^t_{i+1,j}$, $Q^t_{i,j-1}$, $Q^t_{i,j+1}$ are calculated as follows:

$$Q^t_{i-1,j} = \frac{\lambda}{\Delta x}\left(T^t_{i-1,j} - T^t_{i,j}\right) \cdot \Delta y \cdot 1$$

$$Q^t_{i+1,j} = \frac{\lambda}{\Delta x}\left(T^t_{i+1,j} - T^t_{i,j}\right) \cdot \Delta y \cdot 1$$

$$Q^t_{i,j-1} = \frac{\lambda}{\Delta y}\left(T^t_{i,j-1} - T^t_{i,j}\right) \cdot \Delta x \cdot 1$$

$$Q^t_{i,j+1} = \frac{\lambda}{\Delta y}\left(T^t_{i,j+1} - T^t_{i,j}\right) \cdot \Delta x \cdot 1$$

Heat of the internal heat source in the control volume in unit time, $Q^v_{i,j}$, which in this case corresponds to the deformation heat, is obtained from:

$$Q^v_{i,j} = (q_P + q_f) \cdot \Delta x \cdot \Delta y \cdot 1$$

Where q_P is the strength of the heat source due to deformation and q_f is the strength of the heat source due to friction:

$$q_P = \frac{Q_P}{t_r};\ q_f = \frac{Q_f}{lh_c t_r}$$

$$t_r = \frac{l}{v_r}$$

Where:

Q_P	deformation heat (J)
Q_f	friction heat (J)
t_r	Contact time of roll (s)
v_r	Work roll speed (m/min)
l	Total length of the rolling deformation zone (mm)
h_c	heat transfer coefficient $\left(\frac{W}{m^{2\circ}C}\right)$

Finally, using the law of conservation of energy equation, temperature of the internal nodes is integrated using the explicit forward-difference time integration rule [17]:

$$\Delta E_{i,j}^t = \rho c \frac{T_{i,j}^{t+1} - T_{i,j}^t}{\Delta t} \Delta x \cdot \Delta y \cdot 1$$

$$T_{i,j}^{t+1} = \frac{\lambda \Delta t}{\rho c (\Delta x)^2}(T_{i-1,j}^t + T_{i+1,j}^t - 2T_{i,j}^t) + \frac{\lambda \Delta t}{\rho c (\Delta y)^2}(T_{i,j-1}^t + T_{i,j+1}^t - 2T_{i,j}^t) + \frac{\Delta t}{\rho c}(q_P + q_f) + T_{i,j}^t$$

3.4 CAE explicit solvers

Abaqus explicit is used to study the stress state of the slab under heat generation conditions. Abaqus explicit solver perfectly adjusts to the dynamic analysis required. In dynamic problems, there are inertial effects, and the kinetic energy in the system is not negligible. Abaqus explicit is used for problems that are nonlinear, which is the case in metal rolling processes. Nevertheless, there are different CAE explicit solvers in the market. The main explicit solvers on the market are discussed below.

- **Nastran sol700**

Nastran explicit sol700 is a software tool developed by NASA engineers written in FOTRAN. It is one of the most important solvers for structural analysis with high non-linearities like crashes. Its main disadvantage is not having any tool to generate the geometry and meshing, which have to be done my means of Patran or APEX. [23]

Until recent years, it was the only solver widely used in the aerospace industry for this kind of non-linear analysis, but nowadays, solvers like Abaqus are gaining importance in the Aerospace industry.

- **Pam-crash**

This software's predecessor code simulated the frontal impact of a full passenger car structure in an overnight computer run. This was the first successful full-car crash simulation. [24]

Using Pam-crash it is possible to model complex geometries with structural and continuum elements like beams, shells, membranes or solids. This program includes a large library of materials, even the most difficult to model which are the multi-layers composites. Linear and nonlinear problems like failure models or damage can be approached using Pam-crash. [25]

- **ls-dyna**

The software package contains a single executable file, LS-DYNA.exe . LS-DYNA is a command-line driven software package that can be used to solve problems in turbomaching and aerospace industry in general.

The LS-DYNA software package provides solutions for solving a variety of problems from many branches of science and engineering. The modular structure of LS-DYNA makes it easy to add new functionality to the code.

The characteristic of LS-DYNA that stands out is its capability of solving multiphysics problems, including [26]:

- Heat Transfer
- ALE, EFG, SPH, particle methods
- Navier-Stokes Fluids(version 980)
- Radiation transport (version 980)
- Electromagnetics (version 980)
- Acoustics

- **Radioss**

Altair Radioss is a commercial, multidisciplinary finite element solver that can be used for a wide variety of applications, including: acoustics, fluid flow, electromagnetic fields, heat transfer and structural mechanics.

One of the main advantages of Radioss is that it is open software so that it can be freely modified or distributed. On the other hand, Radioss support the input in the LS-DYNA input format as well as the Radioss 'Block' Format [27].

Chapter 4. NUMERICAL MODEL

4.1 Introduction

In the numerical models performed, it is analysed how a 20mm plate is worked to obtain a 12mm plate in two passes through the rollers. The model used in this study incorporates boundary conditions based on a realistic case of this manufacturing process. Strains on the workpiece are calculated as a function of time. The main objective of this chapter is to present how the dynamic explicit coupled temperature-displacement finite element model is set in order to predict performance of the process in terms of deformation, temperature and force required. The whole model was developed using Abaqus.

Some limitations exist regarding the speed with which a particular model can be meshed and solved numerically. The time required for this depends on several factors including the computational difficulty of the problem, the amount of parallelism inherent in the computation, and the number of processors available to run the calculations in parallel. In addition, the time required to perform the simulations may be limited by the stability of the software being used. Depending on the complexity of the problem being investigated, it may take several hours to several days to perform an adequate number of simulations and to achieve an adequate level of accuracy.

4.2 Parametric analysis

Firstly, a mesh convergence study is performed and then these results are compared with a model whose roller is made up of rigid shells.

Several models have been created with the aim of performing the aforementioned parametric analysis of the metal rolling process. Then, results are analyzed to understand how variations in the different parameters affect the behaviour of the process.

Starting from a base model, with a certain geometry and materials that will be described throughout this section. The parameters to vary between the different models are:

- Rotation speed of the rollers.

- Linear speed of the plate as it passes through the rollers.

- Material of the plate.

Furthermore, since the main objective of the analysis is to study the behavior of the plate, to simplify the calculations, the roller is assumed to be a rigid body. However, the properties of the elements generated with a non-deformable mesh do not allow the application of thermal coupling time steps. For this reason, it was necessary to use a roller that is minimally rigid, that is, with a modulus of elasticity several orders of magnitude higher than the modulus of elasticity of the plate, so that it does not deform during contact with the plate. In this way, it is intended to fulfill the original assumption of a rigid roller. To verify the low impact that the use of a minimally rigid roller has on the model, its mechanical behavior is compared with a model whose roller is a rigid solid.

4.3 Model set up

In the following paragraphs, the main features of the models created are described. In Annex 1 it is detailed the construction of the model step by step.

4.3.1 Assumptions

To set up the model, following assumptions are taken:

1. The process takes place in a very short time step. With the selected velocity and size of the plate and rollers, the whole process is carried out in 0.3 seconds. This means that the heat disipated to the atmosphere is negligible for air free or forced convection. Therefore it is considered that the rollers and plate conform an adiabatic system.

2. Width of the plate does not vary during the process.

3. No slip condition in the tangential point between the roller and the plate.

4. Change of mechanical properties with temperatures are not taken into account.

4.3.2 Parts

The model consists of a plate and two rollers in the form of a hollow cylinder, arranged with their base on the YZ plane.

- Rollers:
  - Internal radius: 0.1 m
  - External radius: 0.25 m
  - Width (z): 0.15 m

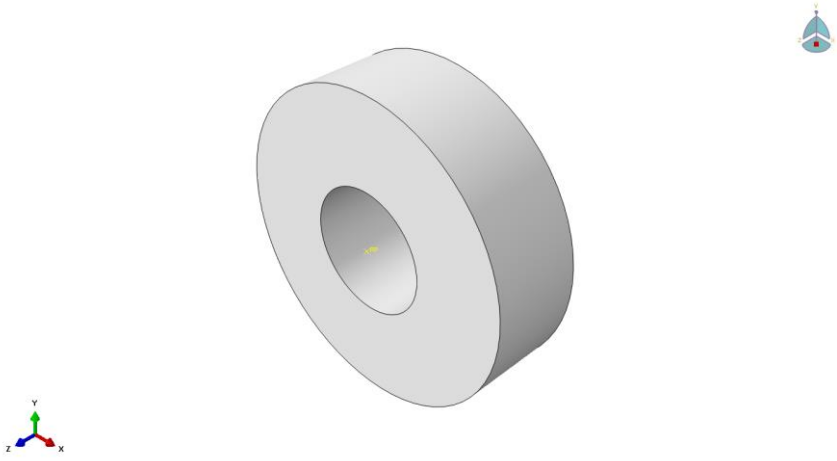

Figure 19. Roller

- Plate:
  - Length (z): 0.2 m
  - Height (y): 0.02 m
  - Width (x): 0.1 m

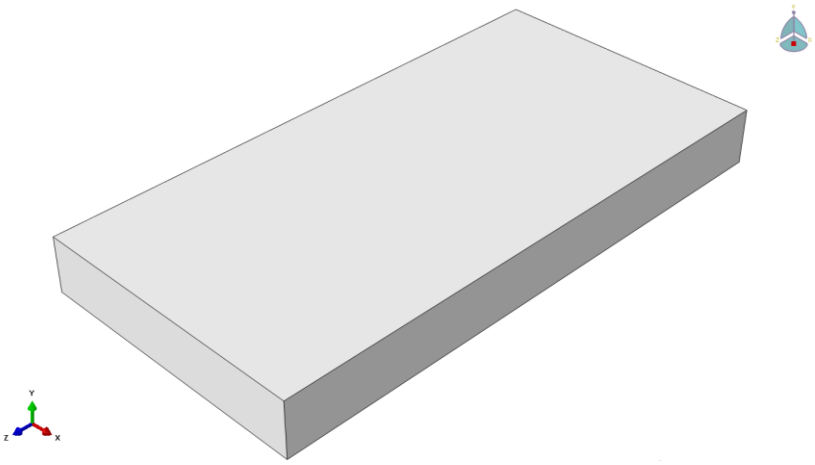

Figure 20. Plate

4.3.3 Assembly

The final assembly of the model with the two roller and the plate would be:

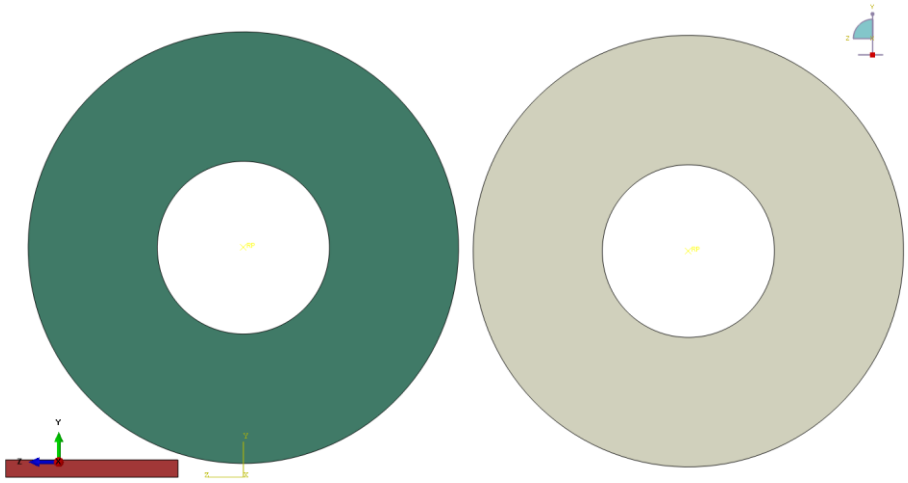

Figure 21. Assembly

4.3.4 Material

The material used in the velocity parametric analysis models is steel St 37-2 G, a material that is typically cold-rolled to build structural elements. This material is used as a carrier material for galvanically refined strips and sheets [28] and it has a high enough melting point to study a wide range of of velocities causing a significant ΔT difference between the models so that the effect of the variation of each parameter can be appreciated.

The properties of St 37-2 G entered in the model have been obtained from the WIAM material database. [29]. El modelaje de este material se ha realizado de acorde con el manual de usuario de Abaqus Simulia. [30].

4.3.4.1 Plate

Material properties introduced in the model for the plate:

- Heat capacity
- Conductivity
- Density
- Elasticity
- Plastic behaviour

Figure 22. Steel St 37 plate [31]

Component	Weight %
Sulfur	0.04
Carbon	0.17
Phosphorus	0.04
Nitrogen	0.007

Table 1. St 37 Composition [28]

The mechanical and thermal properties to be taken into account are:

Property	Magnitude
Density	8000 kg/m^3
Tensile ultimate strength (σ)	4.80E+08 Pa
Young modulus (E)	2.1E+11 Pa
Tensile yield strength (Y)	2.46E+08 Pa
Conductivity	45 W/mK
Specific Heat	460 J/Kg ºC
Melting point	1370°C

Table 2. Mechanical properties of the material [28]

Stress strain curve of this material is introduced to the model, describing the elastic and plastic behaviour of the plate is the following:

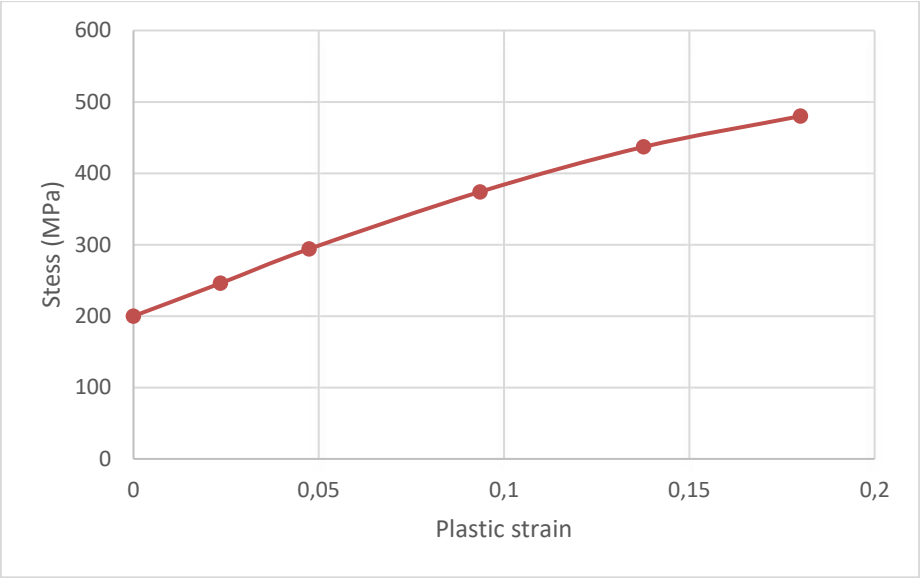

Graph 1. Plastic strain curve for Steel St 37 introduced in Abaqus

4.3.4.2 Rollers

The roller is a minimally rigid deformable solid. To provide stiffness to the roller, the material used has 10 times the Young modulus of the steel of the plate. Plastic behaviour is not introduced to the model. Material used for the rollers has the following properties:

- Heat capacity
- Conductivity
- Density
- Elasticity

Property	Magnitude
Density	8000 kg/m^3
Young modulus (E)	2.1E+12 Pa
Conductivity	45 W/mK
Specific Heat	460 J/Kg ºC

Table 3. Roller properties

4.3.5 Mesh

The mesh used is a fixed mesh since in this case the use of moving meshes complicates the analysis and its reliability, increasing the computation time. The elements used are C3D8T (8-node trilinear displacement and temperature).

It can be seen how the thickness of the mesh depends on the region of interest for the analysis. The study of how the plate behaves is in this case what is intended to be analyzed in detail.

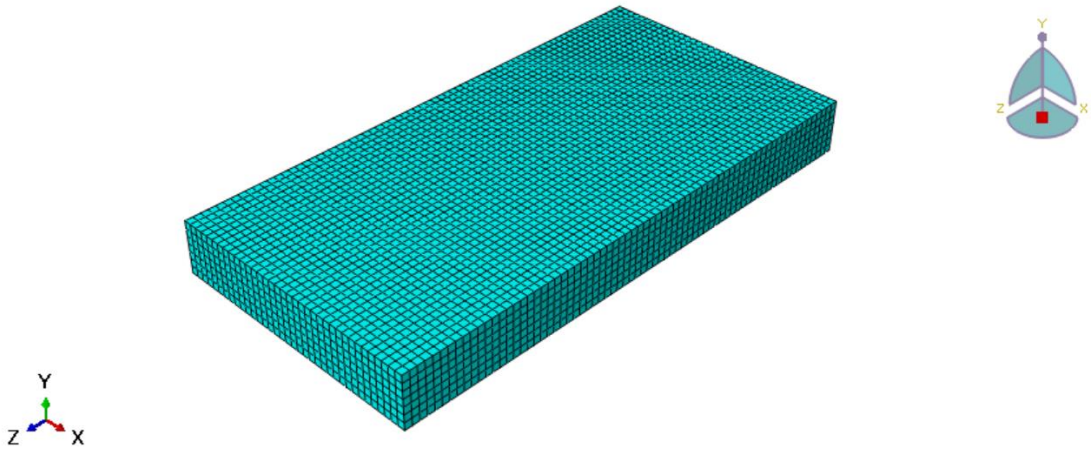

Figure 23. Plate mesh

For the roller, the mesh used is a regular mesh with hexaedral elements. The main region of interest is the plate, so the mesh of the roller is thicker. The global size of the roller is 0.01, while for the plate is 0.0028 being the element size of the roller 3.57 times bigger than the plate elements.

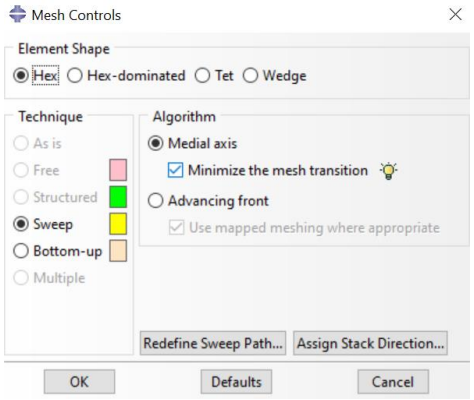

Figure 24. Mesh controls applied to the roller

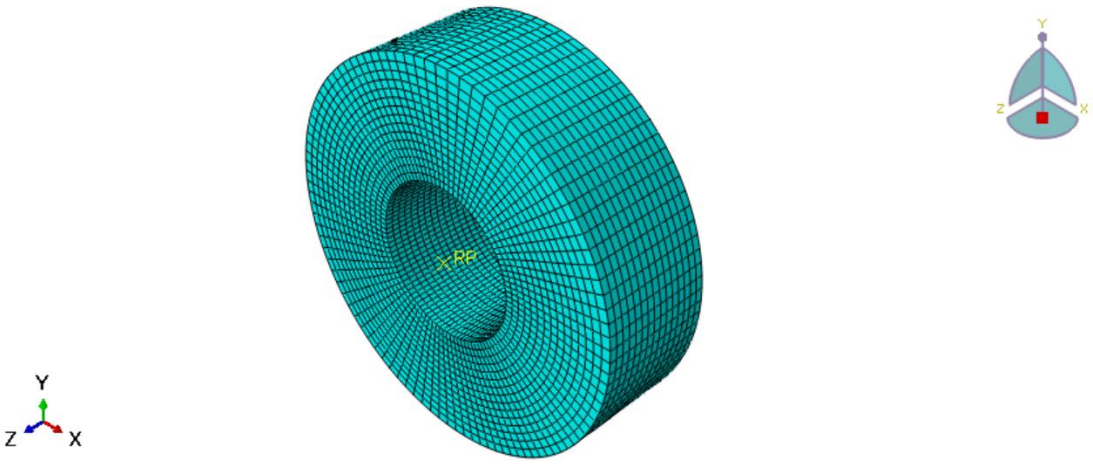

Figure 25. Roller mesh

4.3.6 Boundary conditions

The Boundary conditions applied in the basic model consist of:

- Provide a symmetry to the model.
- Insert a linear speed for the plate of 4 m/s in negative z direction.
- The rollers move with an angular velocity of 40 rad/s in positive x axis.

4.3.7 Step

Step selected, as stated, is the dynamic explicit coupled temperature-displacement. Solution is composed by a temperature field and a displacement field. The temperature field and the displacement field are updated simultaneously according to the coupled thermodynamic-structural condition of the thermo-mechanical problem.

To get an stable solution, the changes of the system in total internal energy (E_I), viscous energy dispated (E_V), frictional energy disipated (E_{FD}) and kinetic energy (E_{KE}) as a result of imposing an external mechanical load (E_W) must be taken into account. The energy balance can be described as:

$$E_I + E_V + E_{FD} + E_{KE} - E_W = E_{total} = constant$$

For example, in the metal rolling process the energy dissipated by the system is equal to the difference between the total amount of heat generated by heating and the amount of heat absorbed by the cooling of the metal strip and absorbed by the roller. The energy dissipation represents the heat dissipation capacity of the system and the efficiency of the cooling system used. In the numerical model E_{total} is only approximately constant, generally with an error of less than 1%. [32]

4.3.8 Unit system

In the models described, the units system used is the SI (mm):

Quantity	SI
Length	m
Force	N
Mass	kg
Time	s
Stress	Pa
Energy	J
Density	kg/m^3
Temperature	K

Table 4. SI unit system is used

4.4 Output variables

In order to study how the metal rolling manufacturing process behaves under different conditions, a parametric analysis is carried out. In said parametric analysis, different models are made by varying the speed and temperature at which the process is carried out. The variables studied when extracting results are the following:

4.4.1 Mises stress

To study the results of the model, first it is represented the contour plot of Von Mises to quantify the internal concentration of stresses along the plate. Von Mises is a scalar magnitude proportional to the distortion energy, which is calculated as a function of the stresses tensor. In this case it is calculated for each node following this expression:

$$\sigma_{VM} = \sqrt{\frac{(\sigma_x - \sigma_y)^2 + (\sigma_y - \sigma_z)^2 + (\sigma_z - \sigma_x)^2}{2}}$$

Comparing Von Mises stresses along the plate with the yield stress of the material, it is possible to check at which points the material has entered a zone of plastic deformation.

4.4.2 PEEQ

In ABAQUS, PEEQ refers to the equivalent plastic deformation parameter. It is a scalar magnitude of all the plastic deformation components in each specific element of the model. These deformations are the ones that do not return to their original shape after the discharge. Plastic deformations are produced in those points where the stress on the plate exceeds the yield stress ($\sigma_{0.2}$).

When the material is stretched under a constant load to a certain point, the slope is approximately linear until the point where the material achieves its yield strength. Until this point, the material returns to its original shape until all of the elastic energy is completely used up. Then, when all of the available elastic energy is used up, the slope of the original curve approaches zero. This is the point when the material achieves maximum plastic deformation. At this point, the plastic deformation is almost complete and any further elongation will be permanent, resulting in a permanent increase of thickness and a decrease of the cross-sectional area of the material.

As shown in figure below, an elastic-plastic transition occurs when the stress needed to deform a material increases from its elastic value to its ultimate plastic value. For most metals, this transition occurs somewhere between 10% and 30% of the total strain. This phenomenon is known as the Yield Point or Yielding Point. Since the elastic and plastic components of the material are related, once the yield point is reached, no additional elastic deformation is possible and the material will become permanently deformed at this point. If the plastic material can bear a higher load without breaking, then the stress required to achieve maximum plastic deformation will increase continuously until the material reaches its maximum stress or breaking strength.

In engineering, to estimate when a material begins to deform plastically, the stress strain curve is used to draw a line parallel to the linear part of the curve displaced by 0.2% on the strain axis. The corresponding stress at the intersection between this line and the strain strain curve will be considered the yield stress, expressed as $\sigma_{0.2}$.

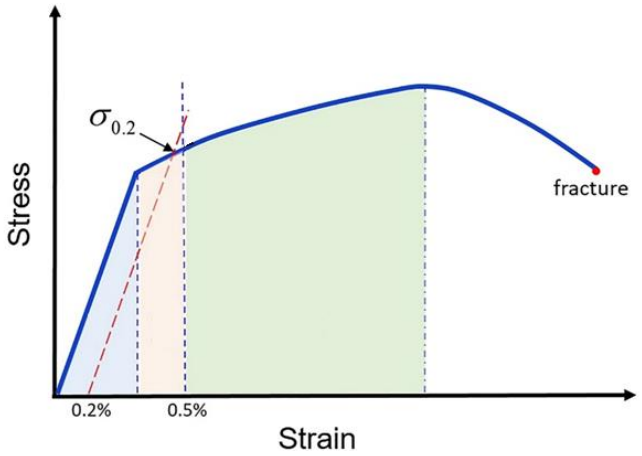

Table 5. Plastic deformation criteria

4.4.3 Reaction Force (RF)

The reaction force in the Y component (RF2) is interpreted as the force applied during the process by the roller. To do this, the center of one of faces of the roller is taken as a reference point, and the reaction force value obtained concentrates all the stress exerted by the roller on the Y component multiplied by the contact area between the plate and the roller.

4.4.4 Nodal temperature (NT)

To analyse the temperature of the plate, NT11 nodal temperature is used. NT11 is the reference nodal temperature value. In this case, temperature will be studied at specific points using the nodal variable NTxx. The nodal variable NTxx should not be used for output at the temperature points if the temperatures are specified by defining the value at the origin of the cross-section and specifying the gradients in the local 1- and 2-directions. In this case output variable NT should be requested; NT11 (the reference temperature value) and NT12 and NT13 (the temperature gradients in the local 1- and 2-directions, respectively) will be output automatically. [22]

In the models performed in this project, reference temperature is zero, so all temperatures are shown with respect to zero, and can be understand as the value of the temperature increment with respect to the initial temperature.

4.5 Dynamic behaviour of the model

The following screenshots show how the plate moves through the rollers at different timeframes.

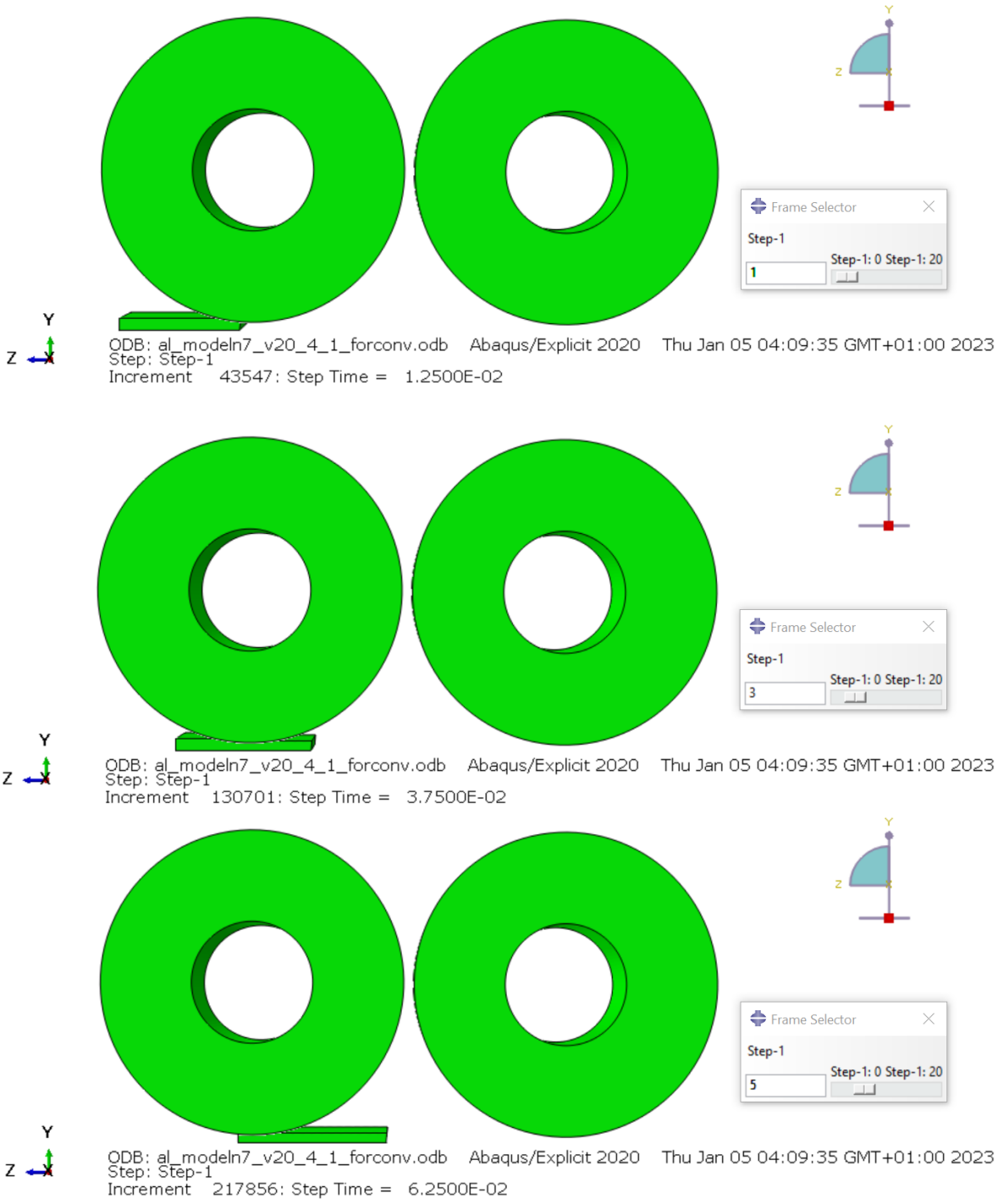

Figure 26. Plate passing through the first roller

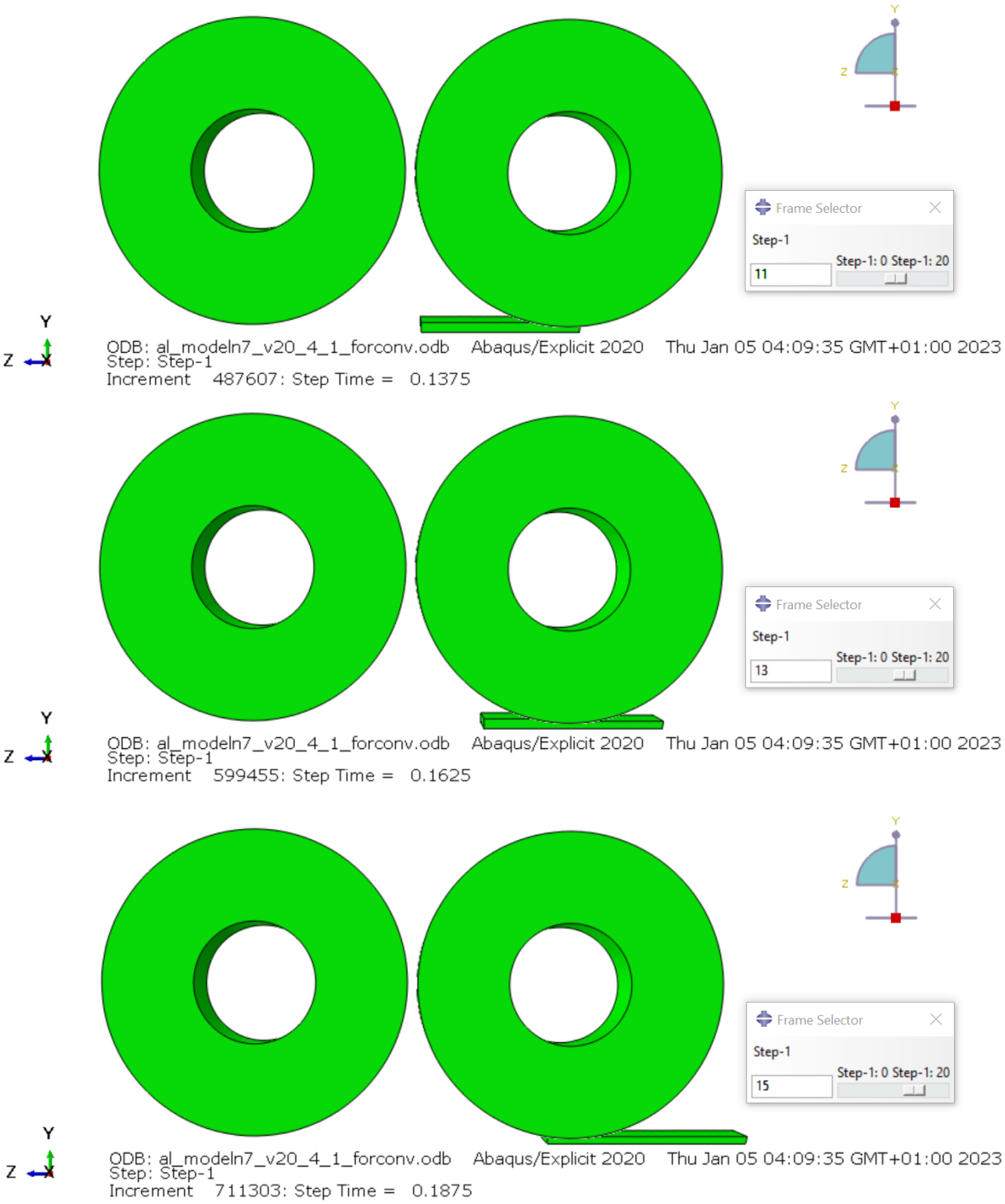

Figure 27. Plate passing through the second roller

4.6 Problem size

The following screenshot shows the problem size of the base model once the mesh convergence analysis has been carried out:

```
                              P R O B L E M   S I Z E


NUMBER OF ELEMENTS IS                                  63792
NUMBER OF NODES IS                                     73538
NUMBER OF NODES DEFINED BY THE USER                    73538
TOTAL NUMBER OF VARIABLES IN THE MODEL                450828
(DEGREES OF FREEDOM PLUS MAX NO. OF ANY LAGRANGE MULTIPLIER
 VARIABLES. INCLUDE *PRINT,SOLVE=YES TO GET THE ACTUAL NUMBER.)
```

Figure 28. Problem size

The computation time varies depending on the selected time period, which will depend on the linear velocity of the selected plate. For this project, all analysis are performed within the range of 4 to 8 hours.

The specifications of the computer used to run these models are:

Sistema operativo:	Windows 10 Home 64 bits (10.0, compilación 19045)
Idioma:	español (configuración regional: español)
Fabricante del sistema:	Micro-Star International Co., Ltd.
Modelo del sistema:	Bravo 15 B5DD
BIOS:	E158KAMS.105
Procesador:	AMD Ryzen 7 5800H with Radeon Graphics (16 CPUs), ~3.2GHz
Memoria:	16384MB RAM

Figure 29. Computer specifications

Chapter 5. ANALYSIS OF RESULTS

5.1 Introduction

With the purpose of analysing the heat generation variation with the roller velocity, different models are run varying the angular velocity of the roller and the plate linear velocity. The effect of friction on heat generation in a metal rolling process calculated with Abaqus according to the stress-strain equilibrium equations and the thermal equilibrium equations will be discussed.

The aim of this chapter is to examine the thermal effect on the power of the roll in a metal rolling process. During the rolling process, two work pieces are pressed together. These work pieces are the work rollers and a work piece called the strip. As the parts are pressed together, there is a heat generation and energy transferred from the strip to the rollers and vice versa. The amount of heat transferred depends on the amount of pressure and the amount of friction.

5.2 Mesh convergence analysis

Mesh convergence analysis is carried out with the purpose of determining the appropiate number of elements required to obtain accurate results while reducing computational resources. The results of this study will be used to ensure that the mesh is suitable for modeling the dynamic behavior of the process, which will help to increase the confidence in further simulation results. If too few elements are used to represent the part, it may not be possible to accurately capture the geometric details of the part and produce reliable results. However, if too many elements are used to represent the part, it may be computationally expensive and it may become difficult to resolve the interactions among the different elements. It is therefore important to choose an appropriate number of elements that adequately represent the geometry of each part and provide a reasonable balance between computational efficiency and accuracy.

To perform mesh convergence analysis, models with different mesh thicknesses are created for the plate:

Model	n
Model 1	2
Model 2	3
Model 3	4
Model 4	5
Model 5	6
Model 6	7
Model 7	8

Table 6. Models created for mesh convergence analysis.
Where "n" is the number of elements along the cross section of the plate

To determine the optimum mesh size, only the action of the first roller is taken into account. The following variables from the output of the first roller operation are analysed:

- Overall Max σ_{VM}
- Overall Max PEEQ
- Overall Min RF2
- Overall Max NT11
- Max σ_{VM} in timeframe 3
- Max PEEQ in timeframe 3
- Min RF2 in timeframe 3
- Max NT11 in timeframe 3

In timeframe 3, roller is approximately in the middle of the first rolling process. It is an adequate timeframe as the stresses and strains in the plate have already developed while dynamic effects are not mature enough to distort the results. So, comparing both the results at this time frame and the maximum values of σ_{VM}, PEEQ, and NT11 and minimum RF2 it can be determined at which mesh size the model is converging. It has to be noted that min RF2 is selected because the rollers are exerting a force in negative Y axis.

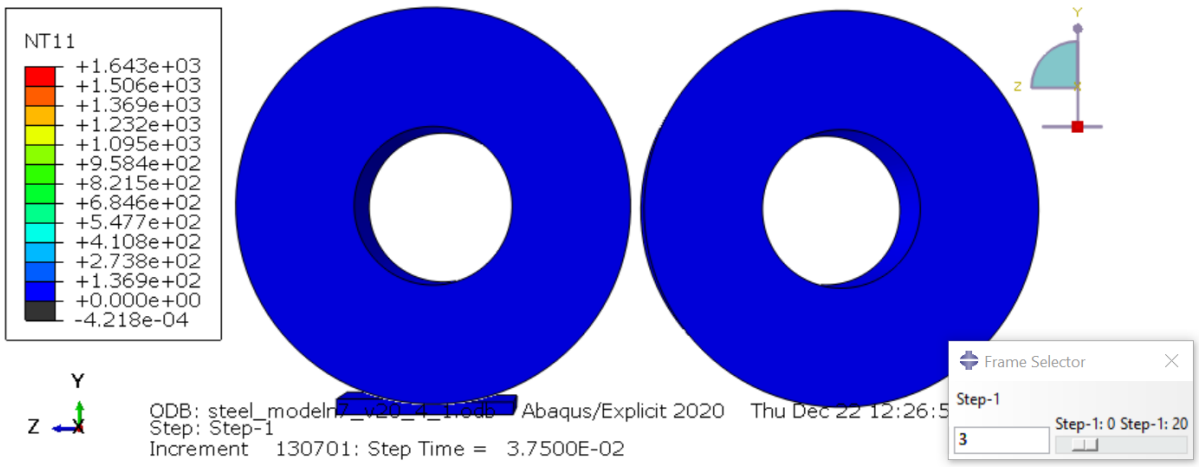

Figure 30. Model 8 at timeframe 3

5.2.1 Convergence criteria

Firstly, an acceptable error is set. In the case of metal rolling, acceptable error is relatively high as the resulting element requires further processes before getting the final product. Here, the purpose is to obtain a sustancial decrease of the thickness of the slab. For these further processes usually used to complement metal rolling such as sheet metal bending, higher precision is required because the final angle of the bending is critical for the piece functionality. In this case, a 5% of deviation will be accepted between one mesh and the upcoming thicker mesh studied. It is to say that, if increasing the mesh density, 5% or less variation from previous model is obtained, it will be considered that the mesh has converged.

5.2.2 Analysis of results

The following tables show the results for overall maximum values of σ_{VM}, PEEQ, and NT11 for the plate, and minumum RF2 for the roller:

MODEL	n	Number of plate mesh nodes	Number of plate mesh elements	σ_{VM} (Pa)	PEEQ	RF (N)	NT (K)
Model 1	2	693	400	8,52E+08	4,16E-01	1,81E+06	3,99E+02
Model 2	3	1800	1218	1,19E+09	4,24E-01	1,73E+06	5,92E+02
Model 3	4	4305	3196	1,15E+09	5,19E-01	1,71E+06	7,21E+02
Model 4	5	7956	6250	9,59E+08	5,85E-01	1,68E+06	8,85E+02
Model 5	6	12180	9918	1,03E+09	6,45E-01	1,66E+06	9,51E+02
Model 6	7	21312	17892	1,21E+09	1,071	1,61E+06	1,01E+03
Model 7	8	29889	25600	1,11E+09	1,107	1,64E+06	1,11E+03

Table 7. Overall maximum σ_{VM}, maximum PEEQ, maximum NT11 and minumum RF2

To find the mesh thickness that provides the most accurate results, the maximum values for σ_{VM}, PEEQ, and NT11 in the plate as well as min RF2 of the roller obtained for timeframe 3 are included. Being the model at the same point of process for each of the models, the results will be comparable to each other:

MODEL	n	Number of plate mesh nodes	Number of plate mesh elements	σ_{VM} (Pa)	PEEQ	RF (N)	NT (K)
Model 1	2	693	400	7,64E+08	3,79E-01	1,54E+06	2,13E+02
Model 2	3	1800	1218	8,69E+08	4,24E-01	1,58E+06	3,18E+02
Model 3	4	4305	3196	7,79E+08	4,77E-01	1,62E+06	4,37E+02
Model 4	5	7956	6250	7,39E+08	4,64E-01	1,62E+06	5,40E+02
Model 5	6	12180	9918	7,37E+08	4,72E-01	1,56E+06	6,43E+02
Model 6	7	21312	17892	8,53E+08	4,92E-01	1,60E+06	7,65E+02
Model 7	8	29889	25600	8,89E+08	4,85E-01	1,58E+06	8,43E+02

Table 8. Maximum σ_{VM}, maximum PEEQ, maximum NT11 and minumum RF2 for timeframe 3

Then, these results are plotted and compared. Von Mises stress máximum overall values oscillate depending on the number of elements in the plate around a value that is between those obtained in Model 2, Model 4 and Model 6, but values do not converge. In each of the models, the maximum σ_{VM} is reached in different instants (see Annex 2), for this reason, the data obtained are not really comparable. For timeframe 3, results are less scattered and a more accurate tendency line can be drawn. Resutls for model 6 and model 7 are very similar.

Nevertheless, σ_{VM} values are not valid to determine the mesh convergence because maximum plastic deformation is already being reached during the process.

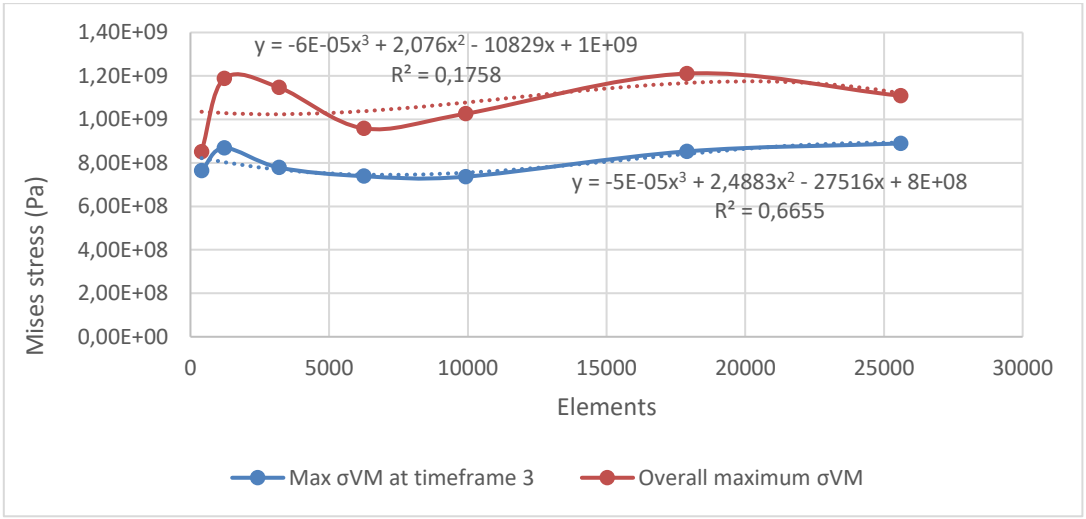

Graph 2. σ_{VM} vs number of elements

As it can be seen in the following screenshot, most of the plate's nodes are on the plastic region, over the tensile ultimate strength, which corresponds to the maximum plastic deformation stress. This is why Mises stresses are not considered as a criteria for mesh convergence.

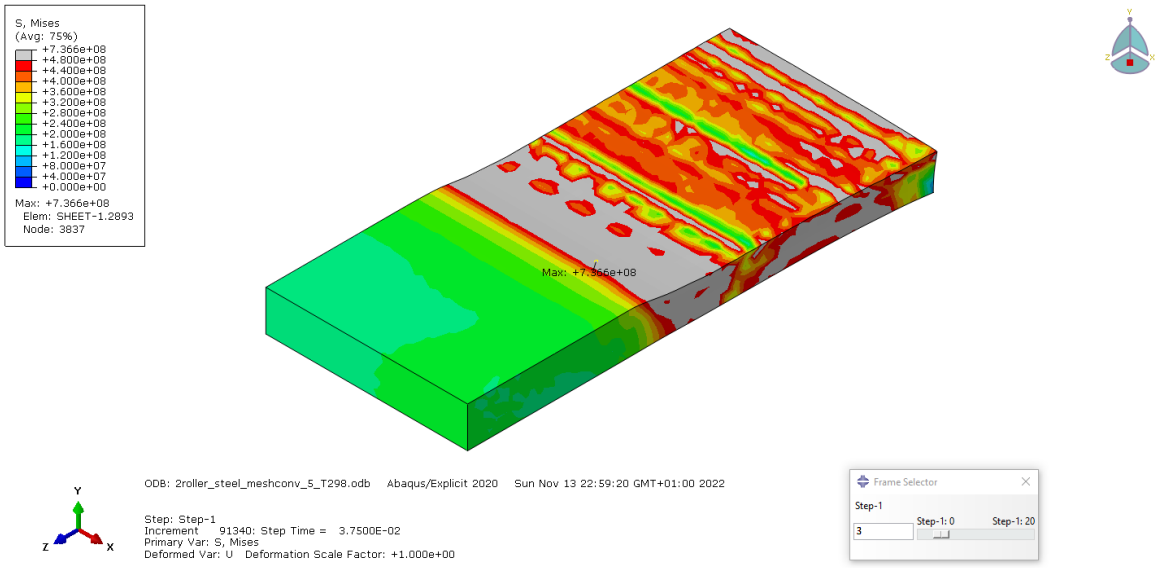

Figure 31. Model 5 Mises stress

For PEEQ, it can be seen that there is a significant increase in its maximum value depending on the number of elements. This occurs due to the dynamic effects of the model, which create a very high PEEQ value in some elements. Nevertheless, if results are compared from the same time step, it can be appreciated how the PEEQ remains almost constant, which is the expected result.

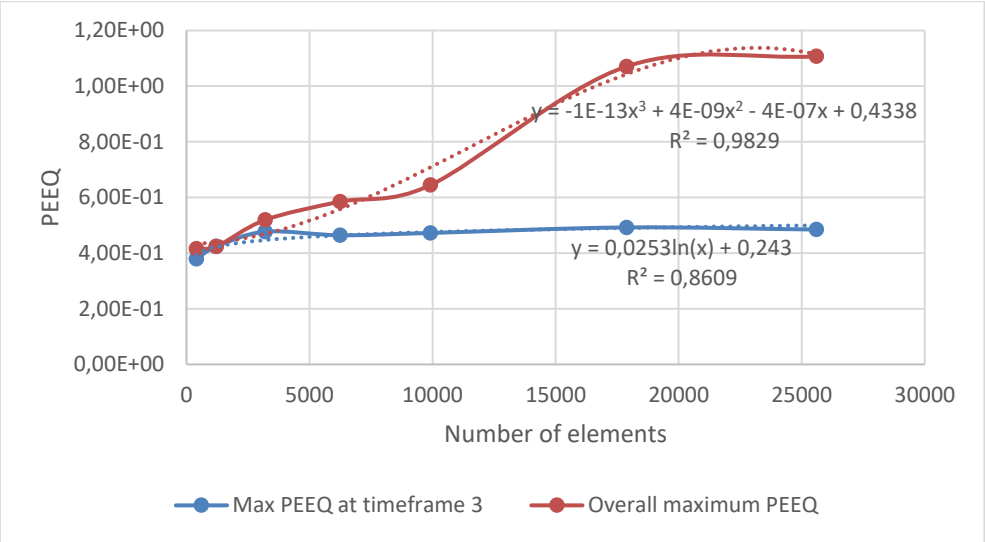

Graph 3. PEEQ vs number of elements

In the figure shown below, it can be seen how in model 6 a PEEQ peak appears in a corner of the plate, but it is a specific stress concentration that is not representative to analyze the convergence of the model.

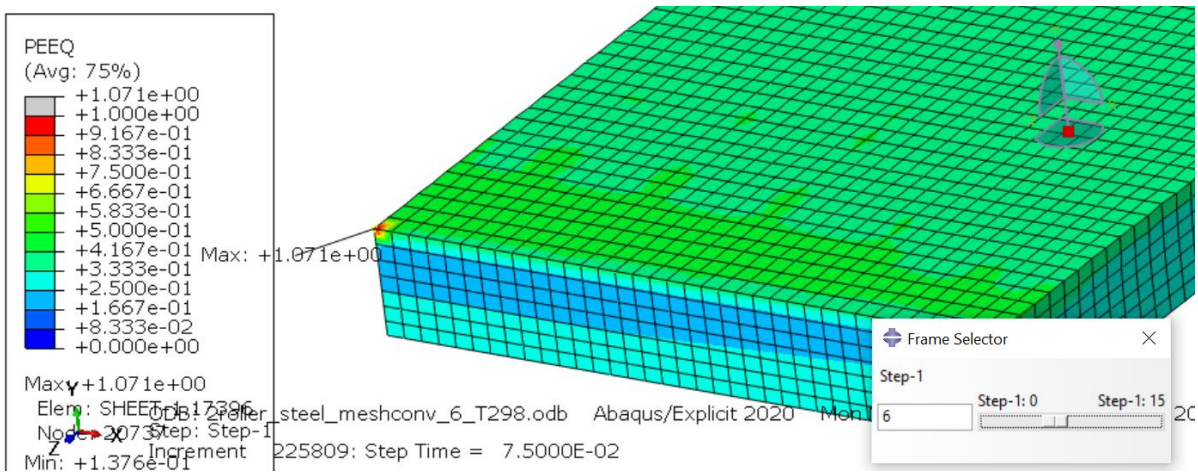

The reaction force generated on the roller maintains similar values in each of the models, since the deformation that occurs on the plate is similar. As the contacts are defined, the deformation that the plate will have will be similar regardless of the density of the mesh, and therefore, the value of the reaction force on the roller will also be similar once the mesh has converged:

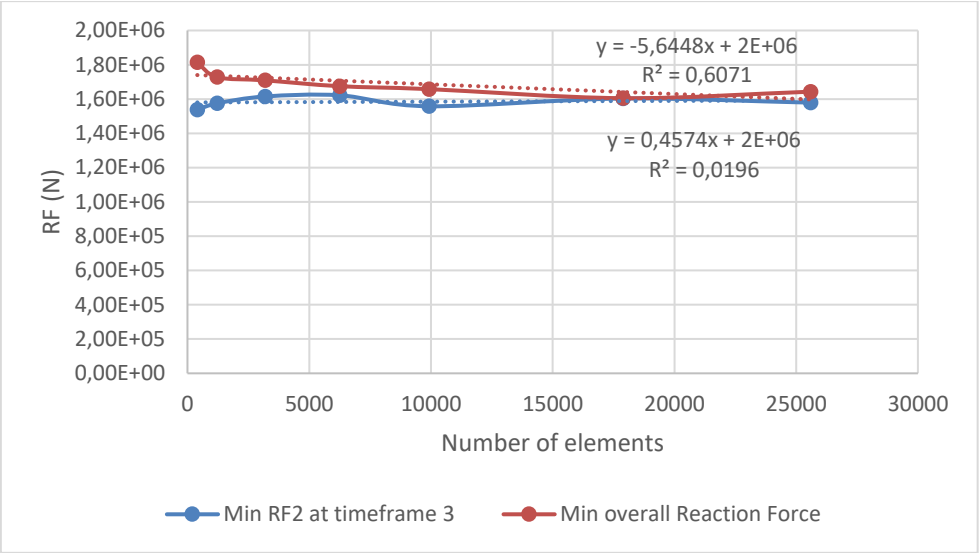

Graph 4. RF2 vs number of elements

The temperature data obtained does not converge due to the temperature peaks that occur in certain areas of the plate in the different meshes tested. This means that the results are not comparable between the different models.

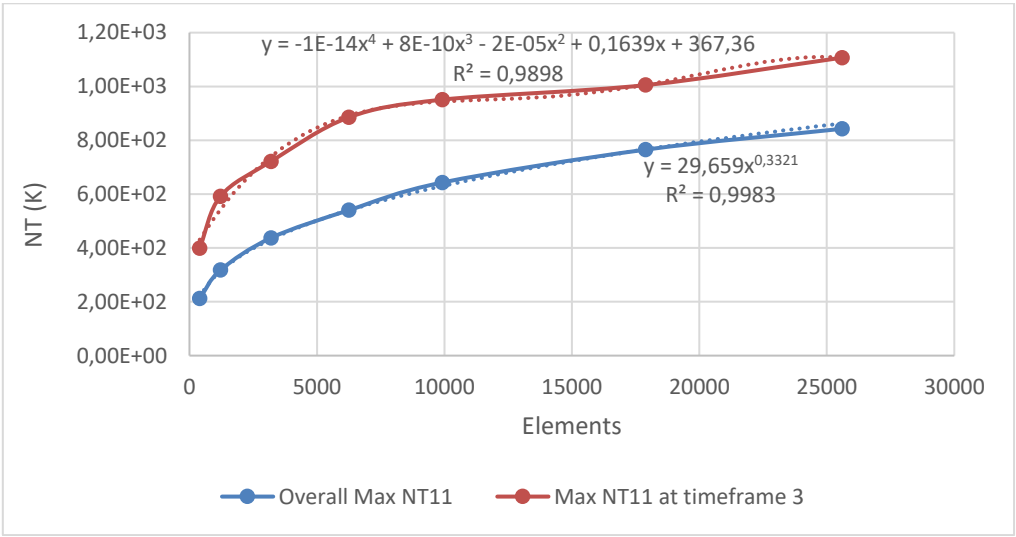

Graph 5. NT11 vs number of elements

For this reason, the temperature values that have been taken for the analysis correspond to those obtained in a node corresponding to the same area of the plate in the same timeframe (timeframe 3 as well as the rest of the variables).

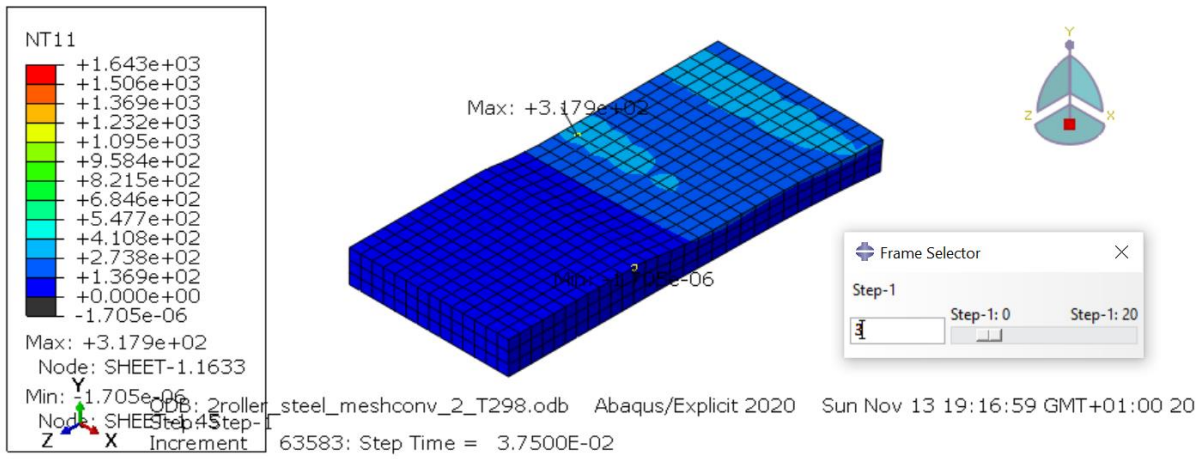

Figure 32. Model 2: Max NT11 location

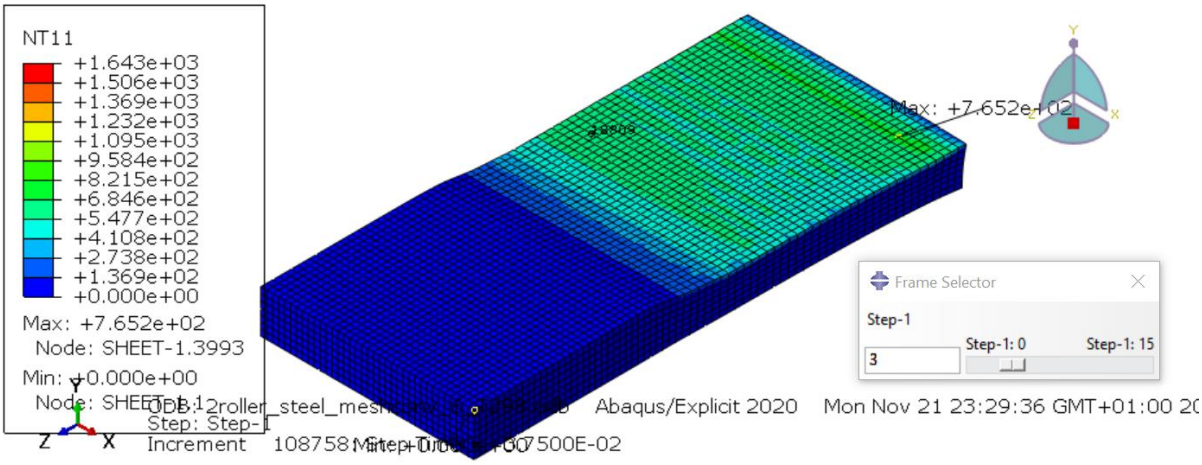

Figure 33. Model 6: Selected node for NT11 convergence analysis. Its location is similar to the location of the node for Max NT11 in Model 2

Annex 3 details how these temperature values have been extracted from the model.

The nodal temperature values grow as a function of the number of elements, but when reaching a temperature slightly above 600 k, the temperature increases very slowly, which means that the mesh is converging.

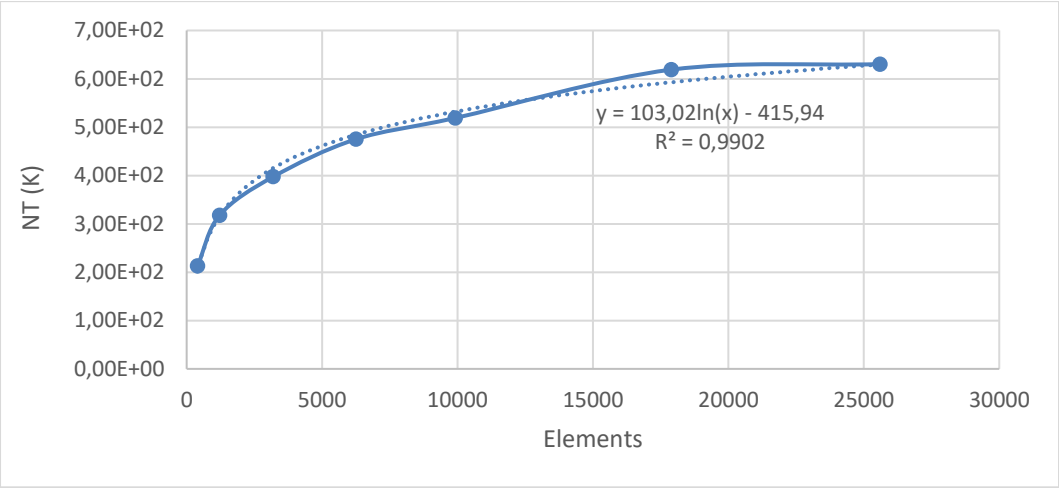

Graph 6. NT11 vs number of elements

Once the results have been extracted, the ideal mesh thickness must be determined. The table shown below contains the values of increase of each magnitude with respect to the value obtained in the previous model with a coarser mesh:

n	Increment of max. PEEQ (%)	Increment of RF (%)	Increment of NT (%)
2	-	-	-
3	10,57	2,35	33,09
4	11,16	2,48	20,02
5	-2,76	0,43	16,34
6	1,76	-4,11	8,46
7	4,02	2,81	16,16
8	-1,57	-1,52	1,81

Table 9. Increment on the magnitude of the variables in % with respect to the mesh density increment

To conclude which mesh dimension is adequate, the most important parameter to analyze are those that refer to the mechanical behaviour, which are plastic deformation, stress concentration and reaction force. In model 6 it can be seen that the results has converged, because the results are behind the 5% selected as convergence criteria. Therefore, it can be concluded that 7 elements along the thickness of the plate is the ideal mesh density for the analysis that is intended to be carried out.

5.3 Comparation with rigid roller model

Models with thermal coupling require deformable elements, for this reason, it is necessary to make a deformable roller. The increase in temperature depends directly on the deformation of the material, so it is necessary that the roller can be deformed. However, in this case it is important for the deformation of the roller to be very low to simulate a real process, for this, the material of the roller must be considerably less ductile than the material of the plate.

In this case, a steel whose thermal properties are equal and whose modulus of elasticity is 10 times higher is used as material. In order to ensure that the roller does not deform, it is important to create a structured mesh in the roller, which does not give rise to excessive stress concentrations in certain elements that are also accentuated by the dynamic effects of the model.

To analyse the mechanical performance of the model, a deformable roller model is compared with a rigid roller model. Rollers from these models are created as discrete rigid parts. Please refer to Annex 4 to see how rigid model is made.

σ_{VM} values are not evaluated as the deformed part of the plate is enterely inside the plastic zone. Thus, the PEEQ and the reaction force are compared. Both models are expected to provide similar results.

Taking an instant from the first pass, in both models the PEEQ oscillates between 0.25 and 0.4167 as for the color scale. In both cases results are similar despite the fact that in the rigid model it appears a PEEQ peak in a specific node causing the maximum magnitude in the model to be higher than for the deformable roller model.

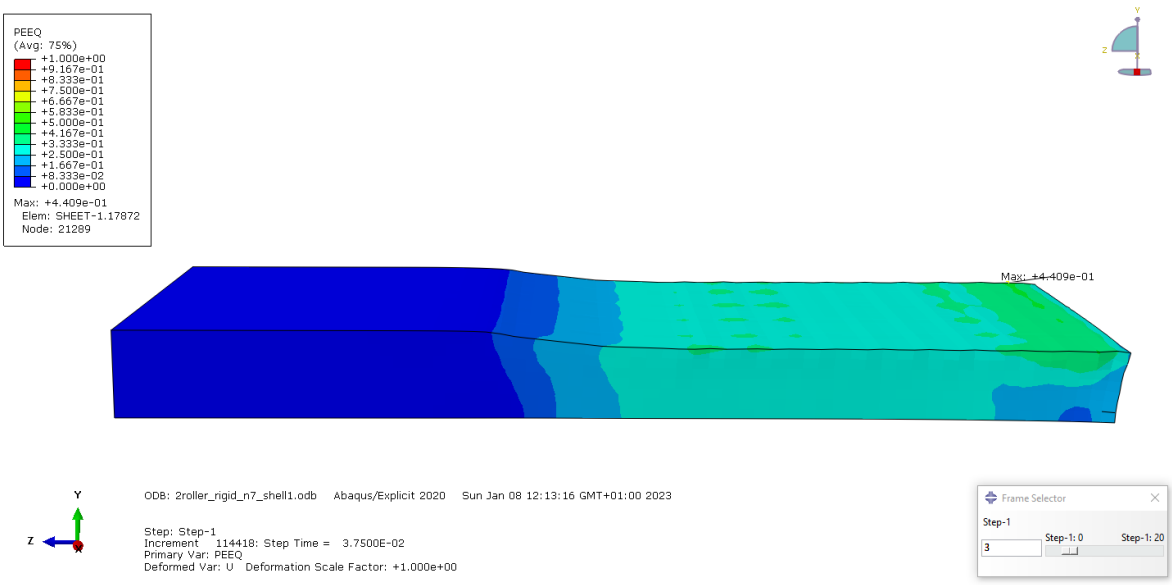

Figure 34. PEEQ at timeframe 3 for rigid roller

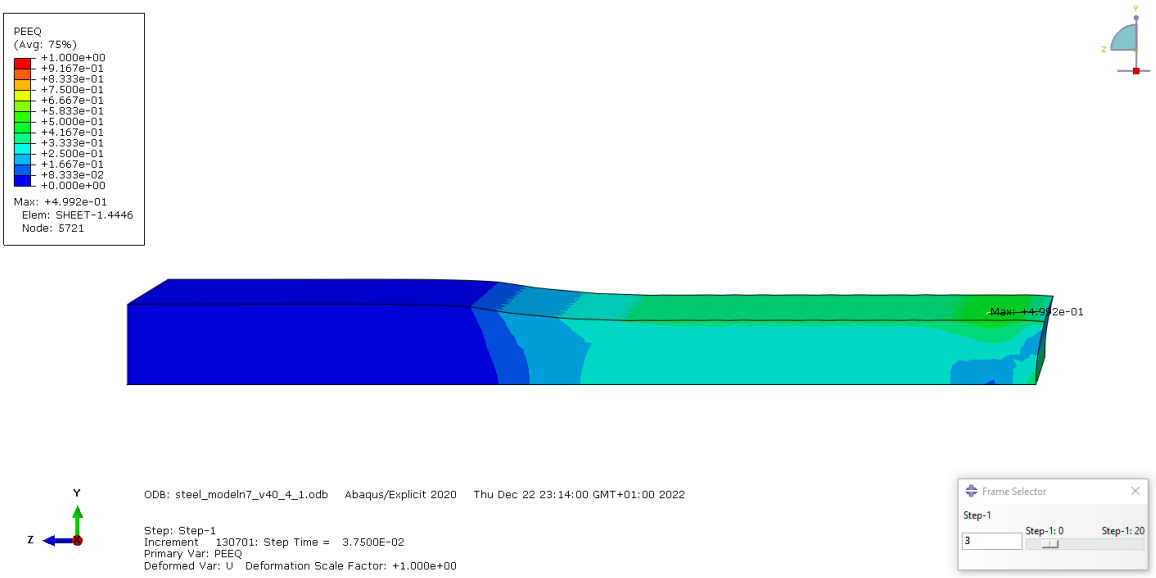

Figure 35. PEEQ at timeframe 3 for deformable roller

In the case of the second pass, a similar peak appears in both models. The following screenshots evidence a trend that began to occur in the first pass, which is that in the deformable roller model the deformation on the surface is slightly higher than in the rigid roller model. This is because, since there is a certain deformation in the roller, there is an exchange of kinetic energy between the roller and the plate which is absorbed by the roller as elastic potential energy and later is transmitted to the plate itself.

Finally, the reaction force values are compared at instants of the first and second passes. It can be verified that the results obtained for the rigid and deformable roller are quite similar for both the first and the second pass.

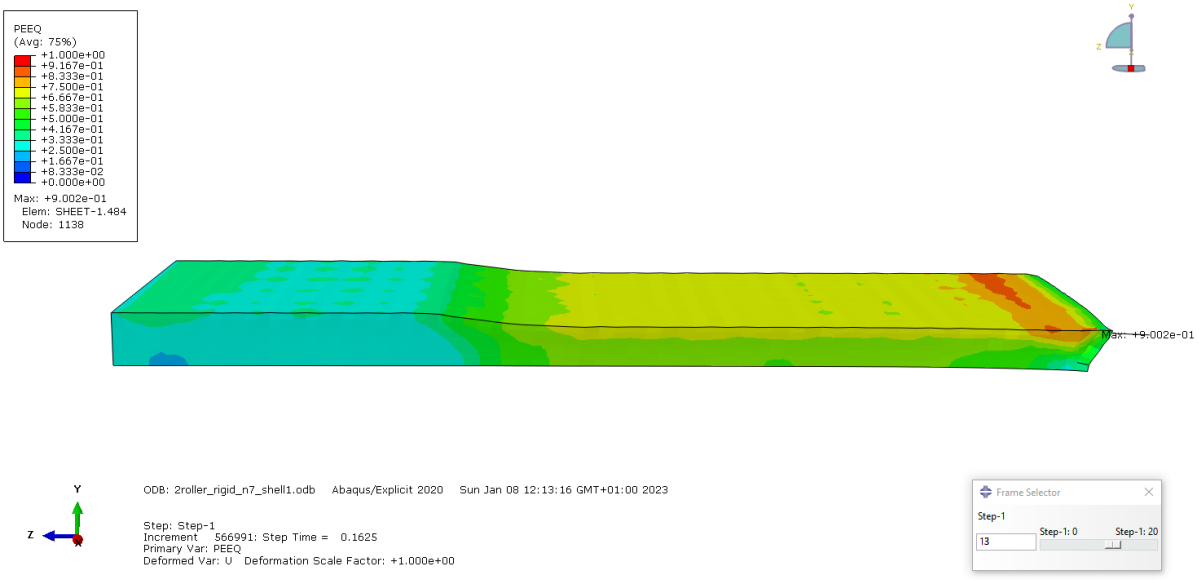

Figure 36. PEEQ at timeframe 13 for rigid roller

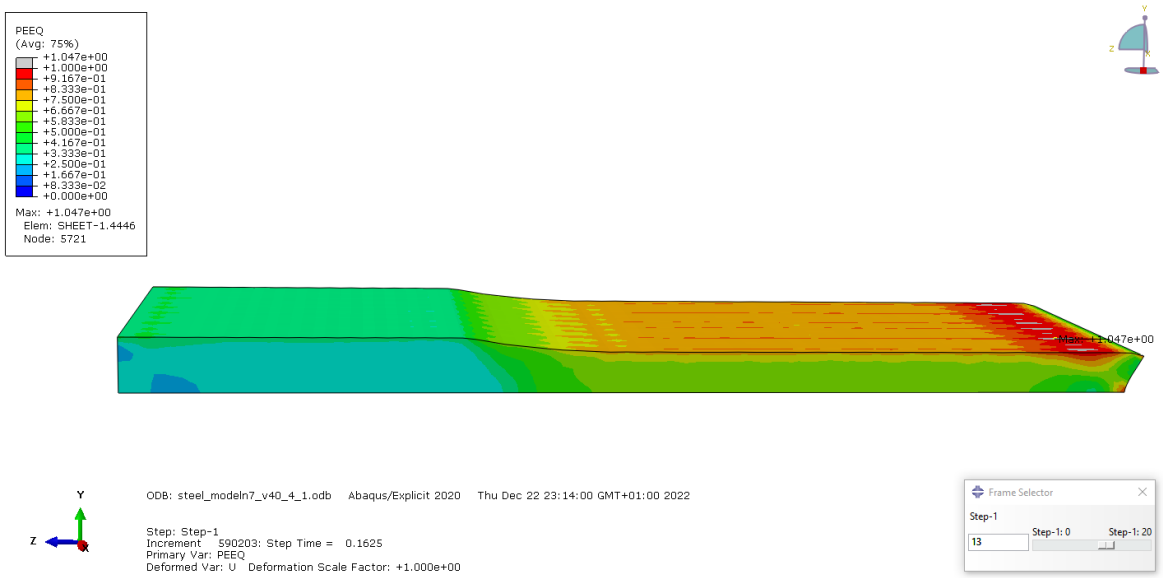

Figure 37. PEEQ at timeframe 13 for deformable roller

The table below shows the comparison of values obtained between the model with a rigid roller and with a deformable roller.

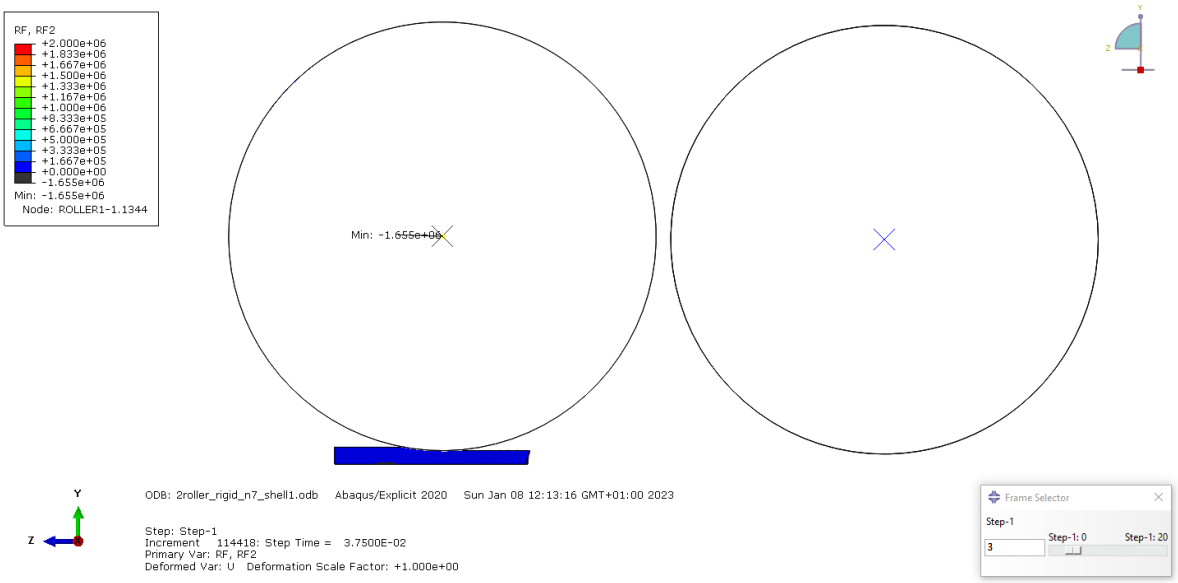

Figure 38. RF at timeframe 3 for rigid roller

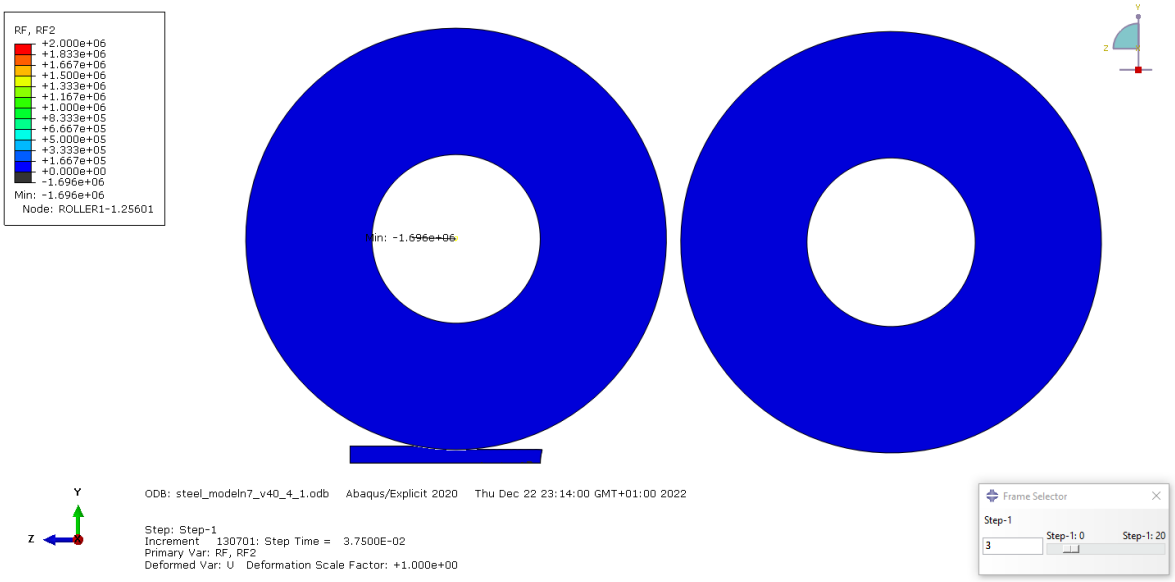

Figure 39. RF at timeframe 3 for deformable roller

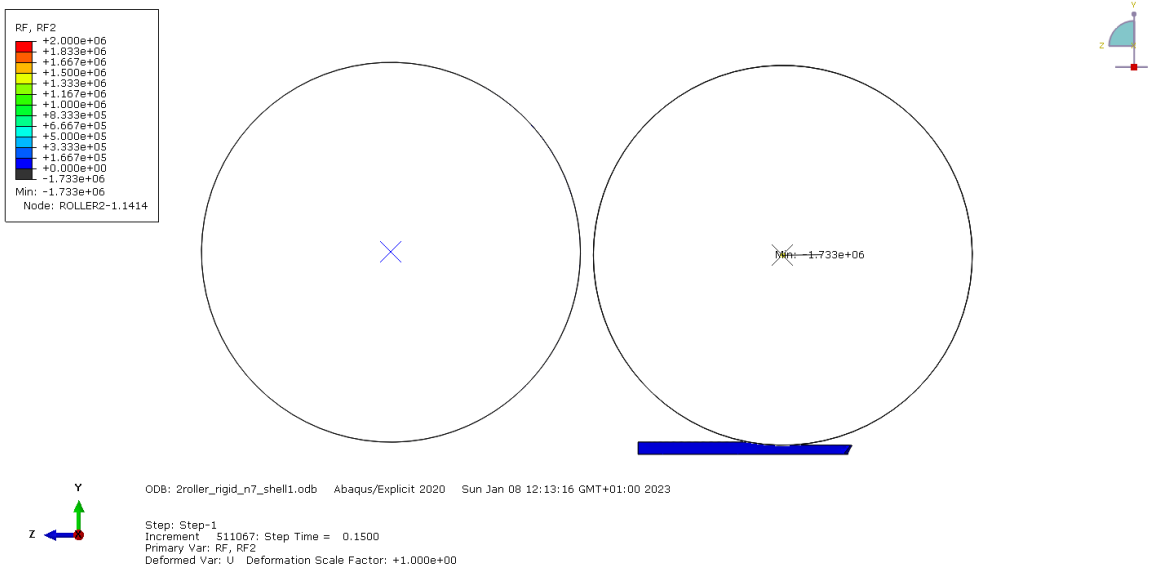

Figure 40. RF at timeframe 13 for rigid roller

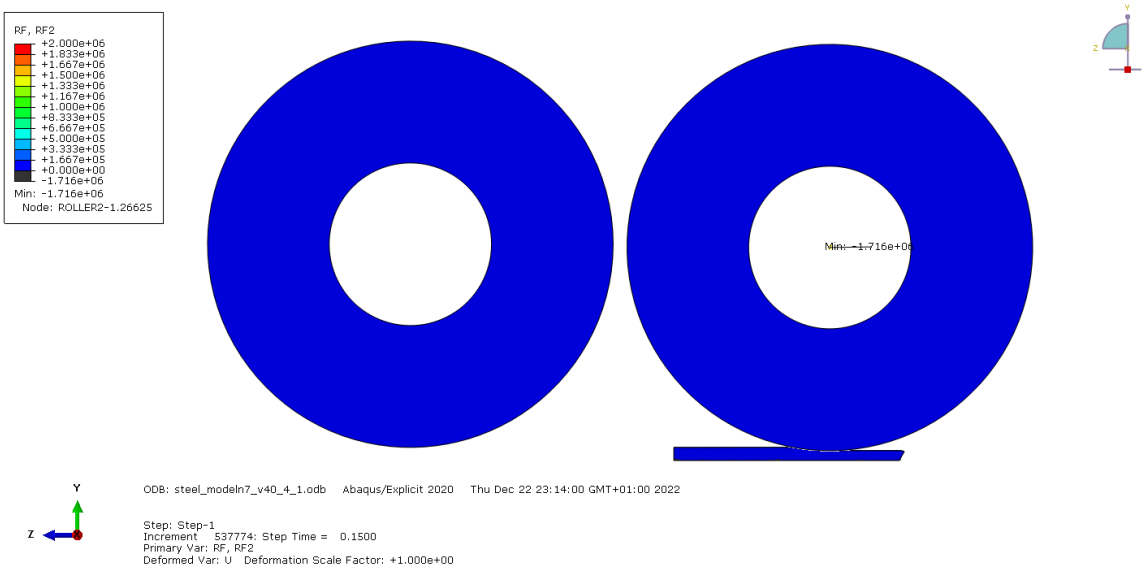

Figure 41. RF at timeframe 13 for deformable roller

	Deformable roller		Solid roller	
	1st pass	2nd pass	1st pass	2nd pass
max PEEQ	4,992E-01	1,047	4,409E-01	9,002E-01
max RF (N)	1,696E+06	1,716E+06	1,655E+06	1,733E+06

Table 10. Result comparation between rigid roller model and deformable roller

In these results it is shown how results from the deformable roller model and the solid roller model are very similar between them, ensuring that using a deformable roller with an elastic modulus 10 times higher than the plate is enough for the intended analysis.

5.4 Thickness reduction of the plate

To check the performance of the simulation, it is imporant to measure the thickness of the plate after the first and the second pass.

During the first pass, the thickness is reduced from 20 mm to 16 mm:

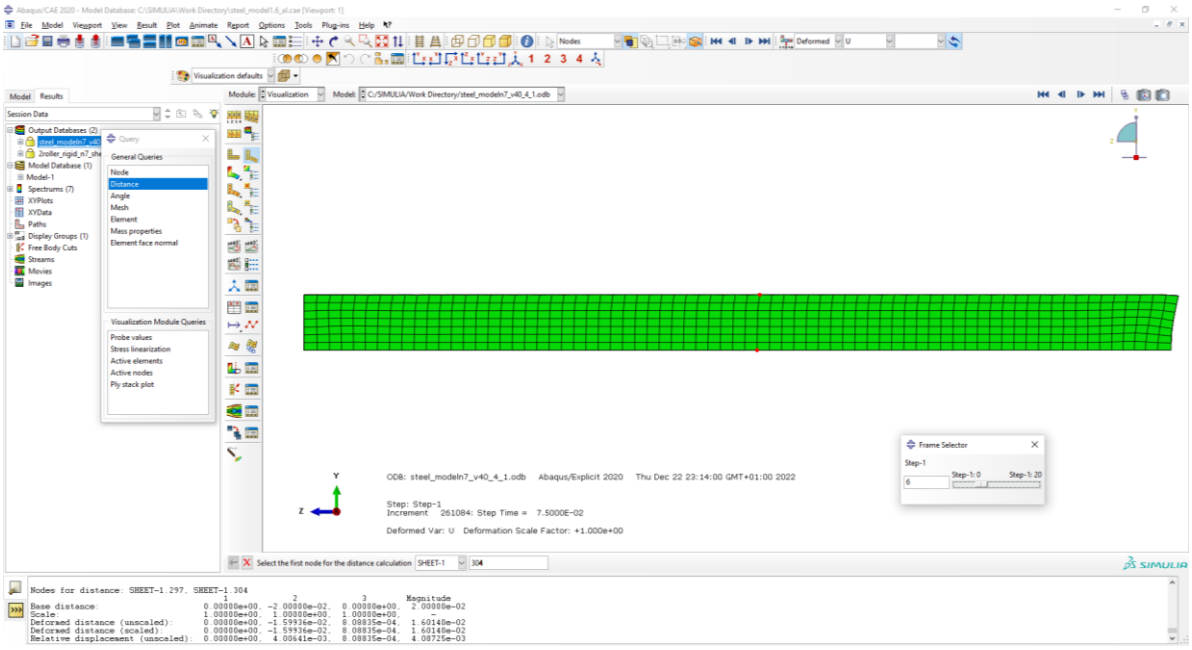

Figure 42. Thickness reduction for 1st pass

During the second pass, thickness is reduced to 12 mm:

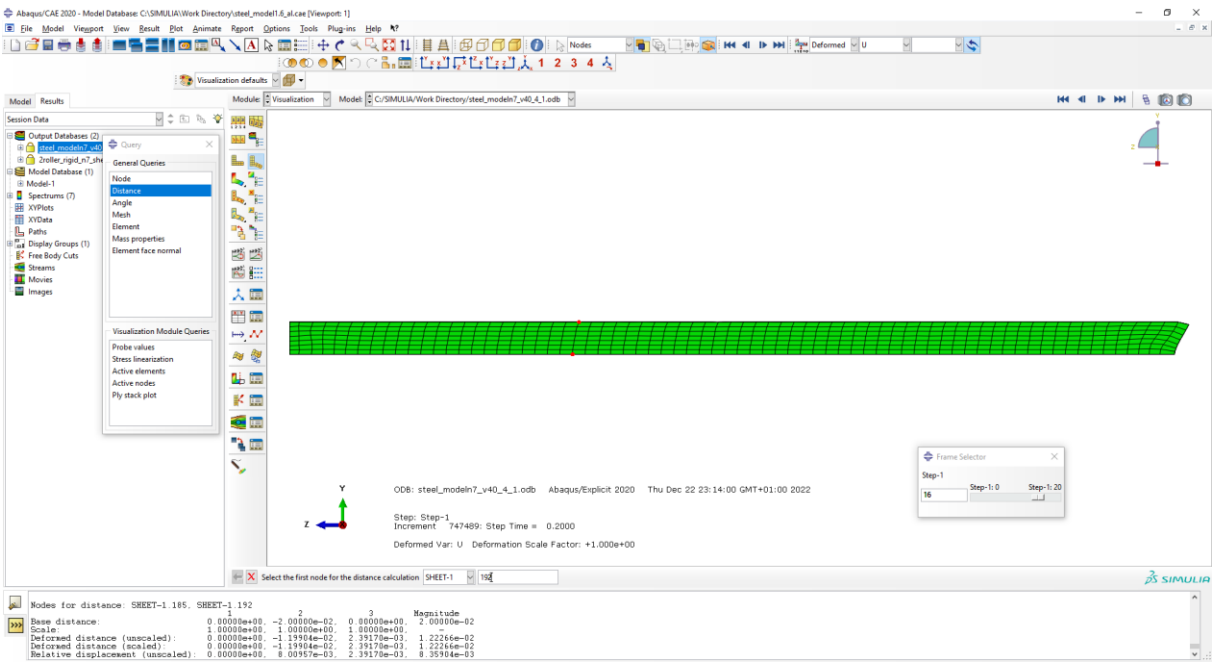

Figure 43. Thickness reduction for 2nd pass

According to Poison's law, when deforming a material in one direction, generates deformation in the directions too. In this case, as width (x axis) is fixed, length of the plate varies from 200 mm to 250.9 mm during the first pass:

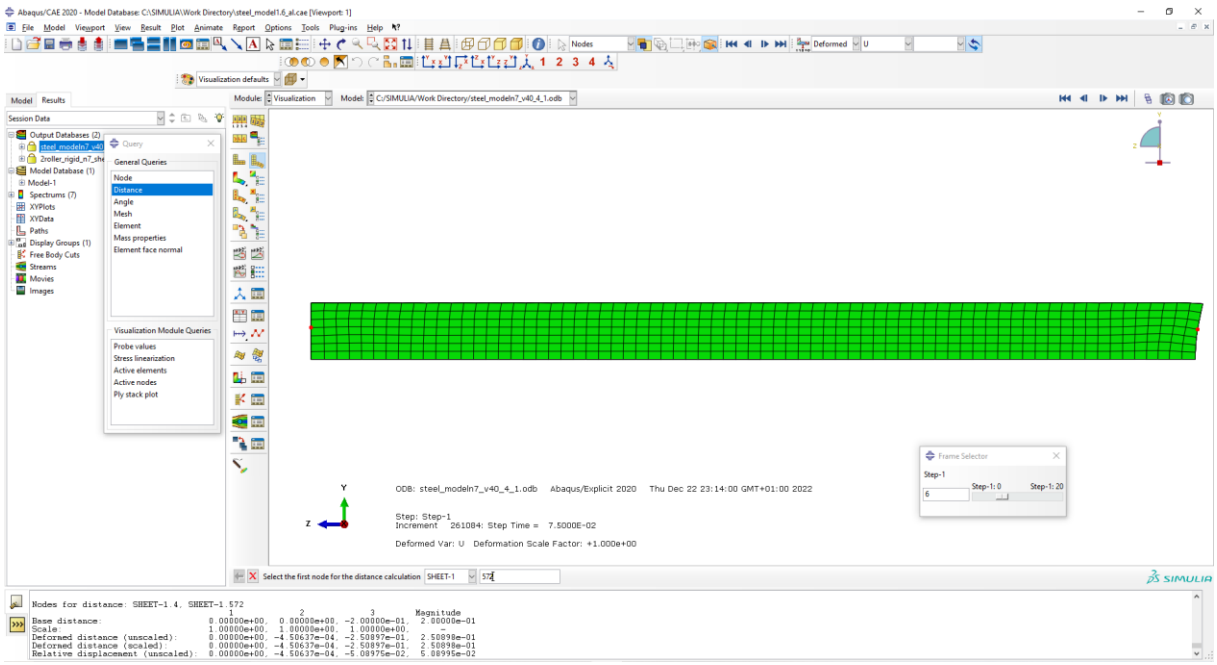

Figure 44. Elongation after 1st pass

On the second pass, length increases to 331.6 mm:

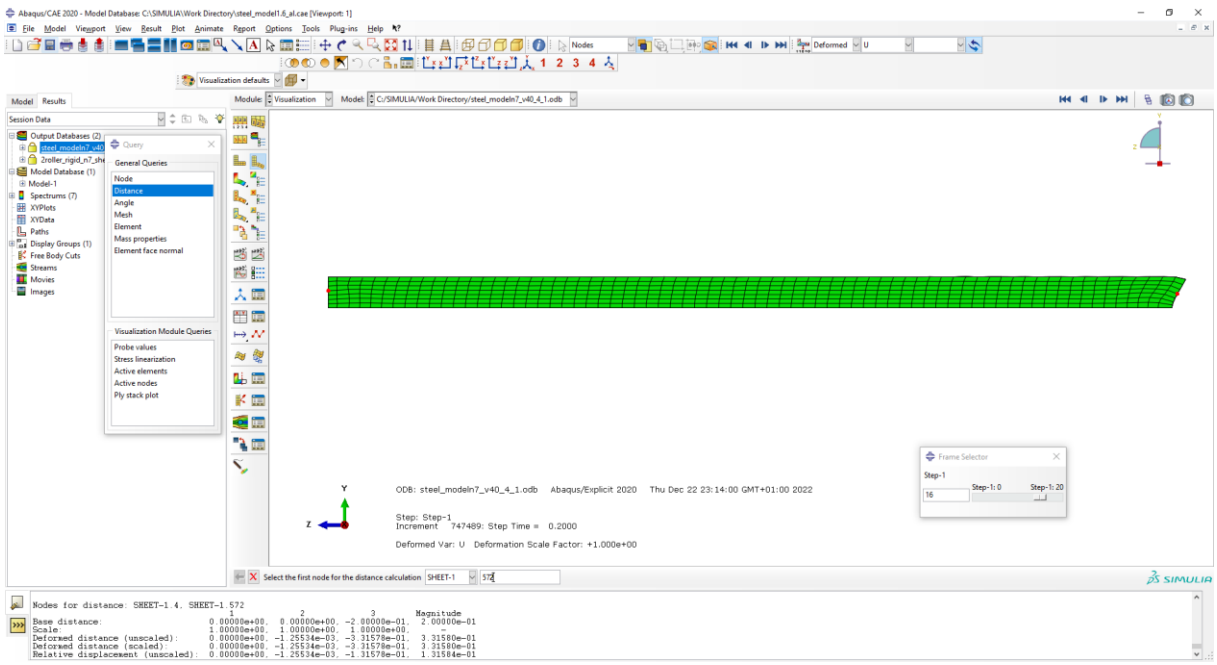

Figure 45. Elongation after 2nd pass

5.5 Velocity parametric analysis

To carry out the parametric analysis of the speed at which the process is carried out, 3 series of models are made:

- Roller angular velocity variation (models 8 to 13).
- Plate linear velocity variation (models 14 to 19).
- Plate linear velocity and roller angular velocity variation (models 19 to 24).

The linear speed of the plate must be less than the tangential speed of the roller so that the impact with the roller does not produce undesired deformations in the plate. The plate, therefore, must enter at a speed lower than the tangential speed of the roller until, due to the effect of the friction of the roller on the plate, the material is dragged inside the rollers and it is at point N in the figure below, where the speed of the plate is equal to the tangential speed of the roller.

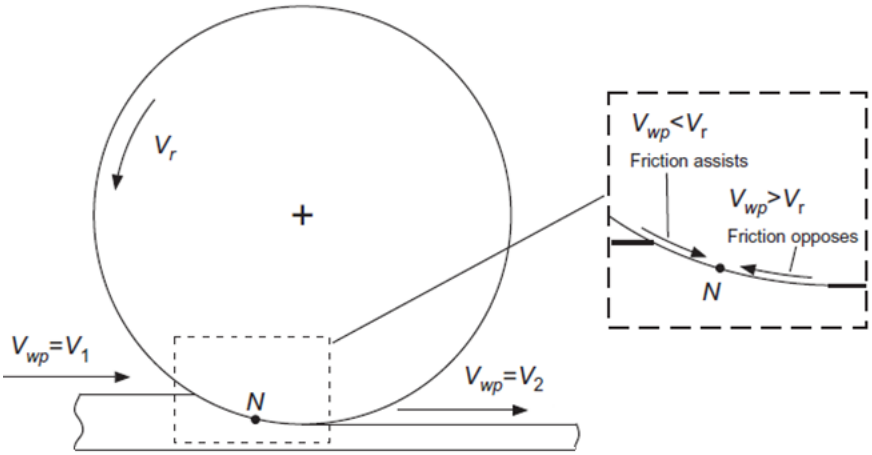

Figure 46. Schematic representation showing how the plate velocity varies during the process

5.5.1 Roller angular velocity variation

First, different models are run by varying the angular velocity of the roller while keeping the linear velocity of the plate constant.

Model	Plate linear velocity (m/s)	Roller ω (rad/s)
Model 8	4	20
Model 9	4	30
Model 10	4	40
Model 11	4	50
Model 12	4	60
Model 13	4	70

Table 11. Roller angular velocity variation models

The values obtained for the maximum temperature increment, PEEQ and reaction force in timeframes 3 and 13 with respect to the initial temperature are shown below. In the same way that it has been done for the mesh convergence analysis, the same timeframes are taken for different models with the purpose of obtaining comparable values between them. By only varying the rotation speed of the roller, the effect of friction on the plate can be perceived, since the higher the speed of the roller, the greater the heat generated by friction. In the table below, results from the main parameters obtained are presented:

1ST PASS				
Roller velocity (rad/s)	Plate linear velocity (m/s)	PEEQ	RF (N)	NT (K)
20	4	3,79E-01	1,84E+06	4,32E+01
25	4	3,78E-01	1,75E+06	2,20E+02
30	4	4,23E-01	1,73E+06	4,40E+02
35	4	4,56E-01	1,69E+06	5,93E+02
40	4	4,99E-01	1,70E+06	7,56E+02
45	4	5,44E-01	1,65E+06	9,14E+02
50	4	6,24E-01	1,61E+06	1,05E+03

Table 12. Results for first pass roller angular velocity variation models

2ND PASS				
Roller velocity (rad/s)	Plate linear velocity (m/s)	PEEQ	RF (N)	NT (K)
20	4	9,37E-01	1,83E+06	1,44E+02
25	4	9,64E-01	1,83E+06	3,60E+02
30	4	1,01E+00	1,80E+06	6,34E+02
35	4	9,93E-01	1,79E+06	9,14E+02
40	4	1,05E+00	1,83E+06	1,20E+03
45	4	1,16E+00	1,67E+06	1,47E+03
50	4	1,23E+00	1,45E+06	1,72E+03

Table 13. Results for second pass roller angular velocity variation models

The plastic deformation of the plate obtained increases proportionally with each pass through the roller. The faster the roller speed, the greater the plastic deformation. In any of the cases shown, the plastic deformation is sufficient to obtain the desired geometry, which indicates that for higher speeds there is an excess of plastic deformation that can be translated into internal stresses in the plate material. These stresses translate into an alteration in the mechanical performance of the material, making it less resistant and more vulnerable to damage.

This can be clearly seen at the edges of the plate, which are flattened by the difference between the tangential speed exerted by the roller on the plate and the linear speed of the plate. This shock produces excessive deformation at the leading edge of the plate.

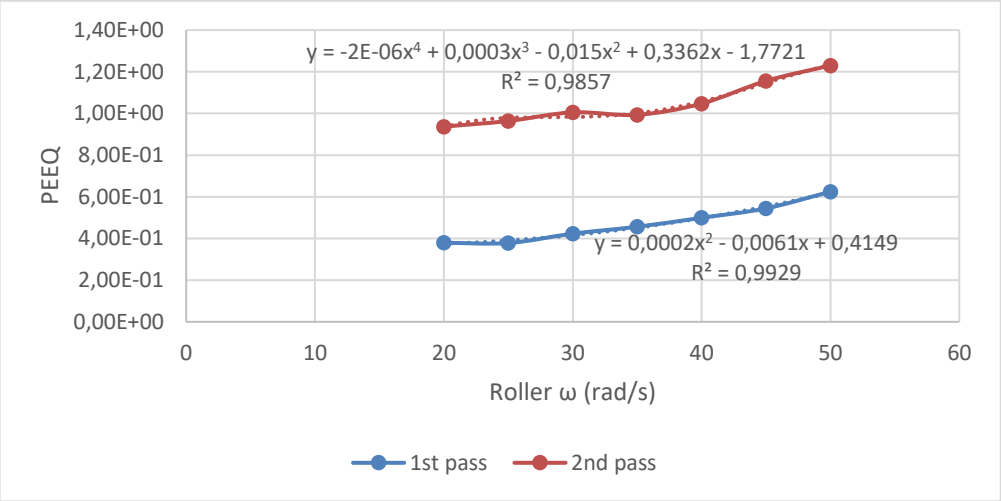

Graph 7. PEEQ results for roller angular velocity variation models

The reaction force is greater at low speeds, indicating that the roller must exert a much greater vertical force during the process. The relevance of this fact depends on the thickness of the part to be manufactured and the available machinery. For angular speeds of the roller between 20 and 50 rps the reaction force remains constant.

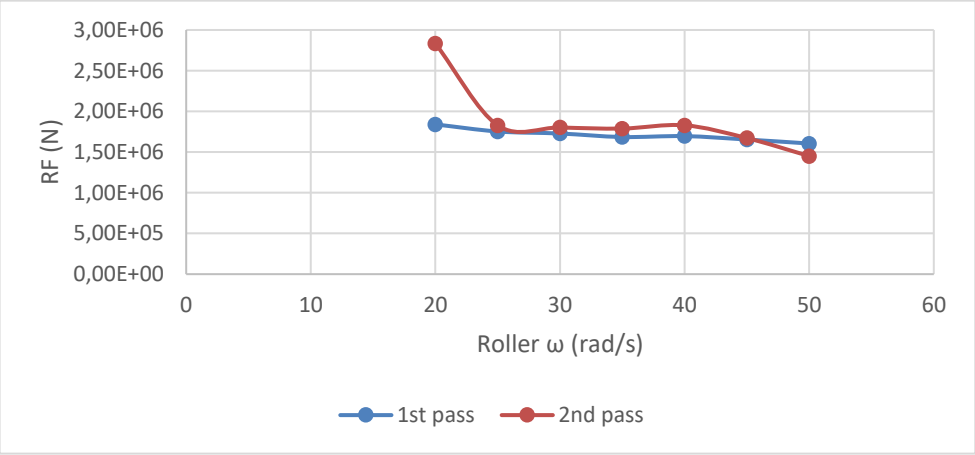

Graph 8. RF2 results for roller angular velocity variation models

In the figures below, it can be seen how the temperature varies along the surface of the plate on the first and second pass for maximum and minimum roller speed simulated:

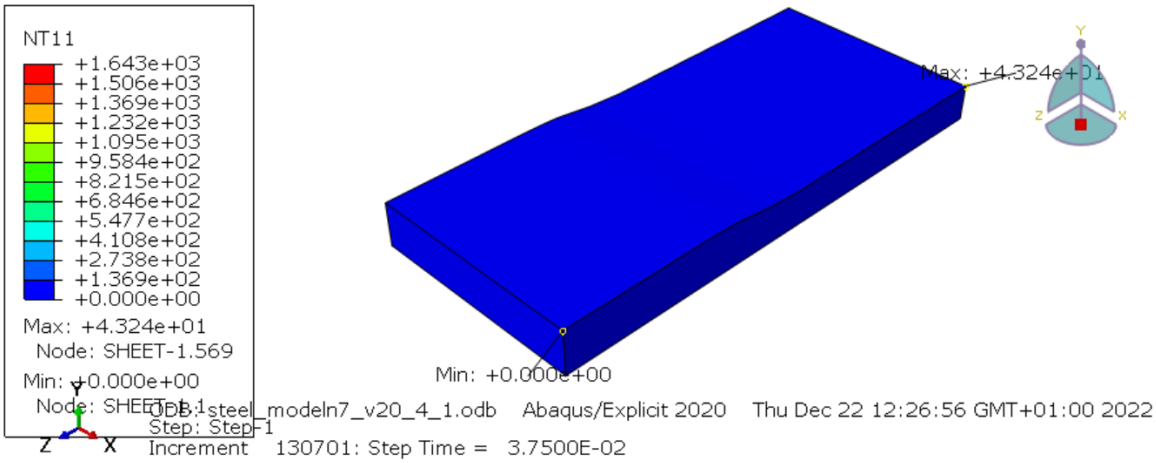

Figure 47. Temperature map of the plate during the first pass for 20 rad/s rolling speed

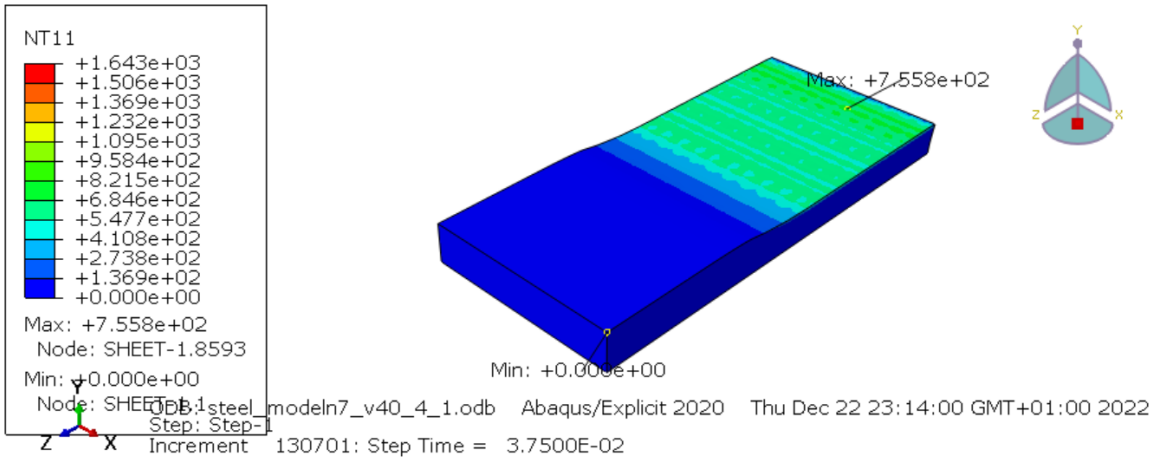

Figure 48. Temperature map of the plate during the first pass for 40 rad/s rolling speed

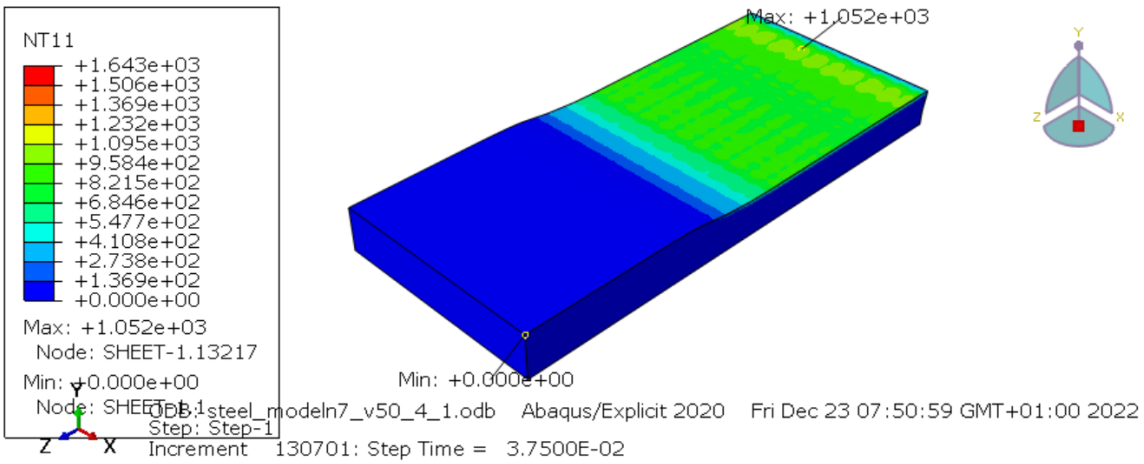

Figure 49. Temperature map of the plate during the first pass for 50 rad/s rolling speed

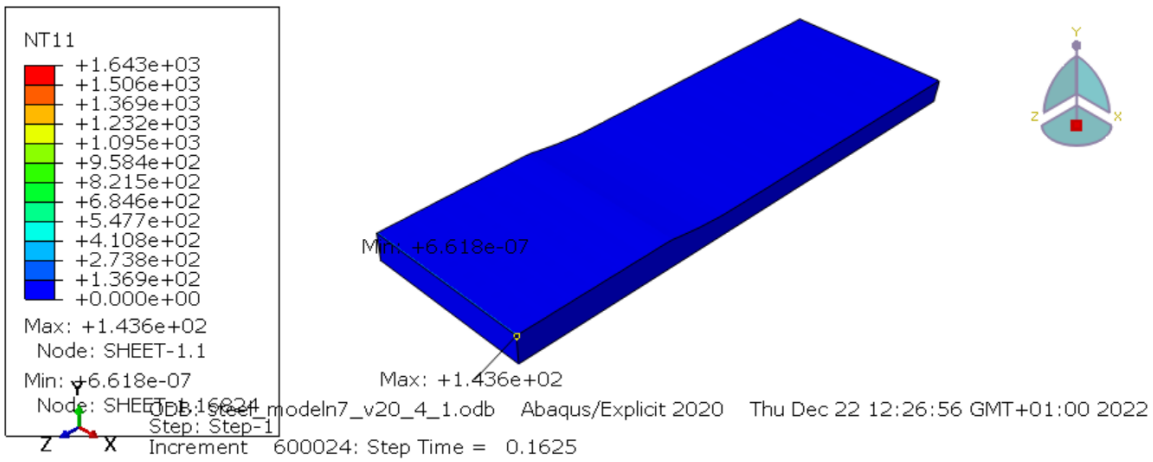

Figure 50. Temperature map of the plate during the second pass for 20 rad/s rolling speed

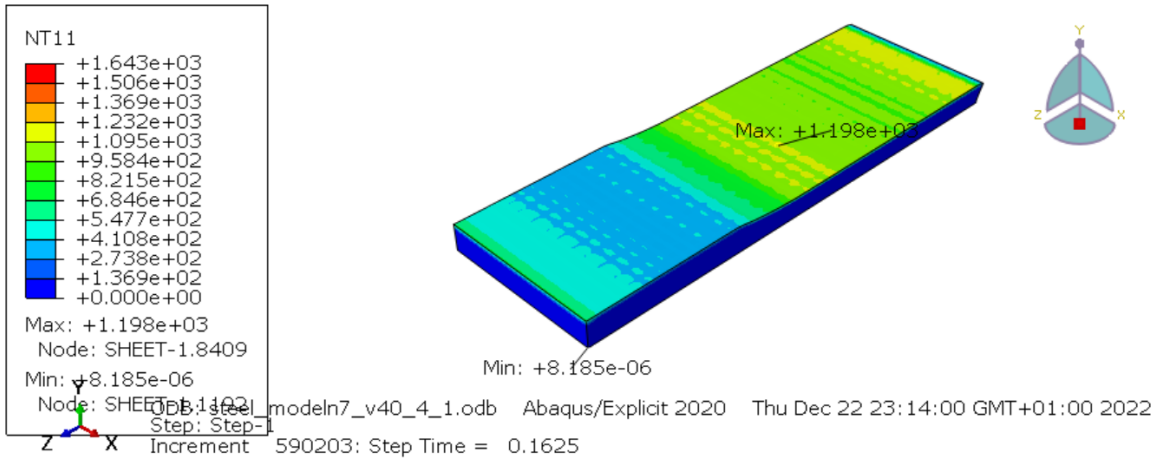

Figure 51. Temperature map of the plate during the second pass for 40 rad/s rolling speed

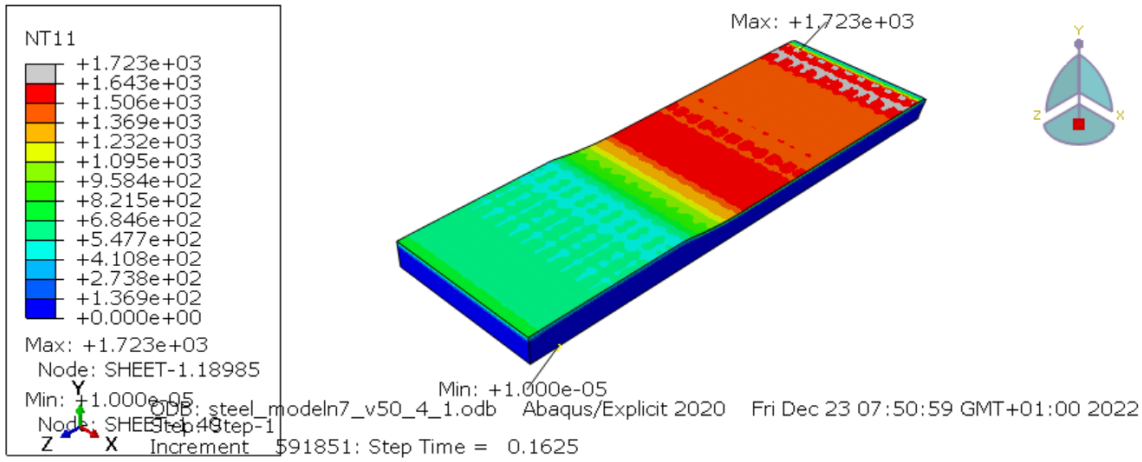

Figure 52. Temperature map of the plate during the second pass for 50 rad/s rolling speed

In these captures it can be seen the great difference in temperatures between the speed of rotation at 50 rad/s and that of 20 rad/s. For 50 rad/s, during the second pass, the surface of the plate that has come into contact with the second roller reaches temperatures above 1506K, while for 20 rad/s, the temperature does not exceed 136.9K, since that the entire plate appears dark blue.

The maximum nodal temperature increases as the rotation speed of the roller increases, and the temperature difference between the first and second pass is greater the higher the rotation speed:

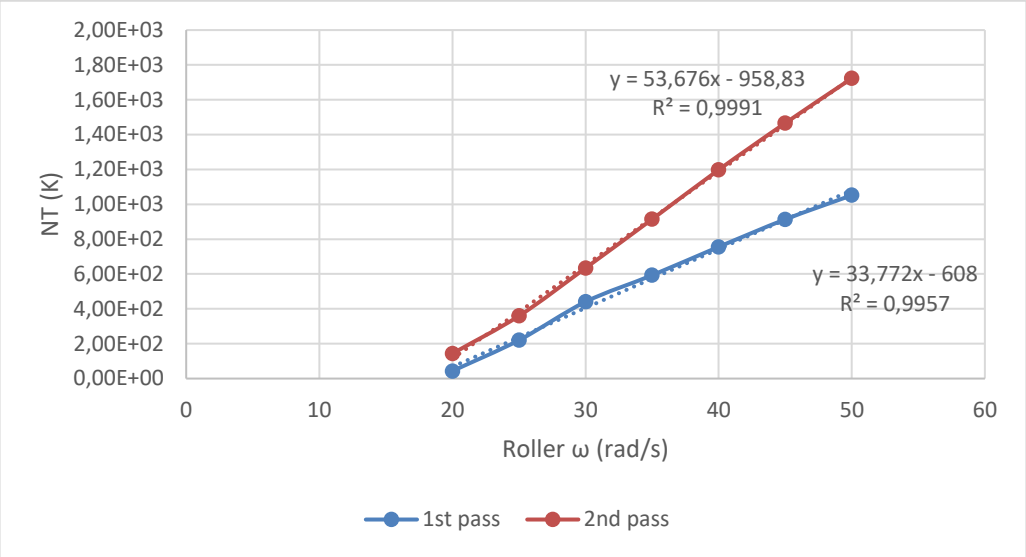

Graph 9. NT11 results for roller angular velocity variation models

5.5.2 Plate linear velocity variation

To analyze the specific influence of the linear velocity of the plate, the following models are run:

Model	Plate linear velocity (m/s)	Roller ω (rad/s)
Model 14	40	2
Model 15	40	3,5
Model 16	40	5
Model 17	40	6,5
Model 18	40	8

Table 14. Plate linear velocity variation models

In this case, only the output of reaction force and nodal temperature are output. Because it has already been verified that the plastic deformation obtained remains invariable with the change in speed of the process. The results are presented in the following tables:

1ST PASS			
Roller velocity (rad/s)	Plate linear velocity (m/s)	RF (N)	NT (K)
40	2	1,43E+06	1,69E+03
40	3,5	1,54E+06	8,92E+02
40	5	1,73E+06	5,09E+02
40	6,5	1,74E+06	2,09E+02
40	8	1,85E+06	3,79E+01

Table 15. Results for first pass roller angular velocity variation models

2ND PASS			
Roller velocity (rad/s)	Plate linear velocity (m/s)	RF (N)	NT (K)
40	2	1,72E+06	2,37E+03
40	3,5	1,50E+06	1,50E+03
40	5	1,84E+06	7,92E+02
40	6,5	1,77E+06	3,79E+02
40	8	2,97E+06	1,91E+02

Table 16. Results for first pass roller angular velocity variation models

The reaction force increases for higher values of linear velocity:

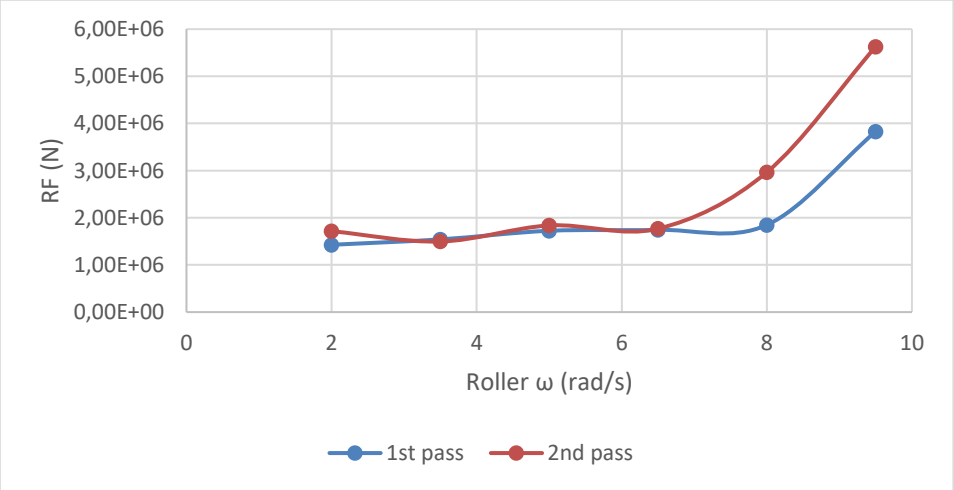

Graph 10. RF2 results for plate linear velocity variation models

The temperature is higher for lower values of linear speed due to the effect of friction, since the greater the difference between the linear speed of the plate and the tangential speed of the roller at the non-slip point, the greater the heat generation.

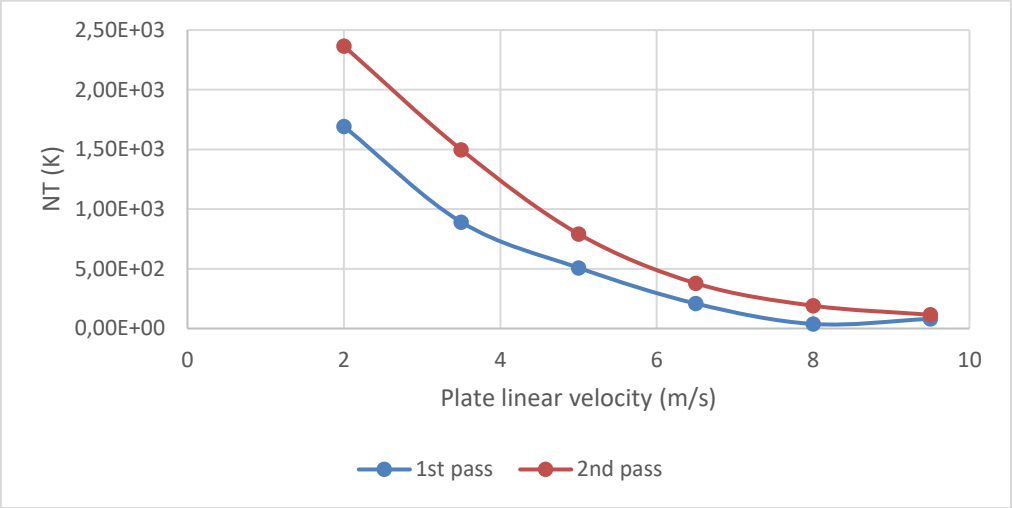

Graph 11. NT11 results for plate linear velocity variation models

The temperature maps below show the similarity between the temperatures obtained in the first and second pass for the linear velocity of 8 m/s.

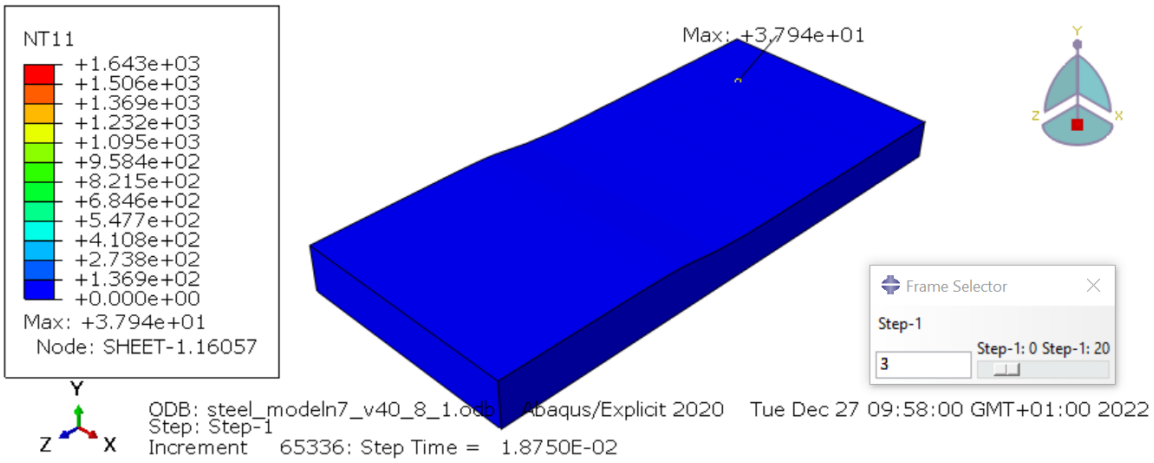

Figure 53. Temperature map of the plate during the first pass for 8 m/s plate linear velocity

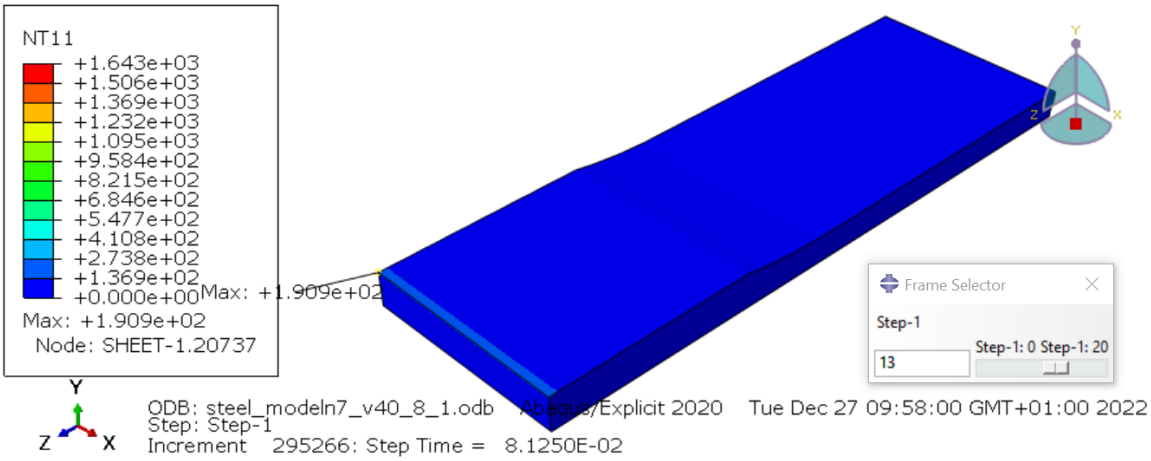

Figure 54. Temperature map of the plate during the second pass for 8 m/s plate linear velocity

The maximum temperature increment is obtained at for the slowest linear velocity model. This is where the maximum velocity difference between roller tangential velocity and plate linear velocity is found.

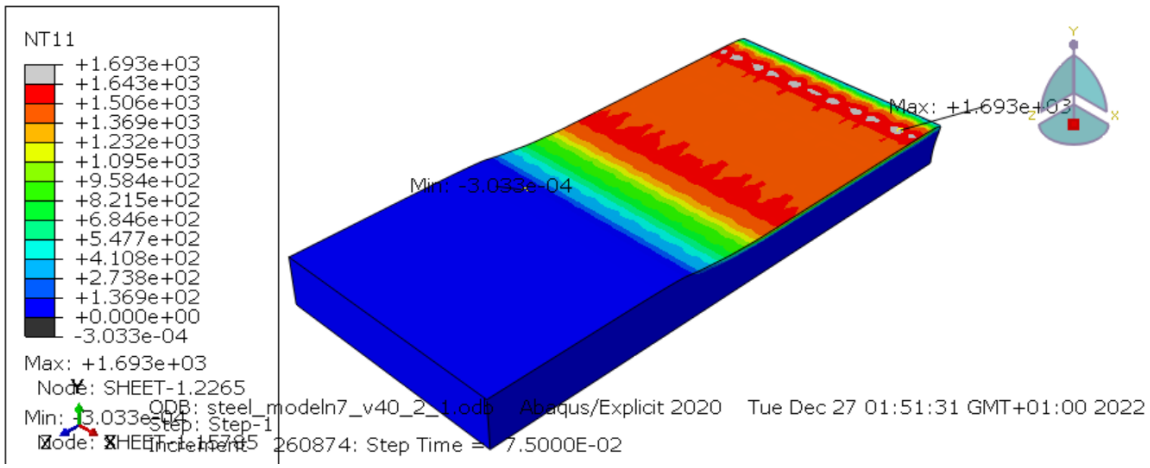

Figure 55. Temperature map of the plate during the first pass for 2 m/s plate linear velocity

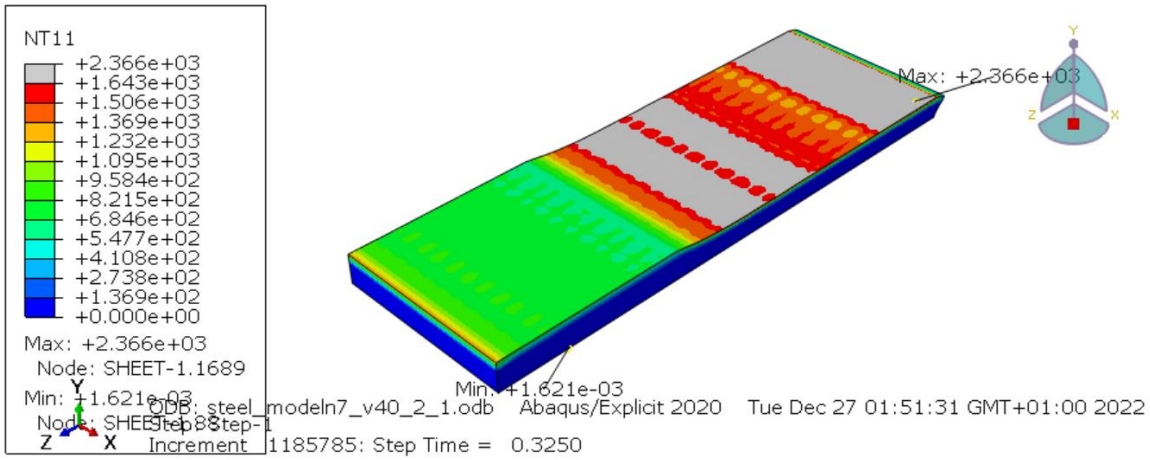

Figure 56. Temperature map of the plate during the second pass for 2 m/s plate linear velocity

5.5.3 Plate linear velocity and roller angular velocity variation

In order to analyse the combined effect of the variation of the angular velocity of the roller and the linear velocity of the plate, the following models are run. The aim of this analysis is to find out which of the two parameters has the greatest effect on the performance of the process.

In this series of models, the input linear speed selected corresponds to the 80% of the tangential speed of the roller:

Model	Plate linear velocity (m/s)	Roller ω (rad/s)
Model 19	4	20
Model 20	6	30
Model 21	8	40
Model 22	10	50
Model 23	12	60
Model 24	14	70

Table 17. Plate linear velocity and roller angular velocity variation models

The results obtained are collected in the following tables:

1ST PASS				
Roller velocity (rad/s)	Plate linear velocity (m/s)	PEEQ	RF (N)	NT (K)
20	4	3,79E-01	1,84E+06	4,32E+01
30	6	3,71E-01	1,81E+06	4,17E+01
40	8	3,71E-01	1,85E+06	3,79E+01
50	10	3,72E-01	1,83E+06	3,84E+01
60	12	3,72E-01	1,76E+06	3,84E+01
70	14	3,73E-01	1,77E+06	3,80E+01

Table 18. Results for first pass plate linear velocity and roller angular velocity variation models

2ND PASS				
Roller velocity (rad/s)	Plate linear velocity (m/s)	PEEQ	RF (N)	NT (K)
20	4	0,9367	2,83E+06	1,44E+02
30	6	9,46E-01	2,79E+06	1,70E+02
40	8	9,32E-01	2,97E+06	1,91E+02
50	10	9,30E-01	2,89E+06	2,00E+02
60	12	9,27E-01	2,78E+06	2,20E+02
70	14	9,25E-01	2,74E+06	2,25E+02

Table 19. Results for first pass plate linear velocity and roller angular velocity variation models

Regarding the mechanical behavior in this series of models, a greater plastic deformation can be observed for the model configured for slower speeds. From Model 21, whose roller rotation speed is 20 rad/s, the plastic deformation remains constant, following the expressions below:

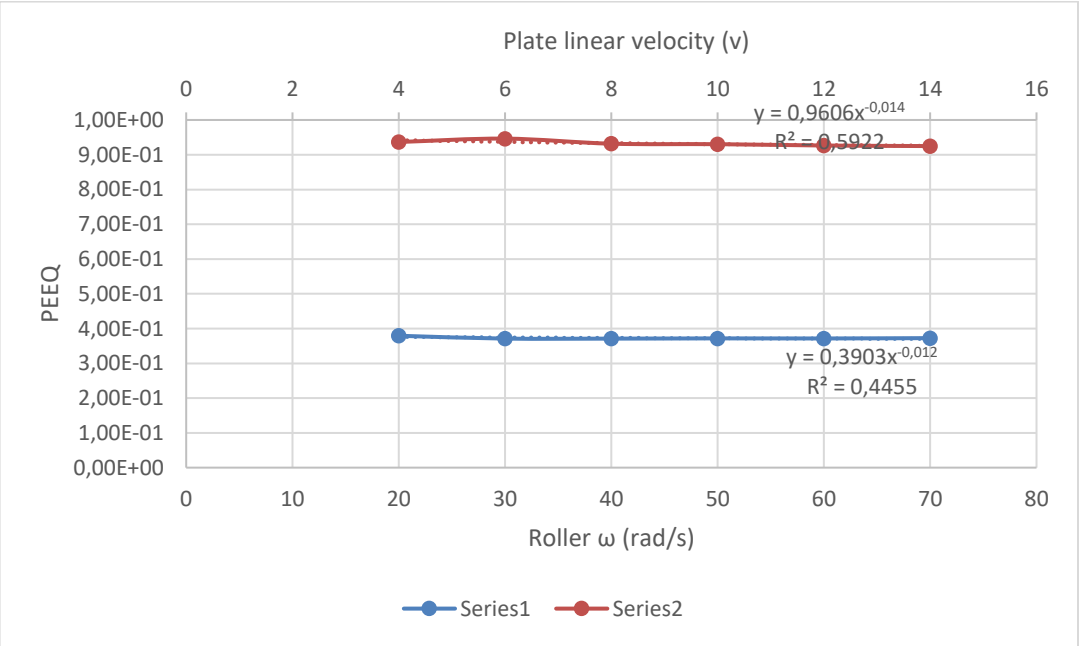

Graph 12. PEEQ results for plate linear velocity and roller angular velocity variation models

For the reaction force of the roller, it remains constant in the first pass, while in the second pass it can be seen that the reaction force increases for low speeds.

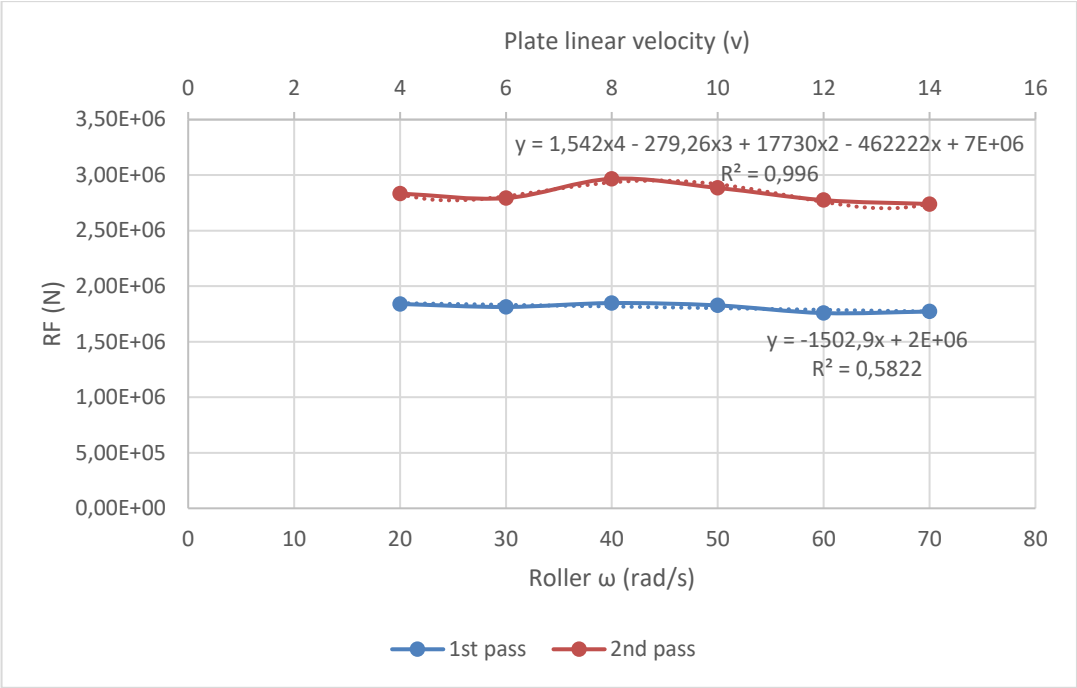

Graph 13. RF2 results for plate linear velocity and roller angular velocity variation models

Regarding the ΔT obtained, it can be noted that for different speeds it remains almost constant in the first pass. However, in the second pass, the temperature increases more with for higher velocity. This increment is logarithmical, indicating that the higher the speeds, the less this effect is. The temperature increases more for each pass as the linear velocity is higher and the surface of the plate has less time to disipate the heat of the surface to internal nodes, leading to a higher surface temperature in the second pass.

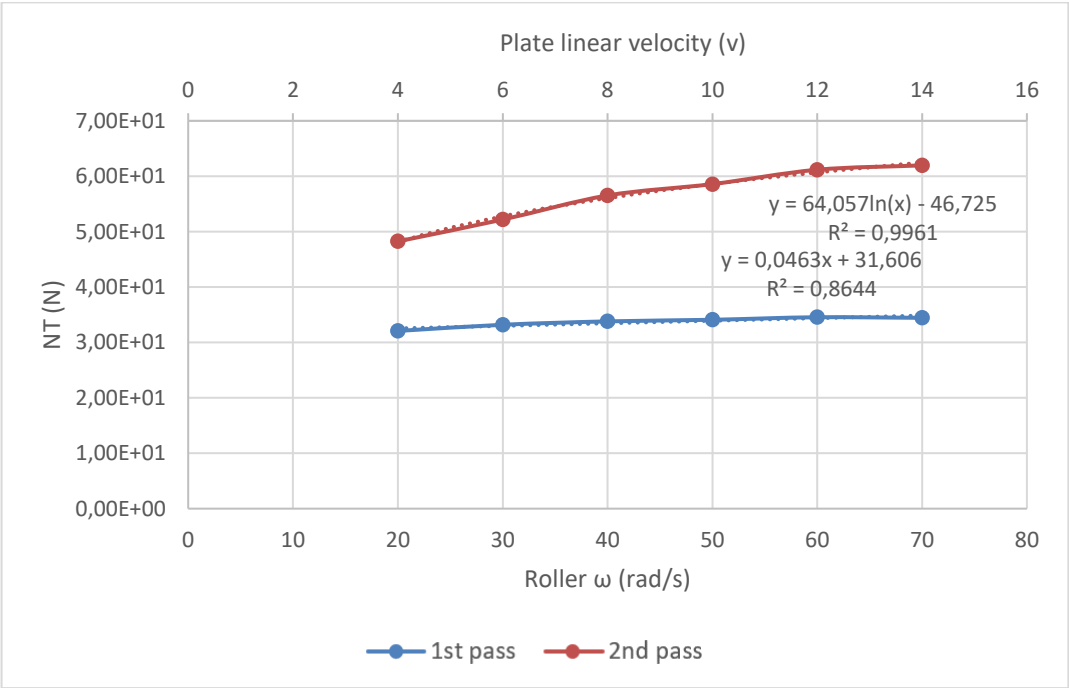

Graph 14. NT results for plate linear velocity and roller angular velocity variation models

5.6 Al2024 simulation

Model 25 is run to analyse the behaviour of an aluminum plate. Linear velocity of the plate selected is 4m/s and roller angular velocity is 20 rad/s. Plate material is changed and the rest of the model set up is mantained as it was for velocity parametric analysis.

The Aluminum Al2024-T3 alloy is used for this model as the plate material. It is a moderately strong and corrosion resistant aluminum-based material. The material is commercially pure aluminum that is aged, or oxidized to produce an alloy with mechanical properties that are better than those of commercially pure aluminum. The most common form of this alloy is sheet stock that is suitable for use in applications such as aircraft skins. It is also useful for the manufacture of brackets, supports and fittings Some variants of this material also have excellent weldability characteristics, which make them well-suited for use in a variety of welding processes. The most commonly used variants are alloys with a composition of between 90.7% and 94.7% aluminum, with the remaining percentage being composed of mainly chrome, copper, manganese, iron, and magnesium.

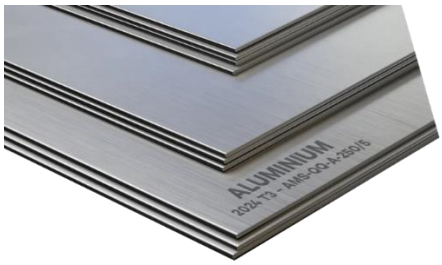

Figure 57. Al2024-T3 [33]

Component	Weight %
Al	90.7-94.7
Cr	Max 0.1
Cu	3.8 – 4.9
Fe	Max 0.5
Mg	1.2 – 1.8
Mn	0.3 – 0.9
Si	Max 0.5
Ti	Max 0.15
Zn	Max 0.25
Other, each	Max 0.05
Other, total	Max 0.15

Table 20. Al2024-T3 Composition. The Wt% are not fixed values, they vary depending on the properties intended to enhance [34]

The mechanical properties to be taken into account to compare the simulation results with the analytical ones are:

Mechanical property	Magnitude
Density	2780 kg/m^3
Tensile ultimate strength (σ)	483 MPa
Young modulus (E)	71700 MPa
Tensile yield strength (Y)	350 MPa
Conductivity	121 W/mK
Specific Heat	875 J/Kg ºC

Table 21. Mechanical properties of the material [34]

Stress strain curve of this material is introduced to the model, describing the elastic and plastic behaviour of the plate is the following:

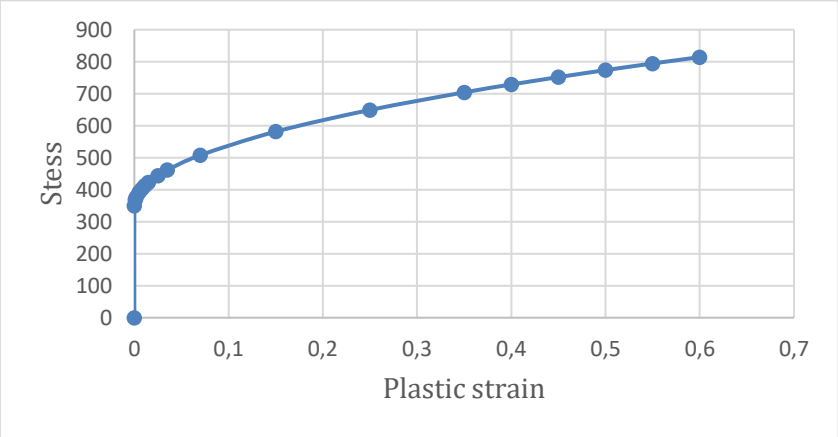

Graph 15. Al2024-T3 Strss vs Plastic Strain curve introduced in Abaqus

The following shows how plastic strain and temperature vary throughout the process.

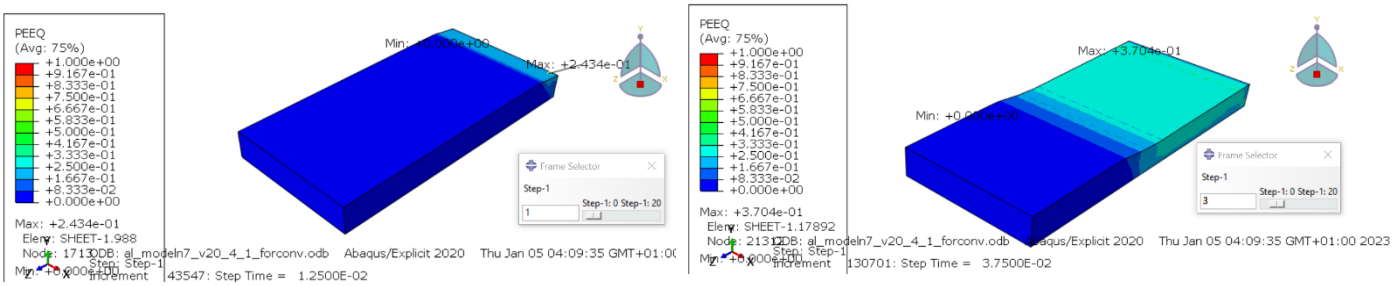

Figure 58. PEEQ for timeframes 1 and 3

For timeframe 5, the first pass is completed, and at this point, the whole plate is deformed plastically, reducing the thickness of the plate from 2E-02 to 1.2E-02 meters (please refer to Annex 5). For timeframe 11, second pass has started:

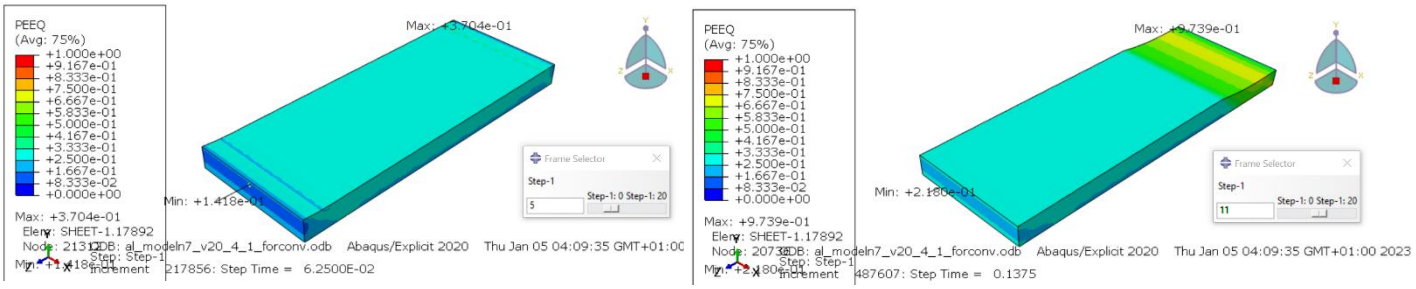

Figure 59. PEEQ for timeframes 5 and 11

During timeframes 13 and 15, the second pass is completed:

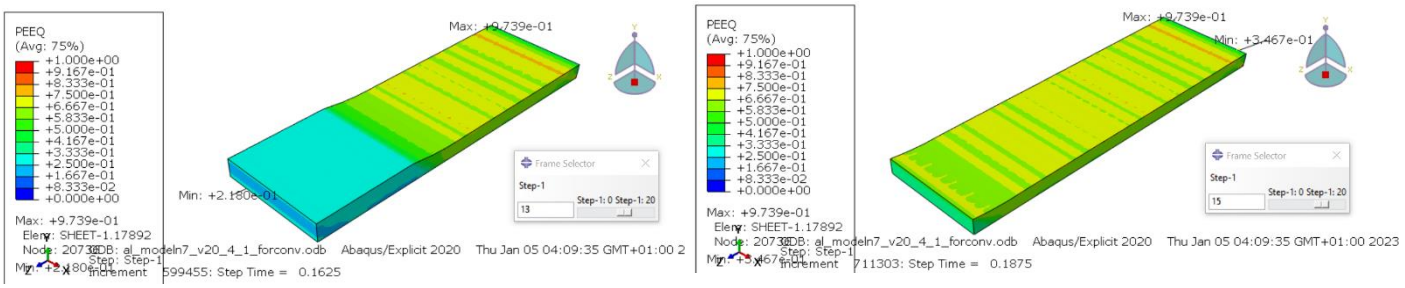

Figure 60. PEEQ for timeframes 13 and 15

After the second pass, the width of the plate is 1.2E-02 m. The elongation of the plate is 1,32E-02m. Please refer to Annex 5.

The evolution of maximum PEEQ is represented in the following graph:

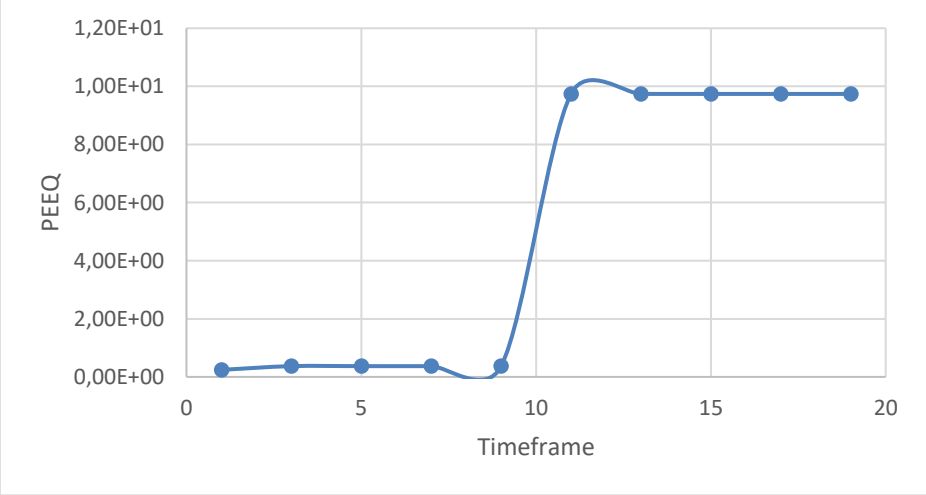

Figure 61. PEEQ vs time

Max PEEQ is mantained constant during first and second pass, which means that there is stability on the model and there is not relevant dynamic effects.

Evolution of temperatures are presented below. The scale has been changed to a maximum of 150K temperature increment, given that for this velocity set up, temperature increment is not high. For timeframes 3 and 5 first pass in completed.

In the last section of the plate, temperature is higher as part of the heat is transmitted from the inflow section of the plate which is worked first.

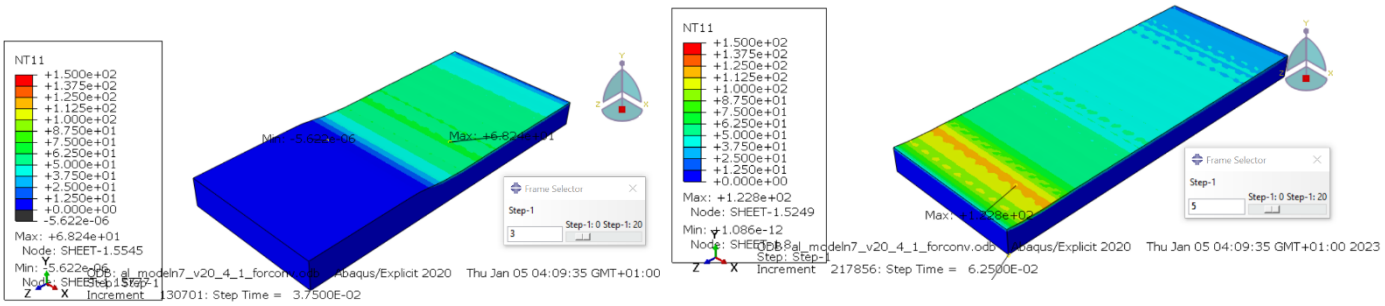

Figure 62 Temperature increment for timeframes 3 and 5

Here this effect can be appreciated even more clearly for timeframe 6, when the outflow section of the plate is worked by the roller. A maximum temperature increment of 432.3k is achieced. Part of this heat is due to the friction with the roller but part is due to conduction from sections of the plate that were heated before. On timeframe 10, an instant before coming into contact with the second roller, it can be seen that at the outflow section of the plate that part of the heat has been transmitted from the surface to internal nodes of the plate. This way, surface temperature gets lower between timeframes 6 and 10.

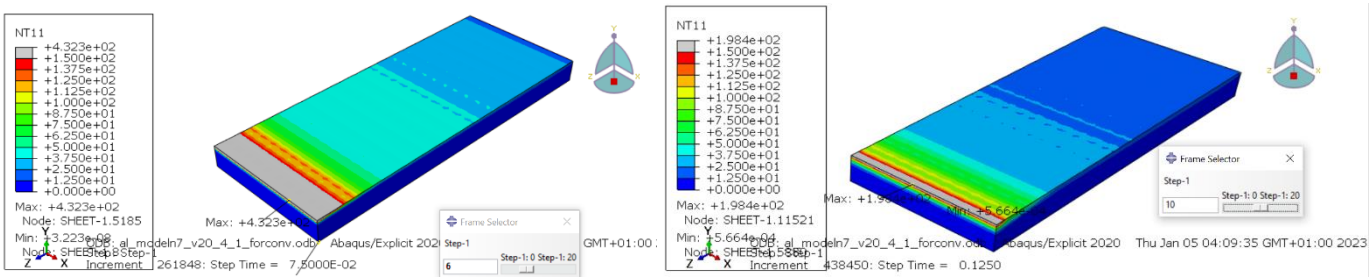

Figure 63 Temperature increment for timeframes 6 and 10

During the second pass, surface is heated again. Higher temperatures tend to accumulate at the plate surface outflow edge because heat from already worked zones is conducted to neighbour nodes.

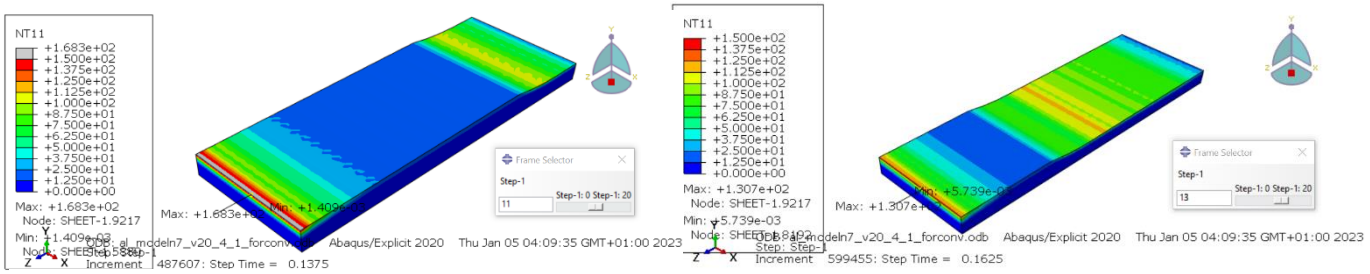

Figure 64 Temperature increment for timeframes 11 and 13

It can also be seen how internal nodes temperature increase.

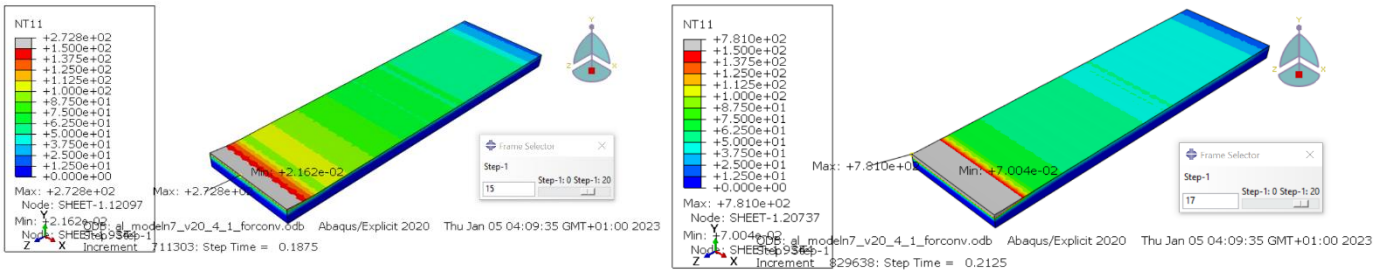

Figure 65 Temperature increment for timeframes 15 and 17

During this process, the roller is also heated. Heat generation in the roller depends on the deformation. For this reason, as the roller has an elastic modulus 29.3 times the elastic modulus of the plate, the roller has considerably less deformation and temperature increase is lower than the plate. Using a scale of a maximum of 50K value to appreciate the temperature change, following temperature maps are obtained for first and second pass:

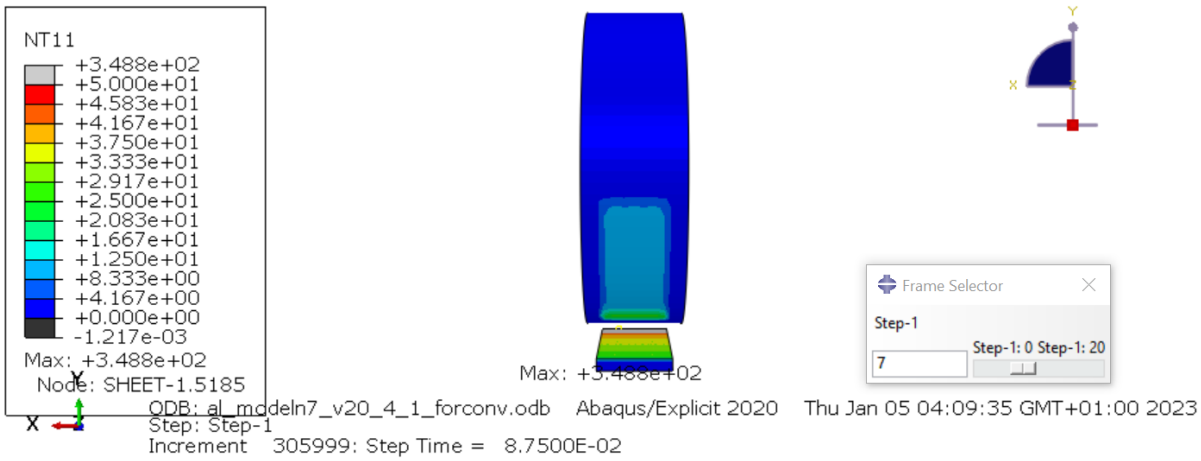

Figure 66. Roller temperature map at timeframe 7

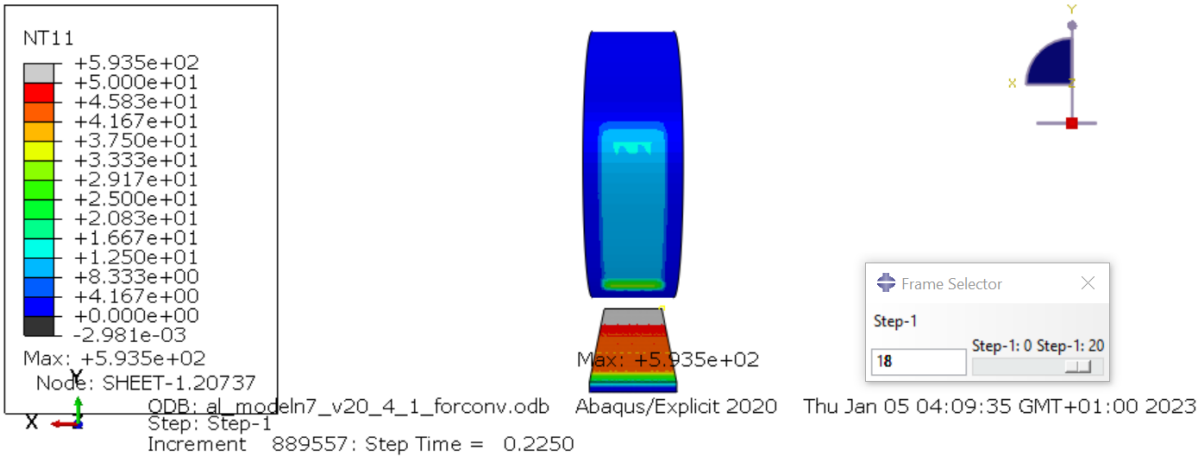

Figure 67. Roller temperature map at timeframe 18

Temperature increment is almost constant for most of the plate surface, but, at the outflow, due to the higher temperature of the plate, higher temperature is transmitted to the roller.

Chapter 6. Conclusions and future work

6.1 Conclusions

From the results obtained, conclusions can be drawn regarding the effect of speed on how a material deforms. It can also be seen that both roller and plate speeds have an effect on the thermal behavior of the plate. Temperature variations (ΔT) that occur when the process is carried out at different speeds have been calculated, and the models used suits the intended parametric analysis, being these methodology for simulating metal rolling process applicable to both cold rolling and hot rolling process and for any material.

6.1.1 Mechanical behaviour

Taking Al2024 plate model 25 to compare analytical results with the obtained in the model, it can be seen that for the first pass, the force results obtained fits with the extracted from the analytical solution. The analytical calculation of the force does not take into account the effect of the speed of the plate and the roller during the process, assuming a steady state:

$$F = \sigma_f \cdot L \cdot w$$

For Model 25:

$$\sigma_f = 8.1428E + 08\ Pa$$

$$L = 3.16E - 02\ m$$

$$w = 0.1\ m$$

The analytical solution is:

$$F = \sigma_f \cdot L \cdot w = 2.57\text{E} + 06N$$

For the simulation of Model 25, with a roller rotation speed of 20 rad/s and a plate linear speed of 4 m/s, a simulated reaction force of 2.56E+06 N is obtained.

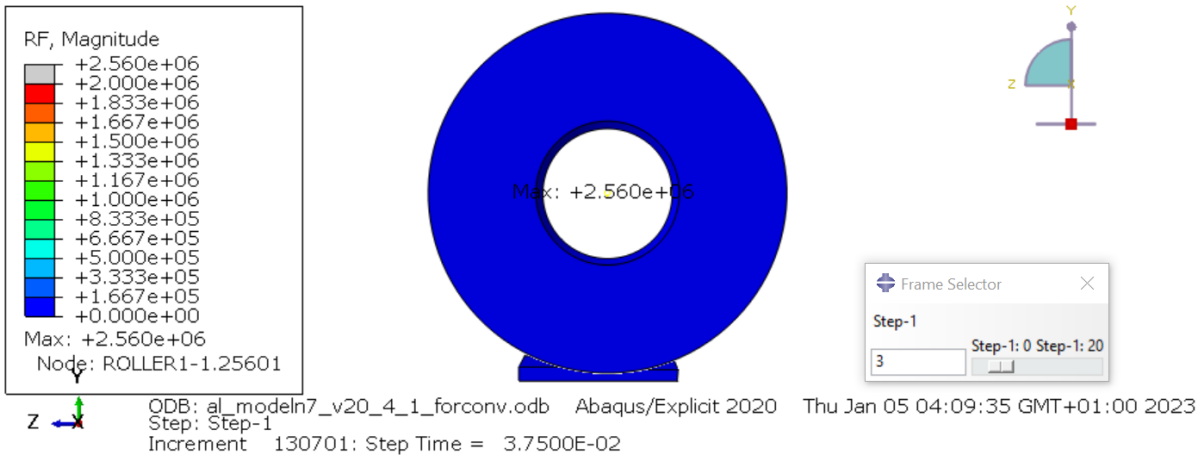

Figure 68. Reaction force obtained from numerical model

This shows that the model is obtaining accurate results. For the first pass the reaction force must remain almost constant. Nevertheless, in some models it may defer because the plate enters the roller with a certain linear velocity, there are stresses generated by this collision between the plate and the roller in the dynamic model, which are not taken into account in the case of the results obtained in the analytical solution. Reaction force is a key variable given that the friction force directly depends on it.

In these metal forming processes there is a high deformation which is produced at a relatively high speed. The effect of the strain rate is greater for greater strain, and it must be taken into account when setting up formation processes where large strains are produced in a short period of time, producing relevant residual stresses in the material. This is because, usually, rolling is carried out hot, so it is necessary to carry out the process quickly enough before the plate material cools down causing relevant changes in the mechanical properties of the material. This cooling, if it is not performed at the correct velocity, could generate residual stresses in the piece.

6.1.2 Thermal behaviour

It has been verified that the heat generation due to friction and deformation, when contact between the plate and the roller occurs, is directly proportional to the difference between the horizontal displacement speed of the plate and the tangential speed of the roller at the non-slip point where contact occurs. If this velocity difference is high, the effect of friction is greater, generating a greater increase in temperatures on the surface of the plate.

This is due to the fact that the kinetic energy of a moving body is converted into thermal energy as it encounters resistance. According to the law of conservation of energy, energy can neither be created nor destroyed. In this process the kinetic energy is converted into heat, which in turn causes the plate to move into the rollers. Heat is a form of energy that is given by the temperature of the object. This form of energy is usually transferred between objects through radiation and conduction. In this case, mainly transferred by conduction from the surface to the bottom of the plate and to the roller.

When changing the angular velocity, it can be seen that the temperature rises linearly in each of the passes due to the heat generated by the friction. The greater the deformation velocity, the greater the temperature difference between the first and the second pass. In the second pass, the temperature increases even more with respect to the first pass, generating a high ΔT, which indicates that depending on the initial temperature and the material of the plate, the temperature at the surface of the plate can be above the melting temperature at some point in the process.

The same effect is shown when changing the plate linear velocity, for higher difference between roller tangential velocity at contact point an plate linear velocity, the effect of the friction is higher and thus, the heat generation is also higher because there is more kinetic energy transformed to thermal energy.

On the other hand, it has been verified that if the horizontal speed of the plate and the rotation speed of the roller are varied simultaneously, the temperature increase remains constant for each of the models in the first pass. In the second pass, the temperature increases are greater as process speeds increase due to the specific effect of linear speed. Since between 1st pass and 2nd pass, the slower the horizontal displacement speed of the plate, the greater is the time for the heat to be transmitted to the neighbor nodes to the surface of the plate. Therefore, part of the heat generated is dissipated towards interior nodes so that the temperature increase is greater for slower linear velocity.

The results obtained are satisfactory from an academic point of view. In this project, the objective was to develop an explicit model with thermal coupling to study how the metal rolling process behaves depending on the speed at which it is carried out. The results obtained are reasonable to study these parameters.

In each of the models there are peaks in some magnitudes and specific elements due to the quality of the mesh, whose dimension is limited by the performance of the computer used for the analysis. However, the results obtained, from the academic point of view, are suitable to draw certain conclusions and it has been possible to demonstrate the relevance of the rolling speed during a manufacturing process. Therefore, it can be confirmed that there is a balance between configuring a simulation fast enough to be carried out on a mid-range laptop and obtaining results that are relatively accurate and adjusted to a real model.

The use of this type of simulation of manufacturing processes saves material, energy and time in carrying out experimental tests, but it does not exempt us from them. In order to verify the veracity of these results, it is necessary to carry out experimental tests, which allow the generation of models and patterns of behavior to be introduced later into a simulation software to predict the performance of the process for different scenarios.

6.2 Future work

During the metal forming process, there is a friction between the roller and the metal sheet that generates heat, producing an increase in temperature both in the roller and in the plate. This increase in temperature alters the mechanical and thermal behaviour of the material, causing thermal expansion. Therefore, the best way to approach our case study is using a coupled thermal-mechanical displacement model.

The control of thermal properties in sheetmetal forming is important to ensure dimensional accuracy and to minimize energy consumption during the forming operation. Thermal properties of the sheetmetal material can be adjusted by using different raw materials or by applying heat-treatments to the sheetmetal during fabrication. The thermal properties of a metallic sheet are influenced by various factors, including the composition of the alloy, the presence of impurities in the alloy, and the thermal history of the metal prior to being formed. Metal forming operations such as forging, bending, and deep drawing result in the formation of permanent residual stresses within the workpiece. These stresses arise from the elastic and plastic deformations of the workpiece as it is heated by the process of forming. As the process continues, the material is repeatedly stretched and subsequently compressed by the roller, resulting in the accumulation of stress inside the workpiece. Once the desired shape has been achieved, these stresses remain in the part and can cause serious problems with part performance and reliability if the stresses are not properly controlled during manufacture.

Furthermore, controling cooling rate is particularly important in processes where material deformations are severe and tend to cause significant internal heating. In rolling operations involving thick sheets (i.e., those thicker than about 15 mm), the metal is heated significantly while it is being rolled. It is therefore necessary to ensure that the temperature drop rate is kept as low as possible in order to avoid excessive heating of the material during forming. One way to achieve this is by using forced-air cooling devices that apply a constant flow of air through the surface of the material to cool it rapidly. Another way to achieve rapid cooling is to use liquids that evaporate quickly, such as water, solvents, or mineral oils.

As future work, it is proposed to simulate the same manufacturing process including material properties that vary with temperature.

ANNEXES

ANNEX 1. Steps for model generation

PARTS

- **Rollers**

First of all, rollers are created. In this case, 3D deformable solid is selected as it is intended to create minimally rigid rollers. The two rollers are created as two independent parts, both with the same dimensions and properties.

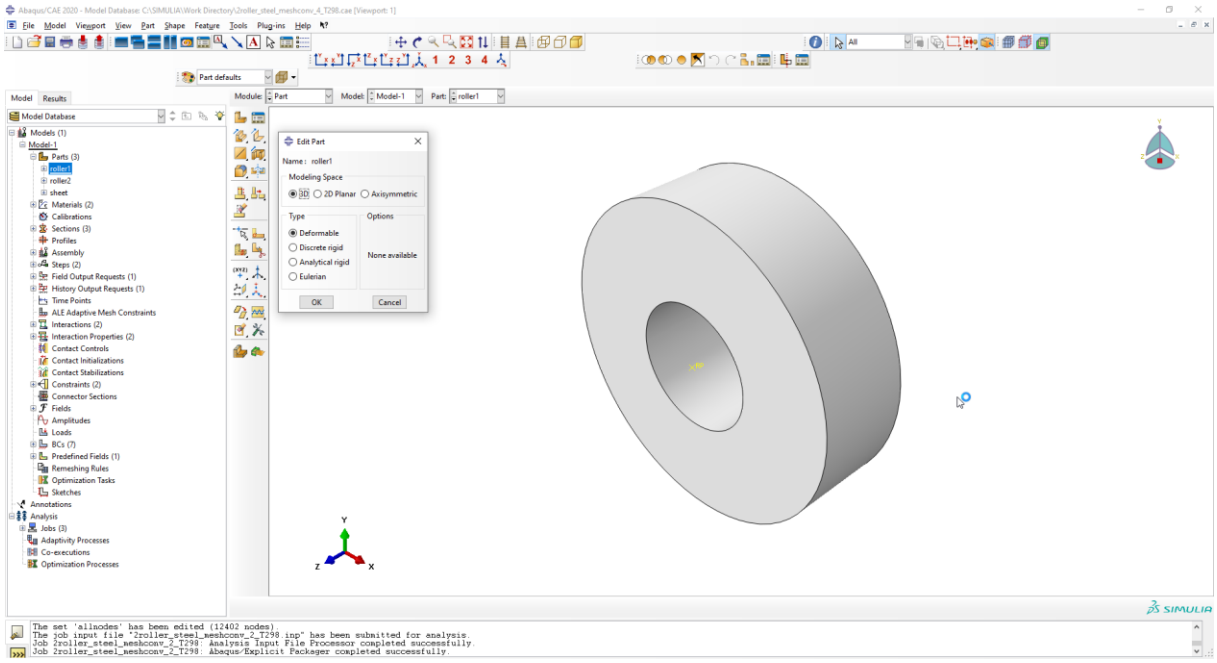

Figure 69. Roller creation

In order to create the roller, a sketch is created. The sketch consists on two concentric circumferences to create a toroidal surface.

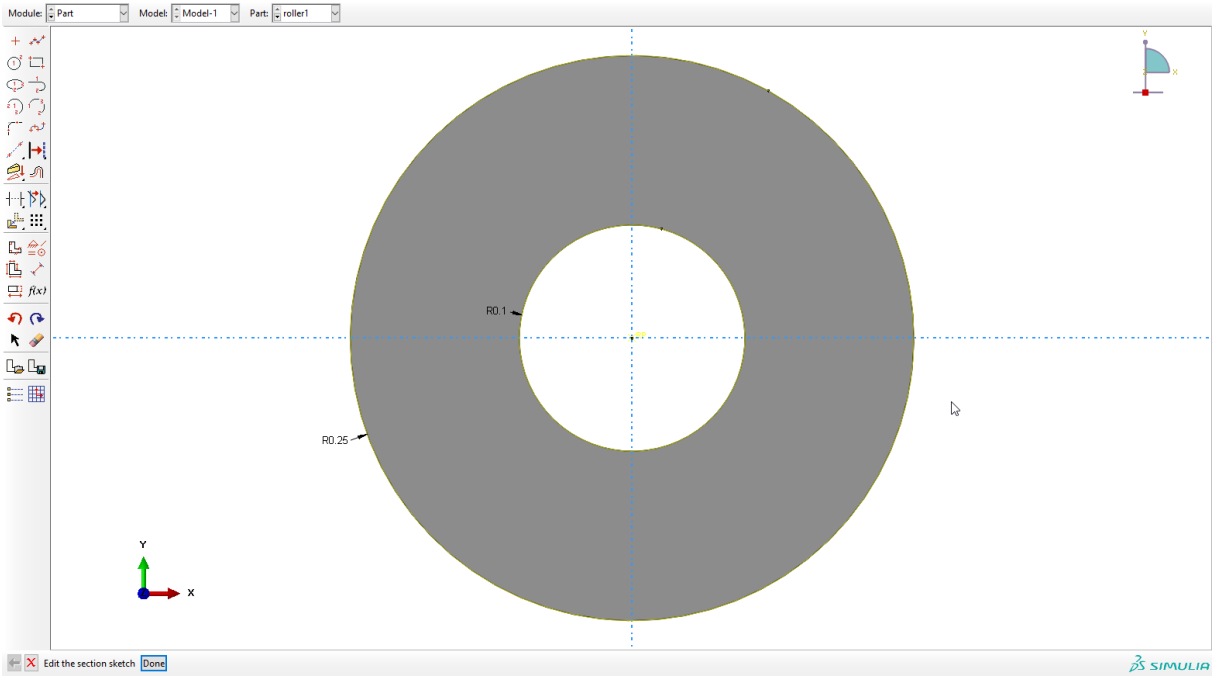

Figure 70. Rollers sketch

Part is finally created when the sketch is extruded:

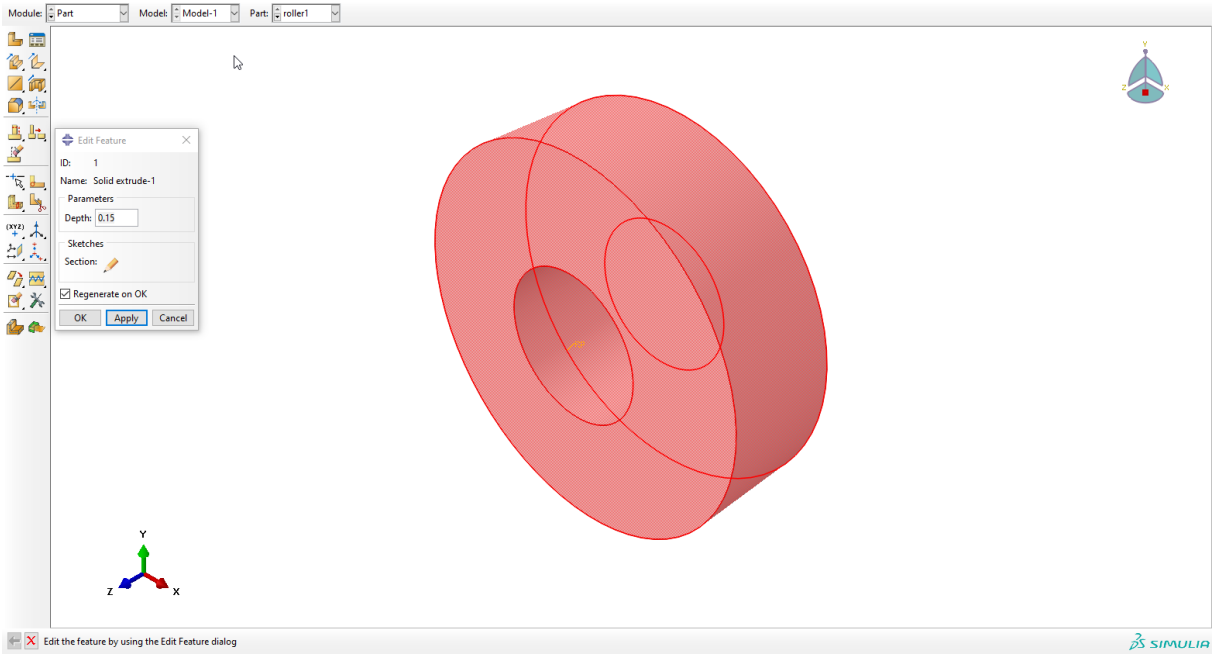

Figure 71. Roller extrussion

- **Plate**

New part is created as a 3D deformable solid.

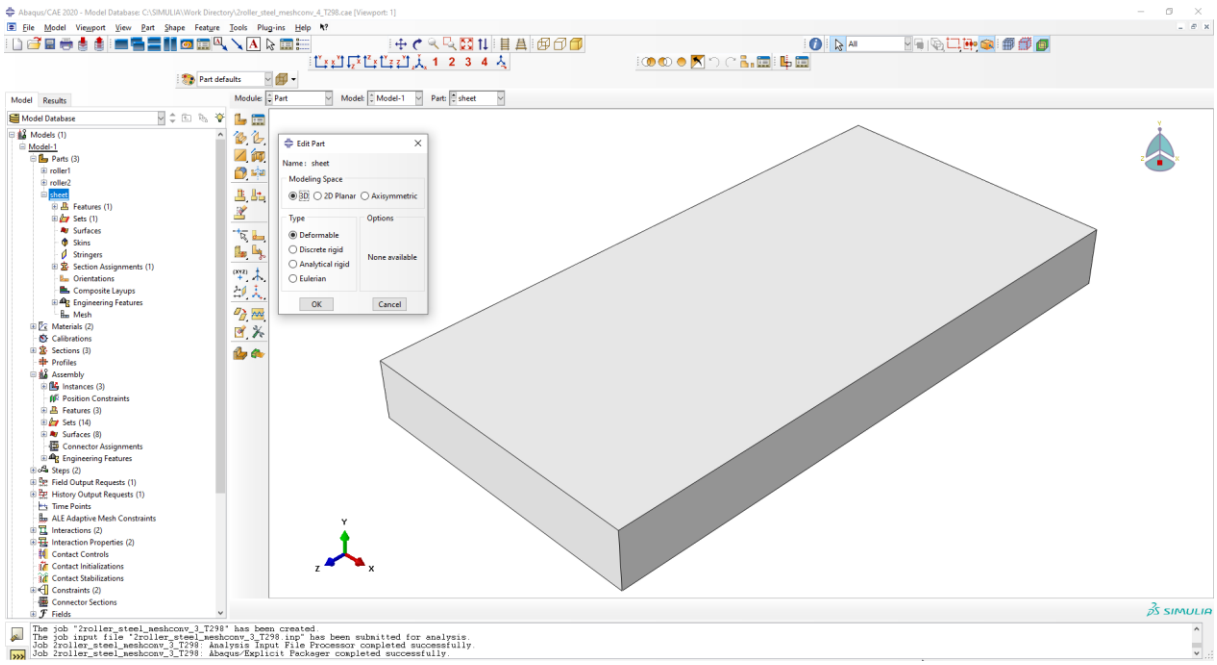

Figure 72. Plate creation

The sketch created is the following:

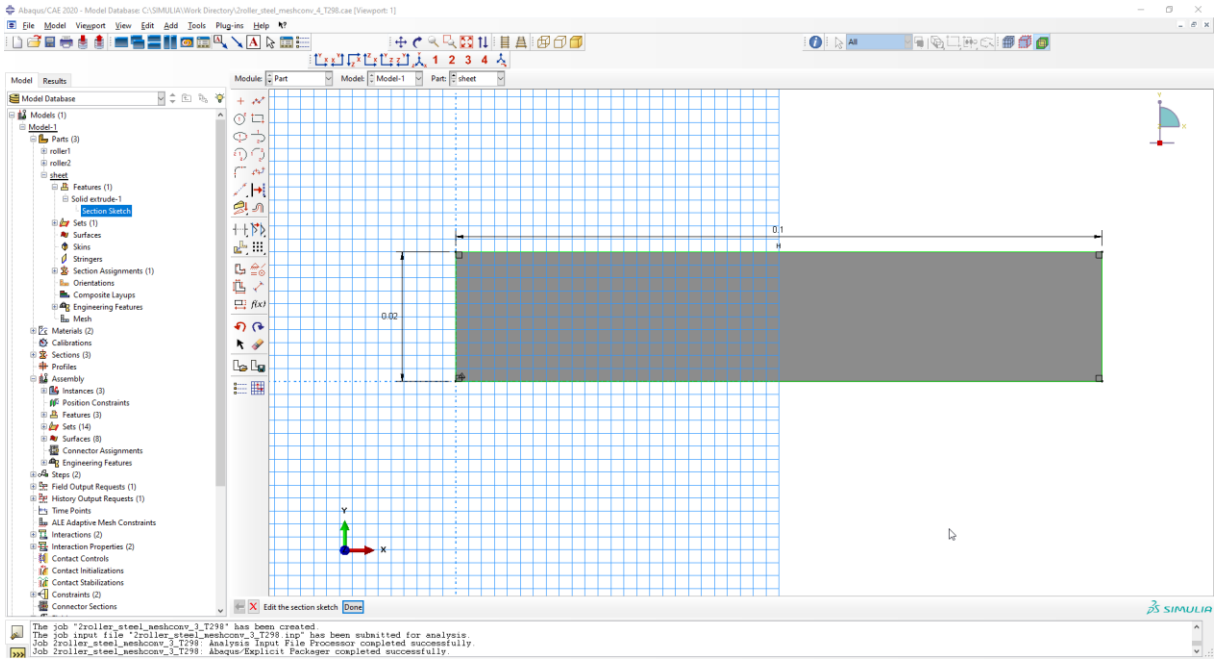

Figure 73. Plate sketch

Then, the part is extruded with 0.2 m depth:

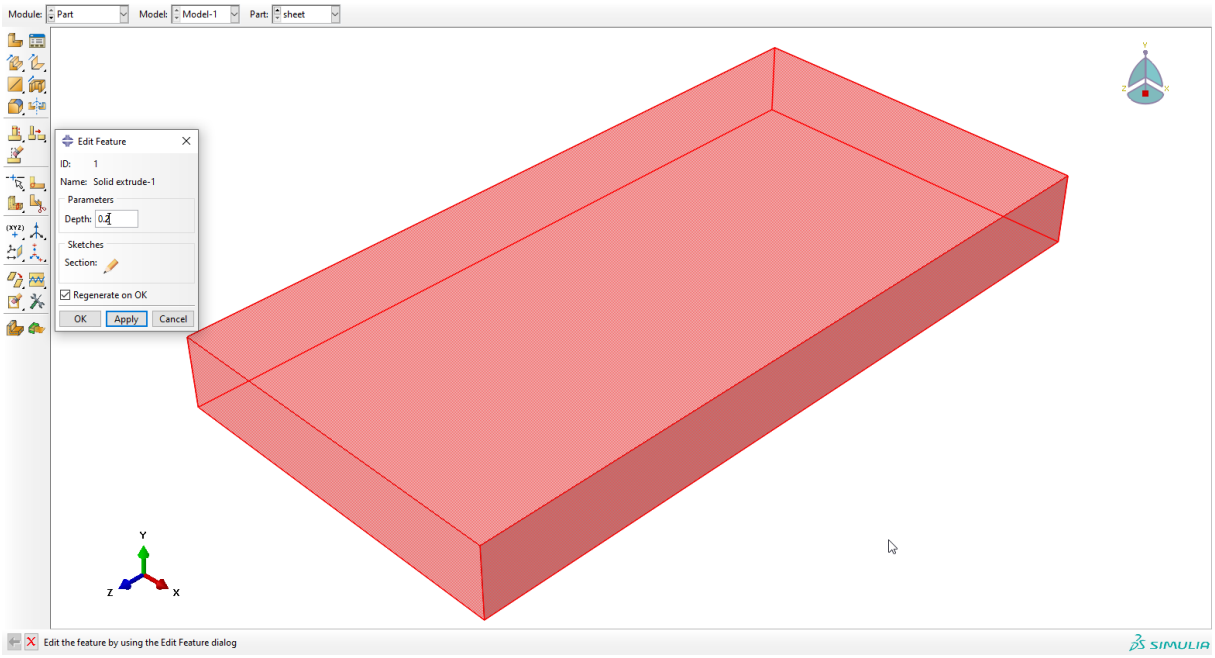

Figure 74. Plate extrussion

Material

The material created for the plate is steel. Mechanical and thermal properties are defined:

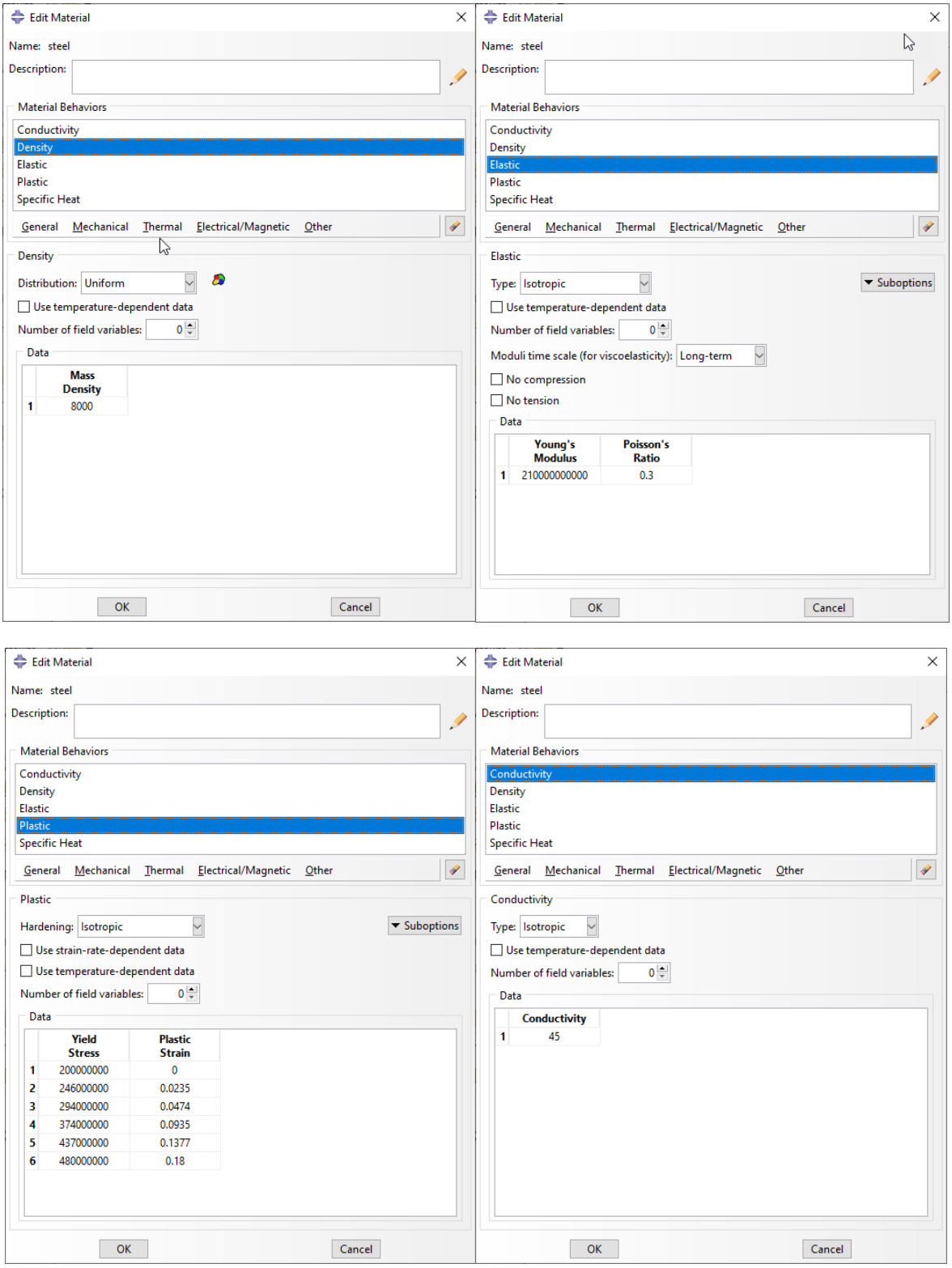

Figure 75. Steel mechanical and thermal properties

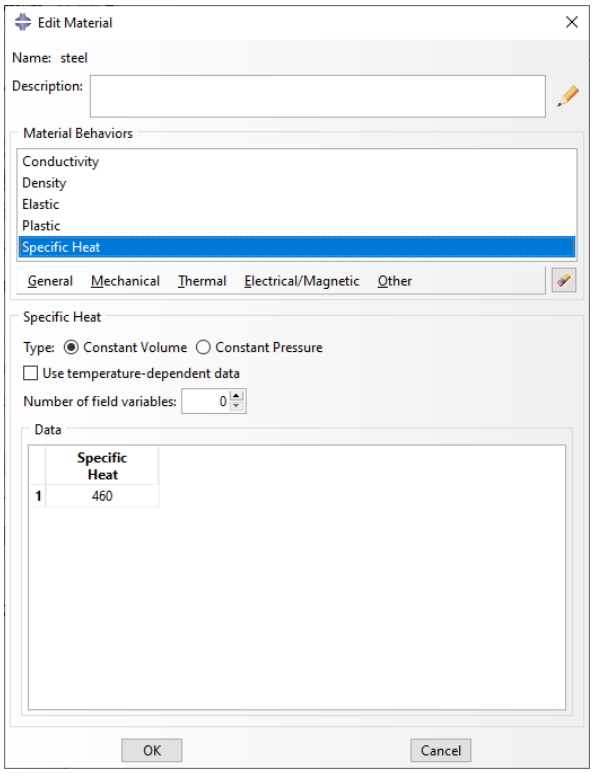

Figure 76. Steel mechanical and thermal properties

Material used for the roller is the same as the used for the plate, but increasing the Young modulus so that it is not deformed during the process. In this case, 10 times the Young modulus of the plate's steel is used.

Sections are created for later material asignation. For it, it is selected the section manager to create a section.

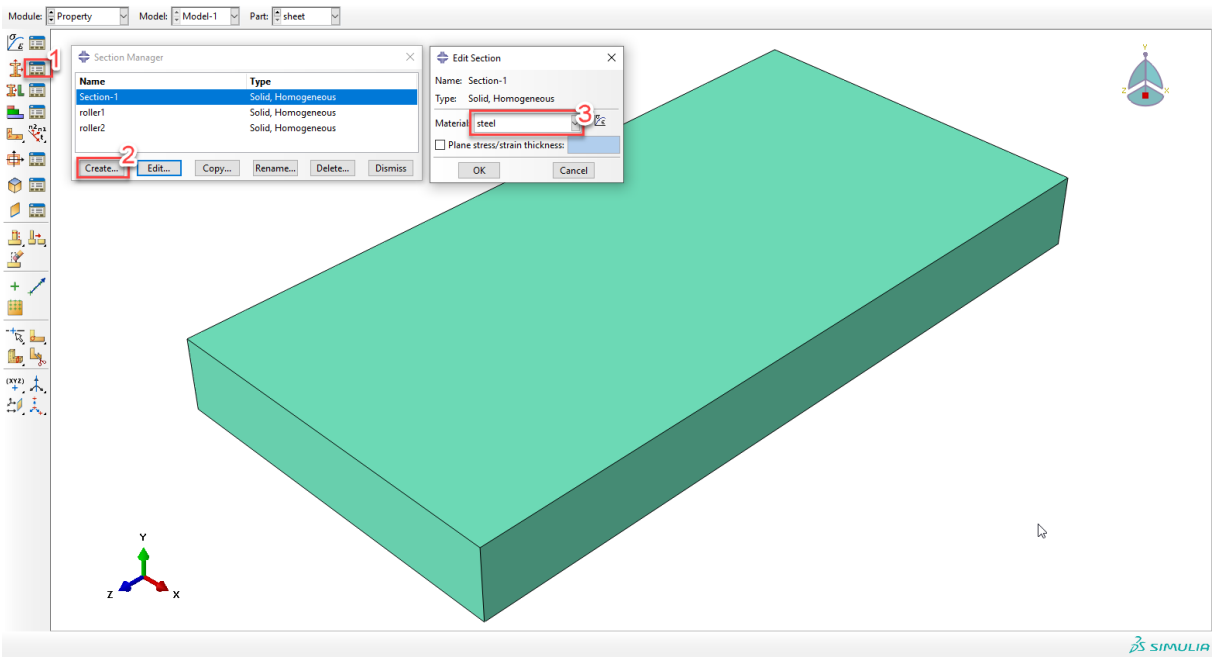

Figure 77. Plate section creation

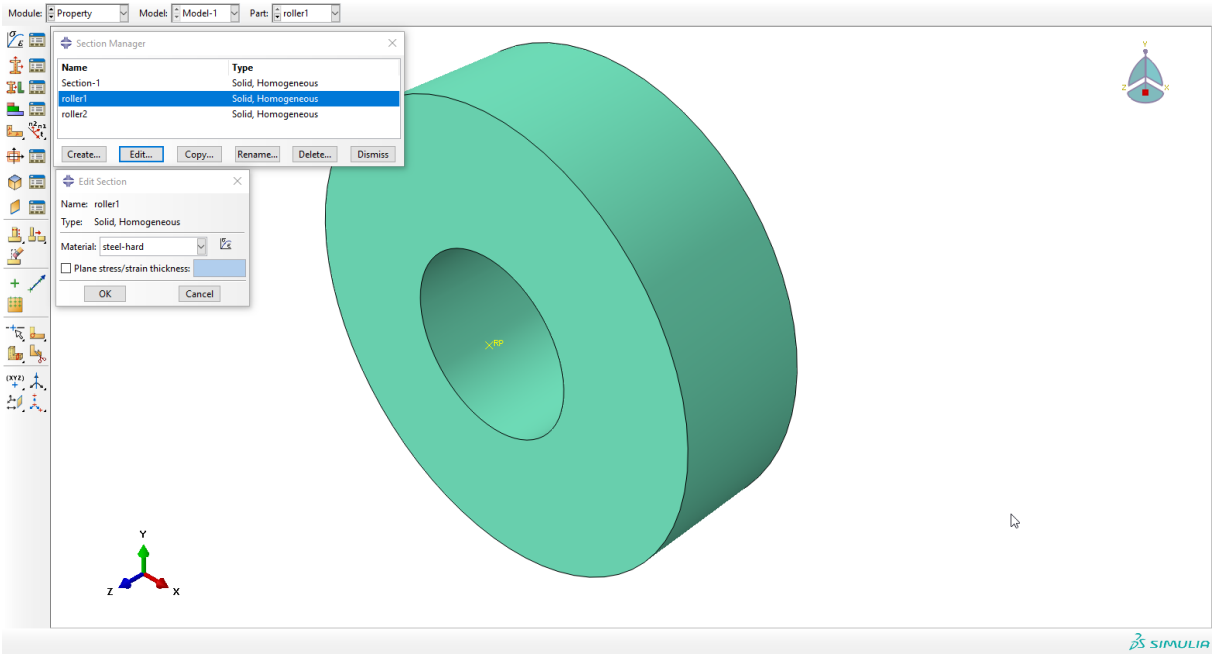

Figure 78. Roller section creation

Then, material is asigned as a property of the section. This is used to set the material properties of the each part.

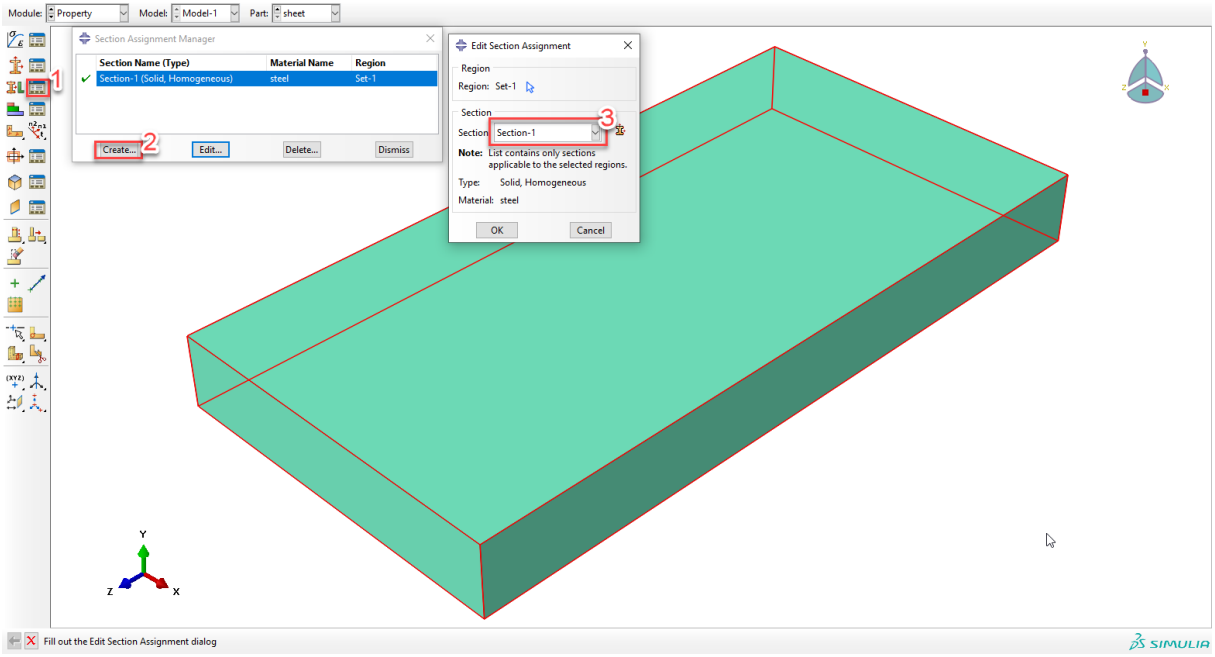

Figure 79. Material properties assignment

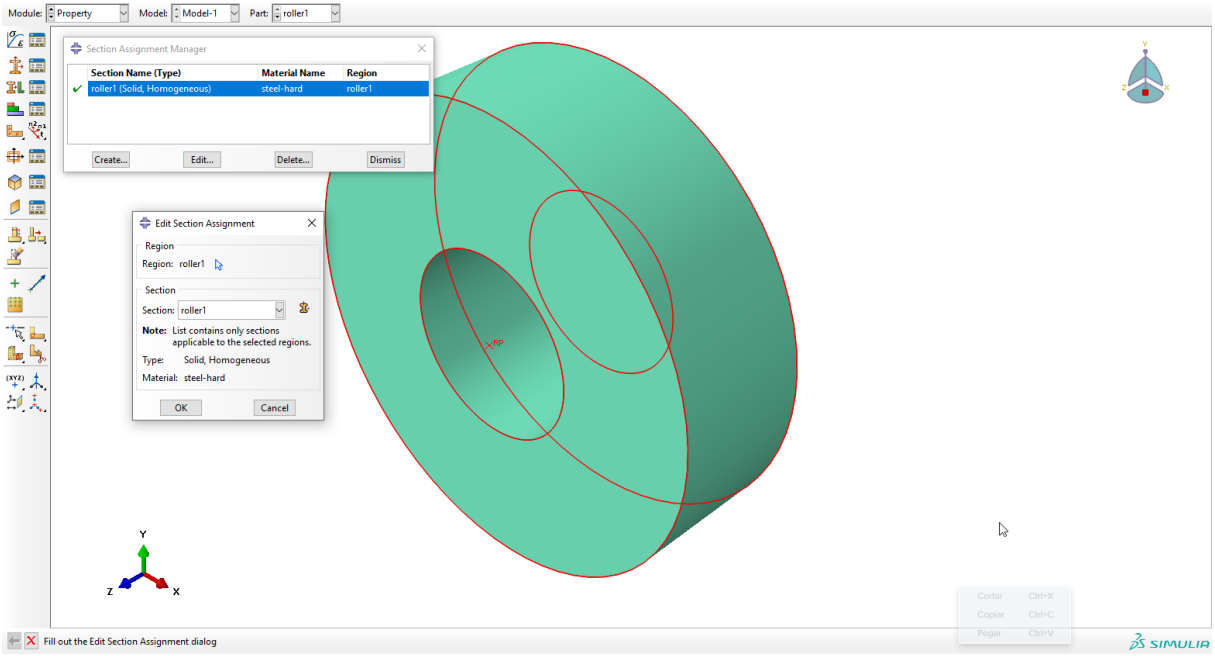

Figure 80. Likewise, material is asigned to the roller

Assembly

First, an instance is created selecting the three parts created:

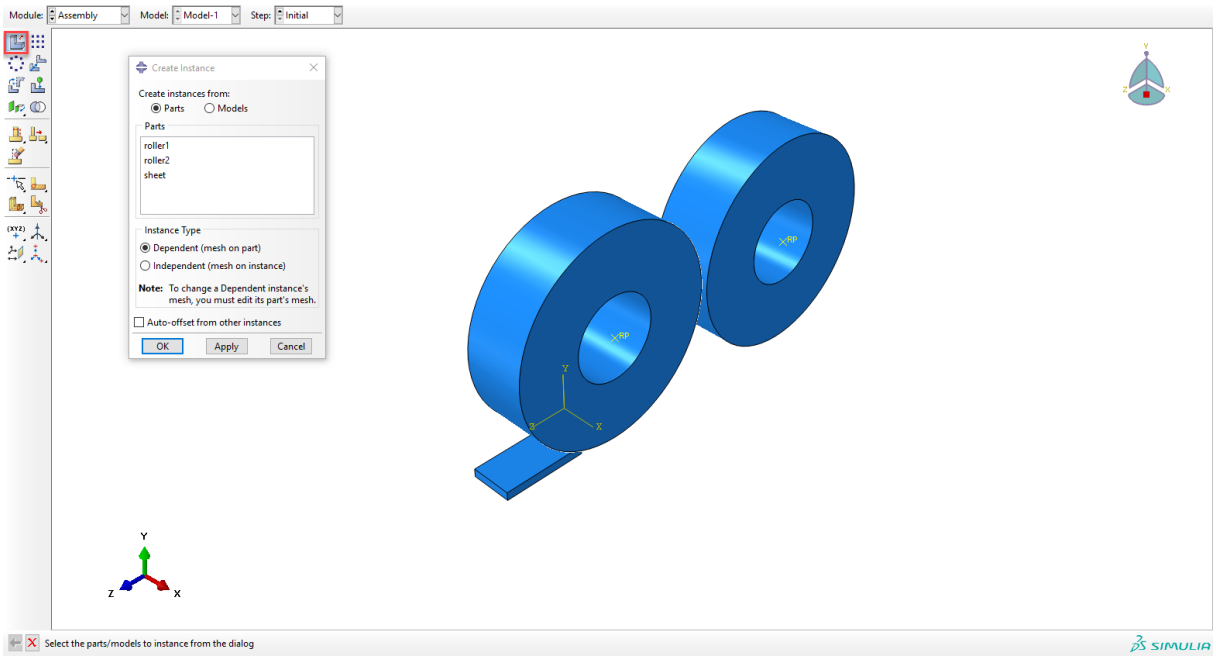

Figure 81. Instance creation

Instance translation is used to place the parts in the correct possition for the analysis. Following transformations are made:

1. Rotation of the rollers along *Y* axis 90 deg.

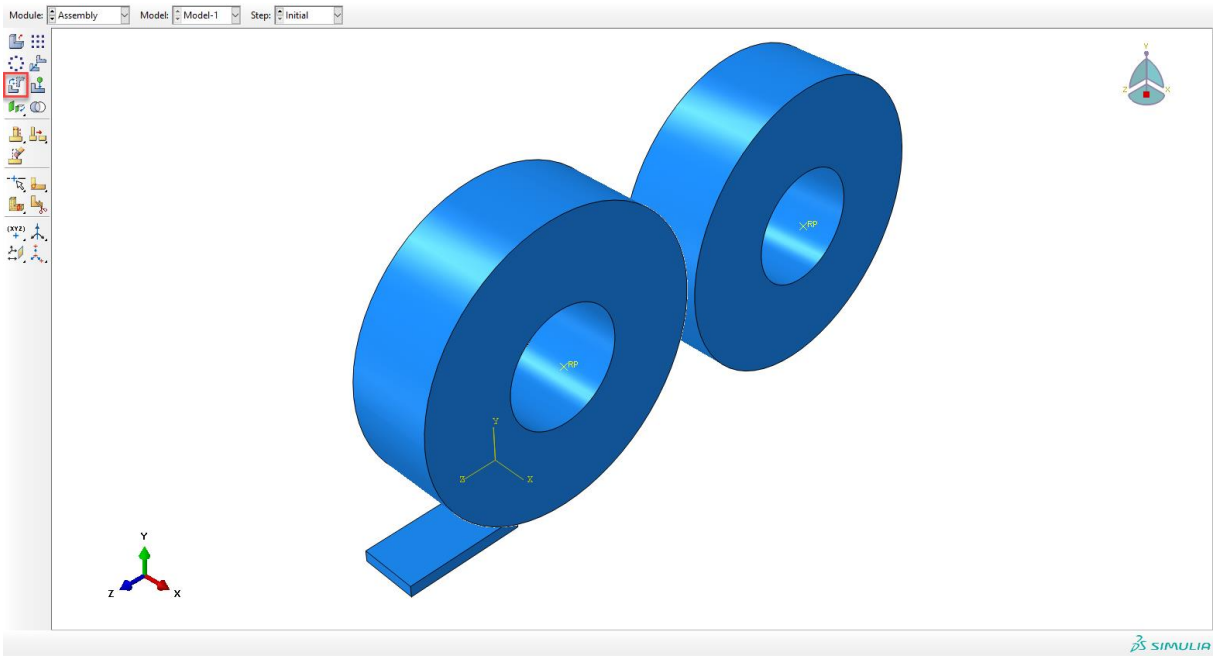

Figure 82. Rotation of the rollers

2. Roller 1: Translate (0, -0.107, 0) *(x,y,z)*
3. Roller 2: Translate (0, -0.105, -0.205) *(x,y,z)*
4. Plate: Translate (0.025, 0, 0.025) *(x,y,z)*

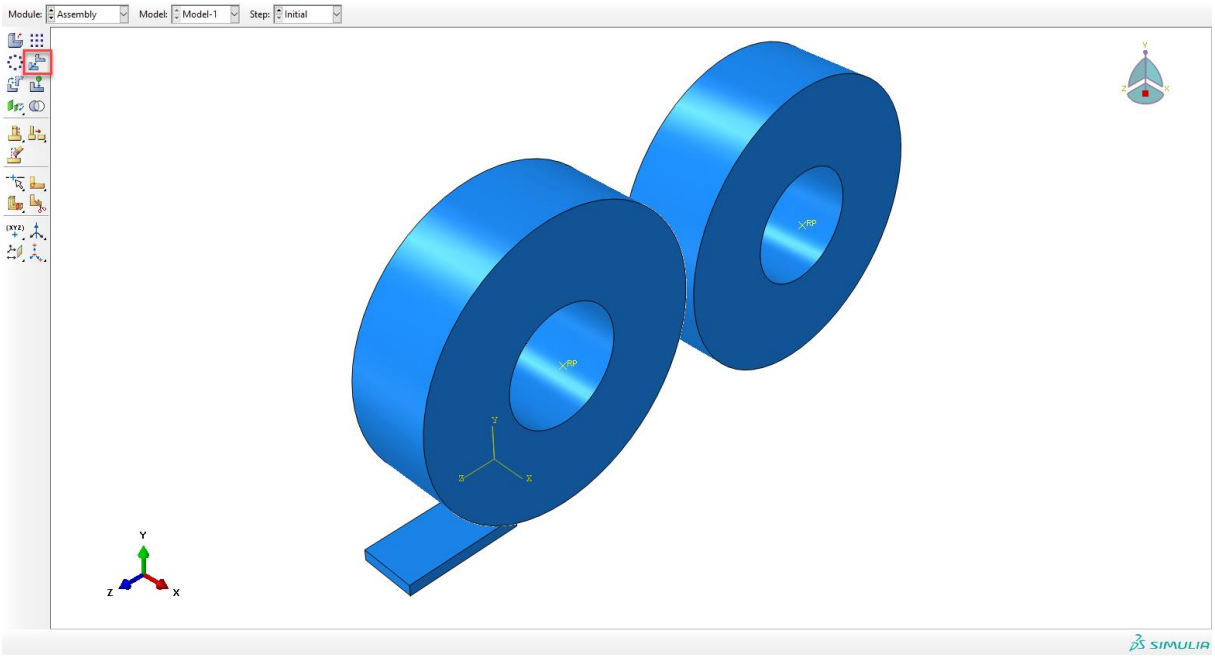

Figure 83. Translation of the rollers and the plate

Reference point associated to the roller is created.

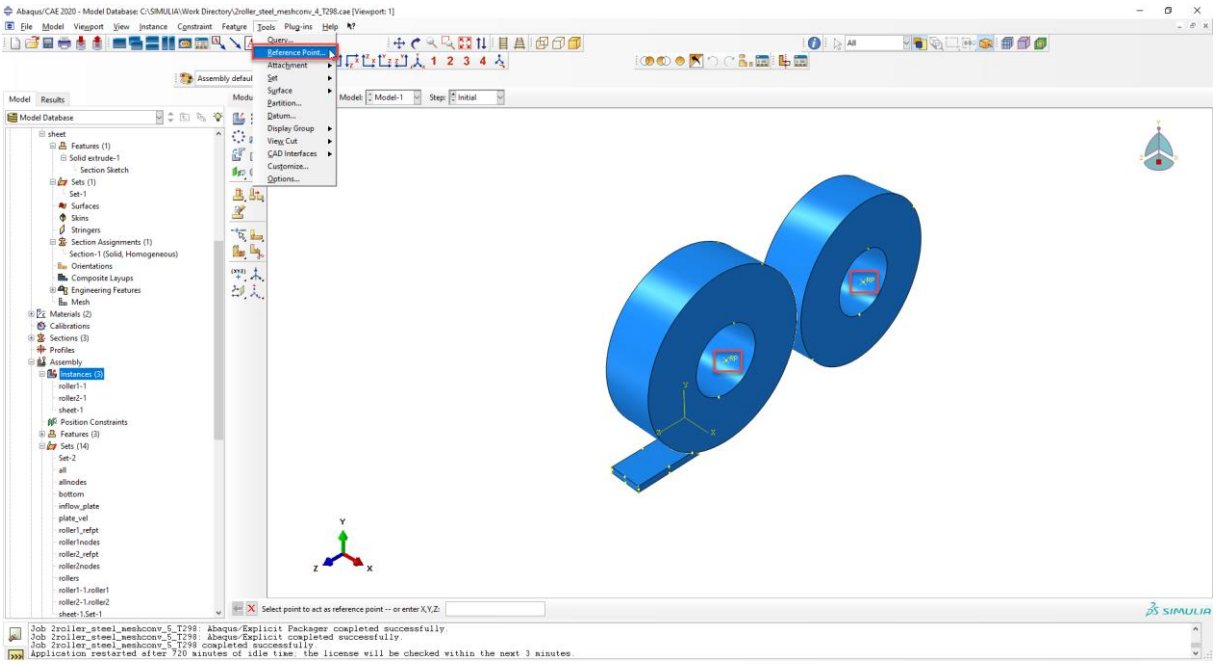

Figure 84. Rollers' reference point

Meshing

To mesh the plate and the rollers, we select the module Mesh and seed part is selected. Approximate global size is adjusted until getting the desired number of elements along the cross section of the part. Mesh of the rollers and the plate are configured in the same way.

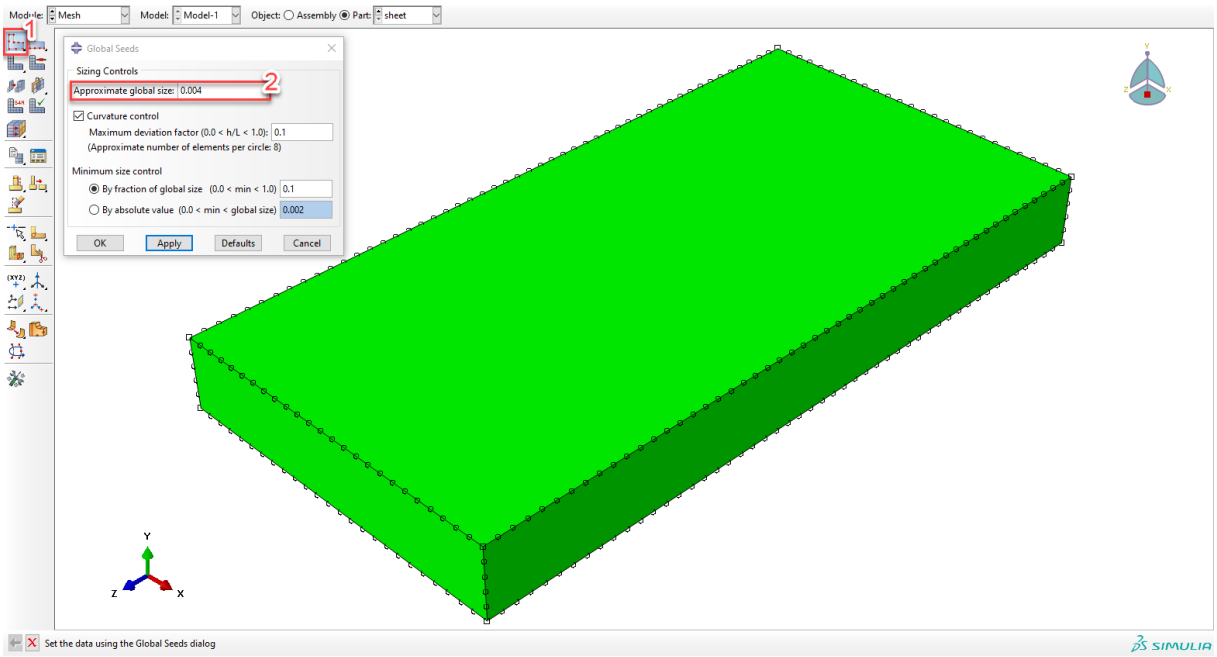

Figure 85. Global seeding

Mesh is created:

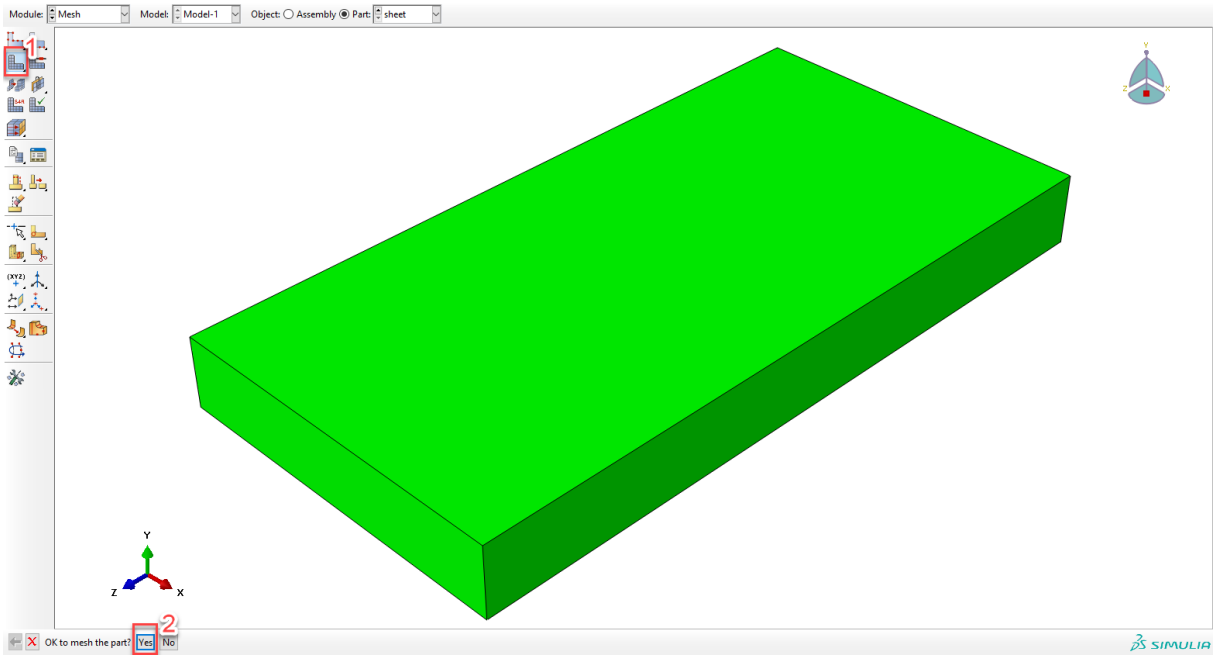

Figure 86. Plate meshing

Element type is selected. In case of the plate, as well as the roller, Explicit-Coupled Temperature Displacement linear elements (C3D8T) are used.

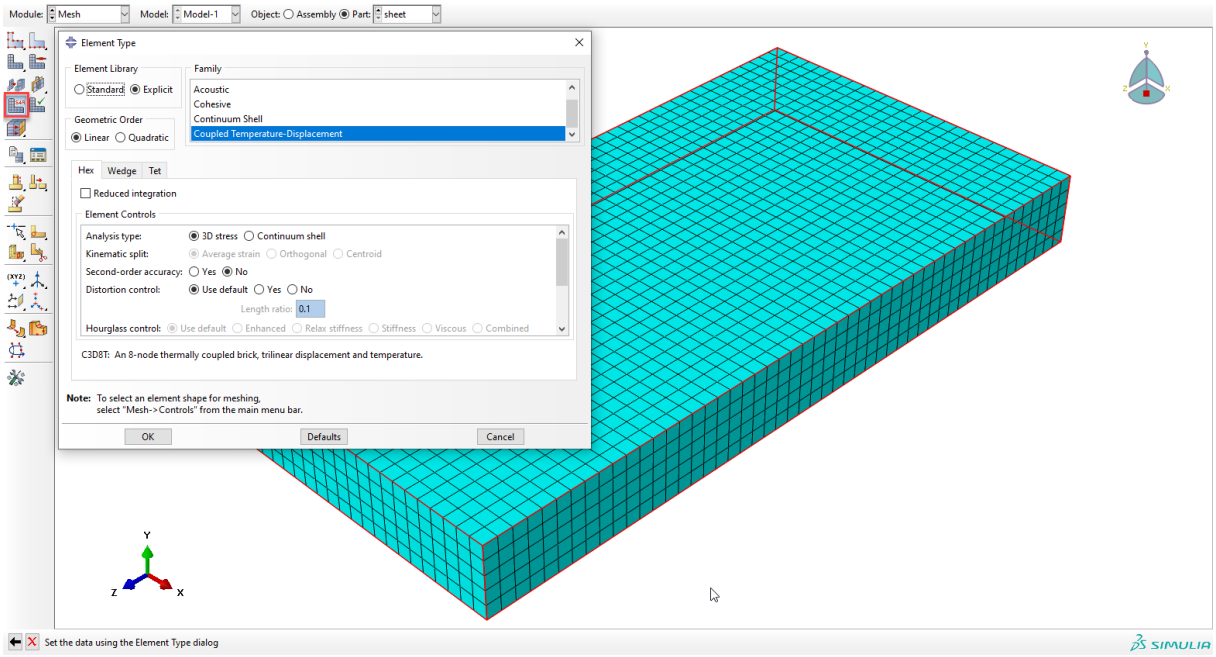

Figure 87. Plate meshing

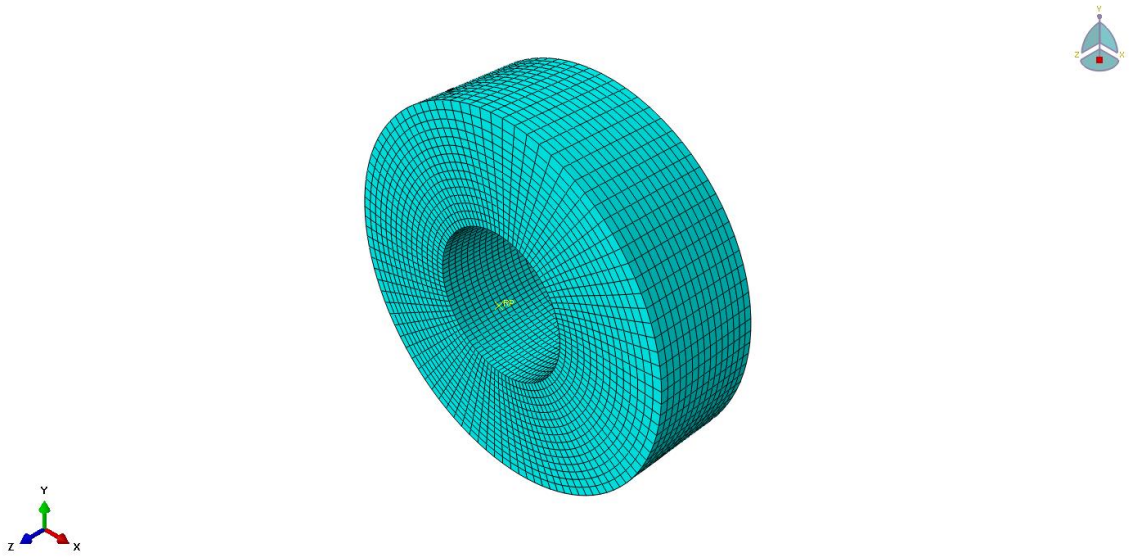

Figure 88. Mesh of the rollers

Interaction

Interation properties are created, to determine the contact between surfaces. Surface-to-surface contact is selected and penalty contact method is defined between surface of the rollers and the plate.

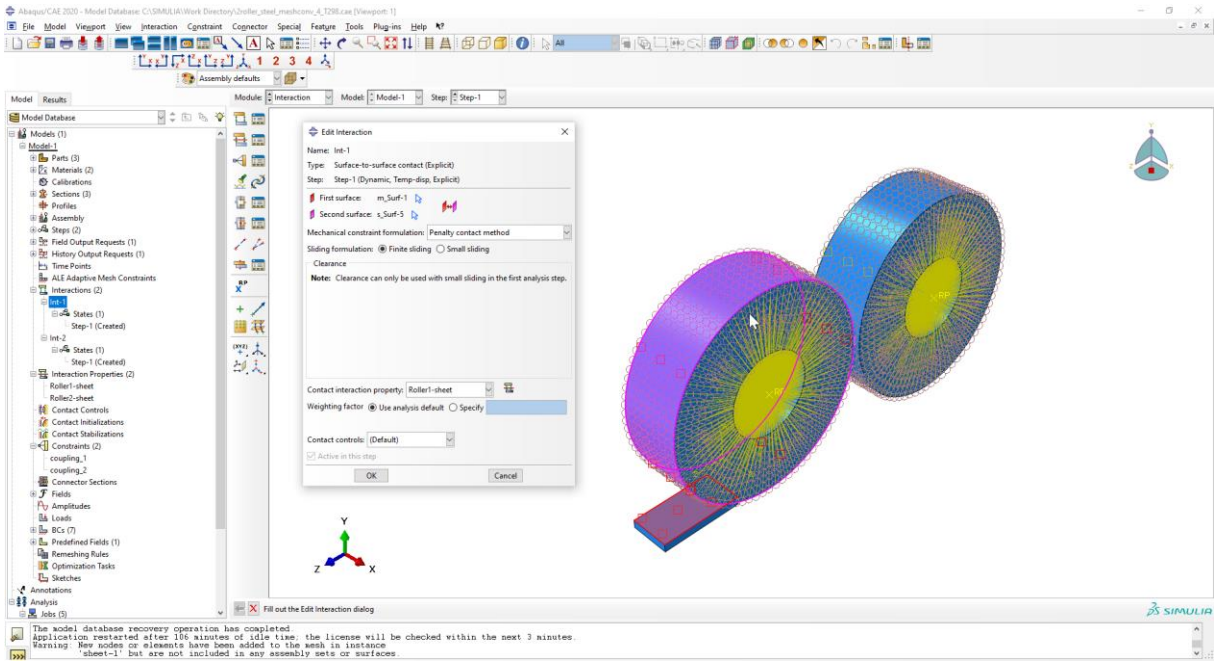

Figure 89. Interation between the plate and the rollers

Then, interaction properties are configured as Tangential behaviour, with a friction coefficient of 0.3. Heat generation is set as default:

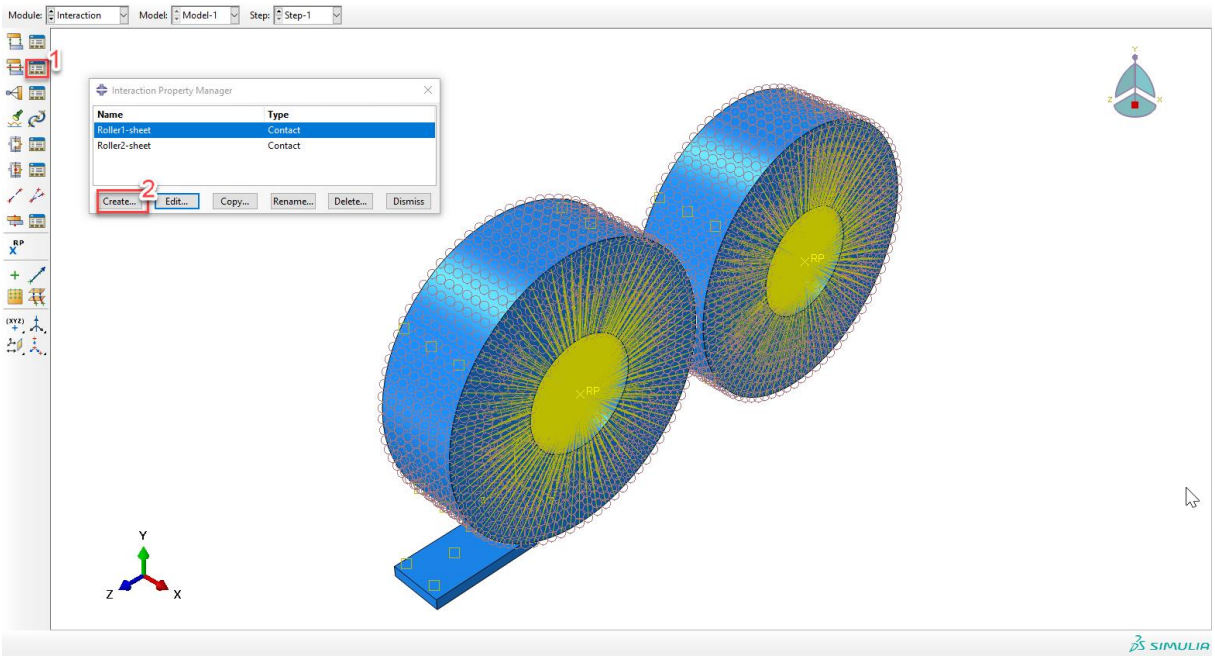

Figure 90. Creation of the interation between the plate and the rollers

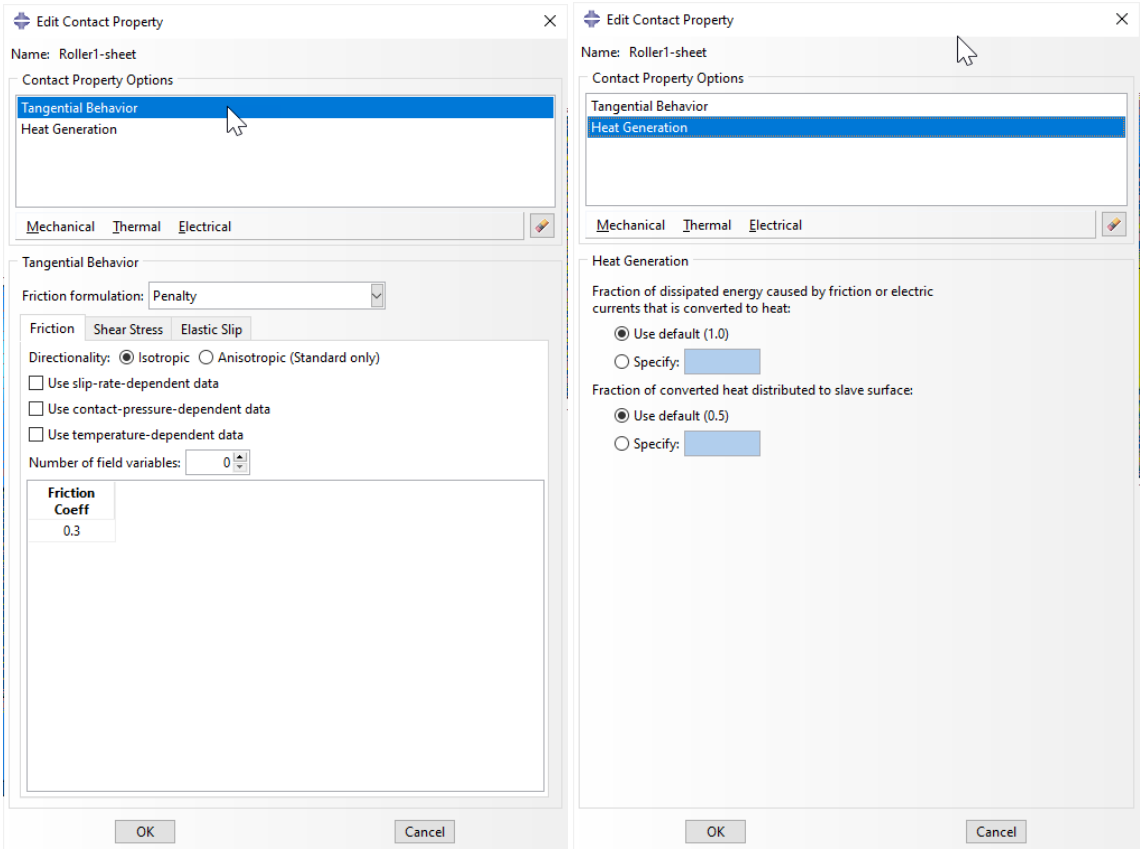

Figure 91. Contact properties

With the purpose of assigning a rotation to the roller, coupling between the all nodes of the rollers and its reference point is required. Roller nodes are selected as control points and the reference point of the roller as the master surface.

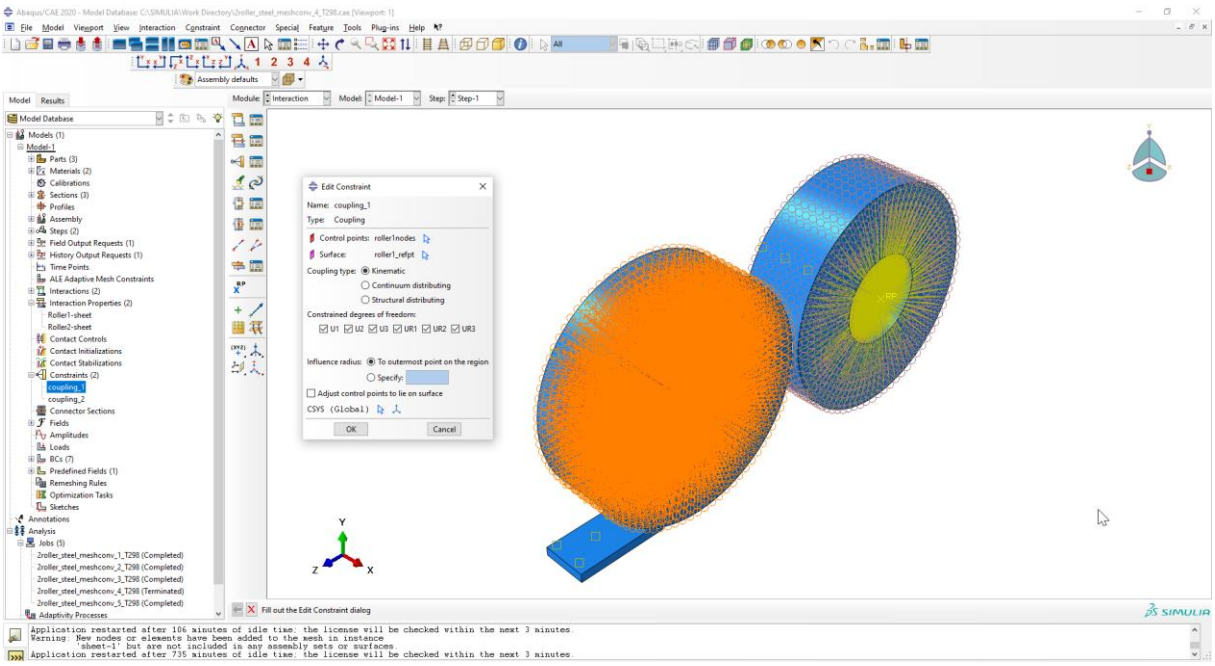

Figure 92. Interation properties

Coupling type is selected as “kinematic” and the 6 dof are constrained.

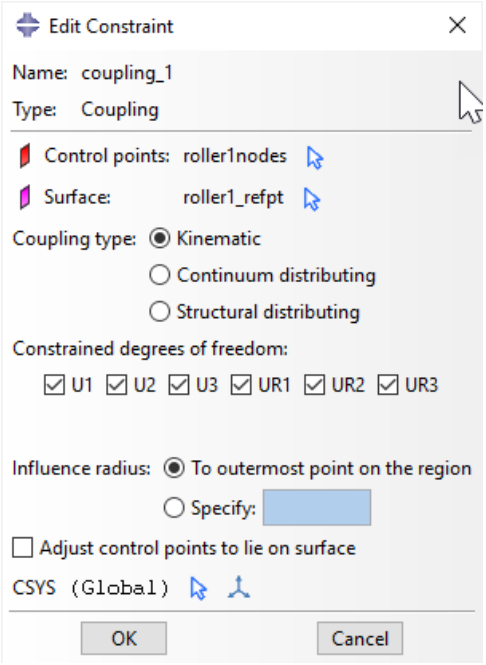

Figure 93. Detailed view of the coupling set up.

Step definition

Now, the steps for the analysis are set, starting with a low increment to ensure the accuracy of the analysis.

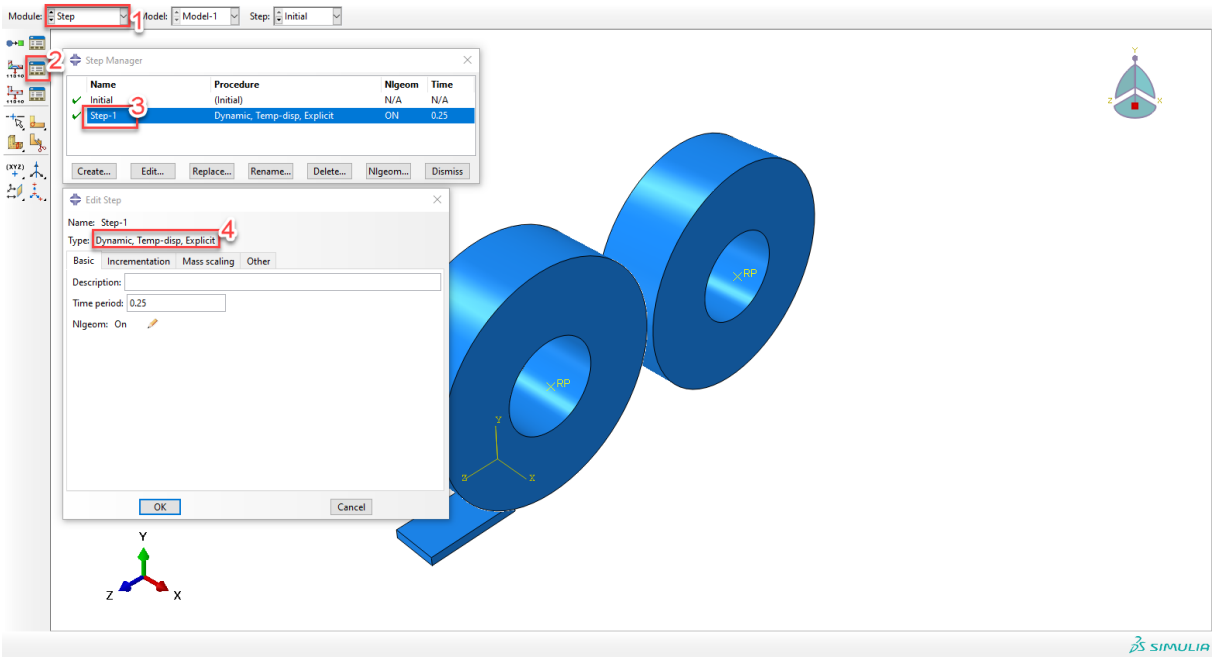

Figure 94. Step definition

Time period selected depends on the linear velocity of the plate. Slower linear velocity will require longer time period to complete the process.

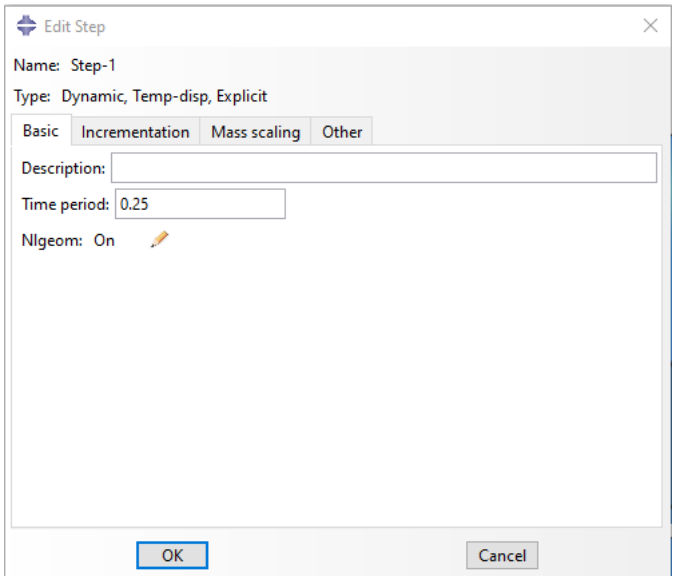

Figure 95. Step definition

For these models, no mass scaling is used.

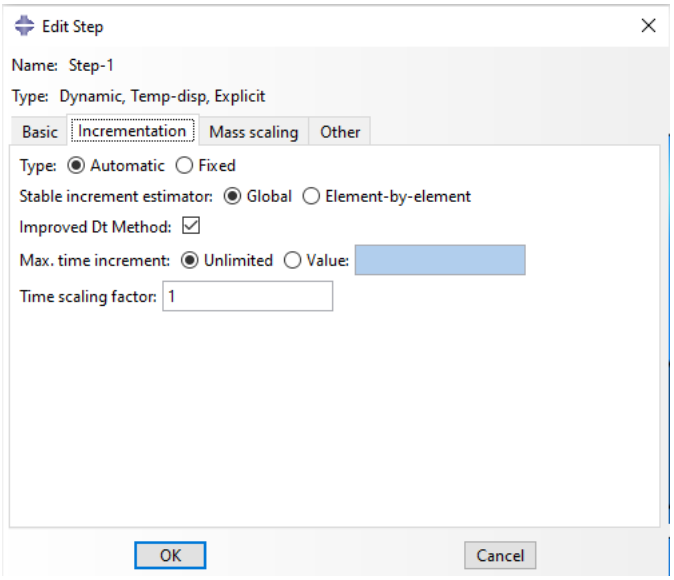

Figure 96. Step definition

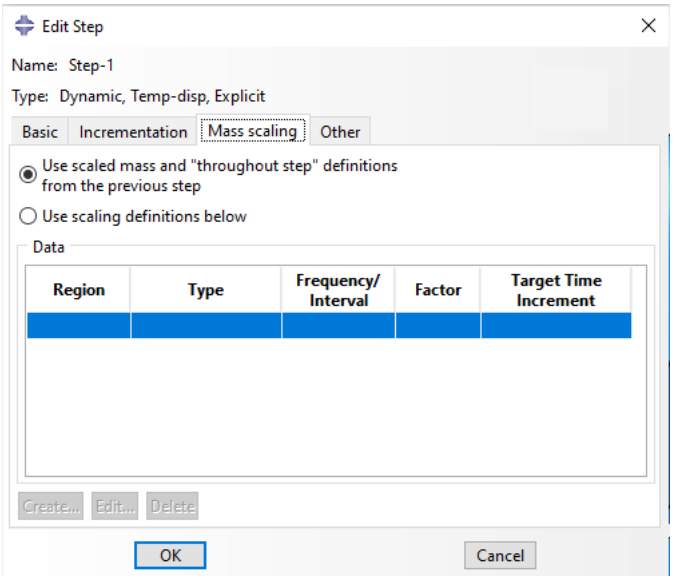

Figure 97. Step definition

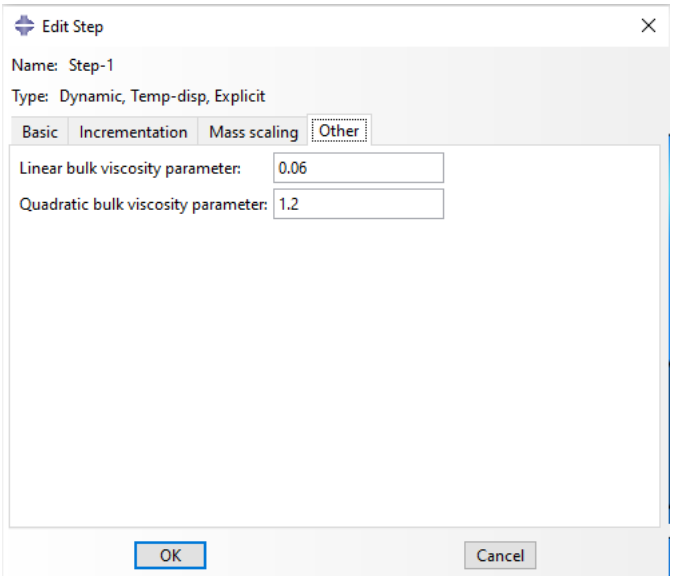

Figure 98. Step definition

Boundary conditions

Boundary conditions are stablished. In the following screenshots, it is shown how are they created:

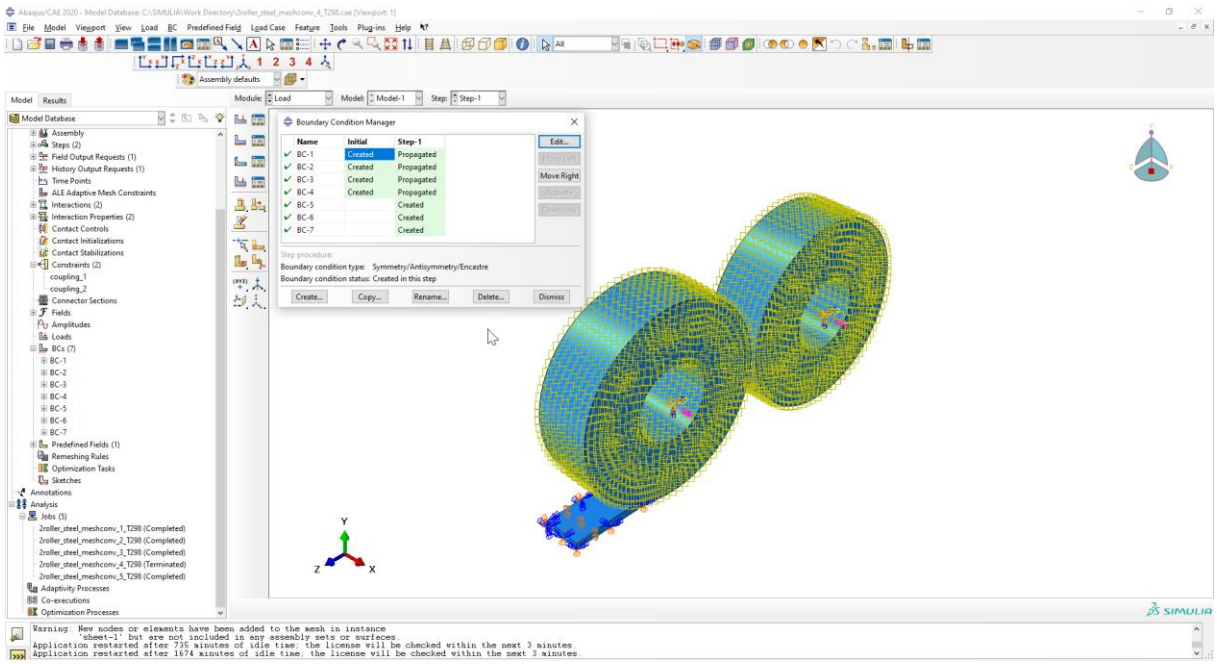

Figure 99. Boundary conditions

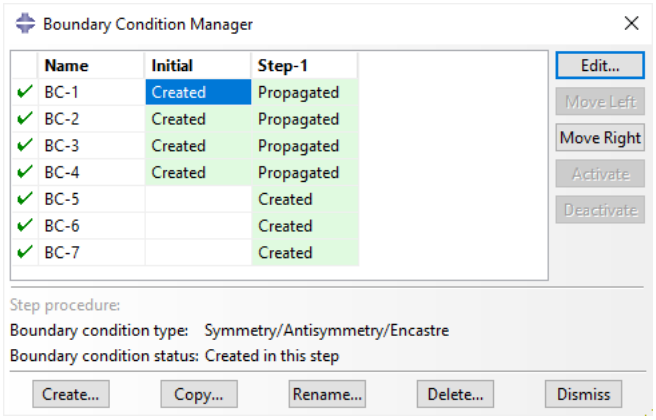

Figure 100. Boundary conditions

Symetry along Y axis is selected for bottom face of the plate. This means that the plate will not move downwards when a force is applied to it.

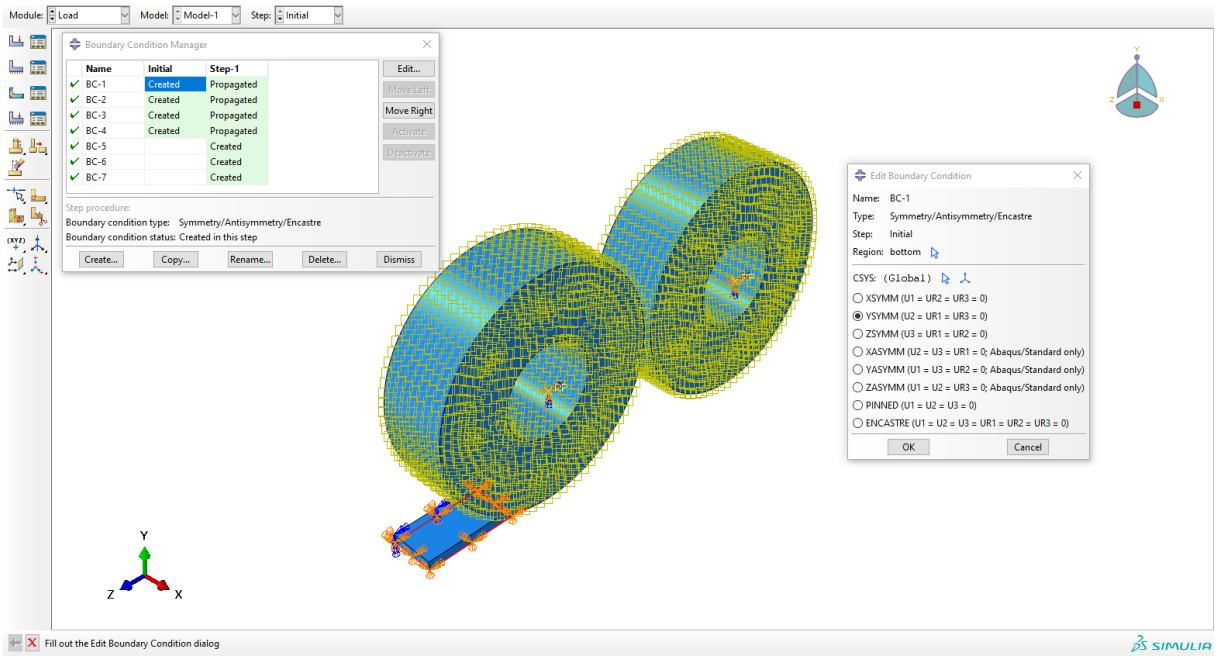

Figure 101. Boundary conditions

Symmetry is also selected for both lateral faces of the plate to ensure it does not spread at the X direction and it remains with the same width during the simulation.

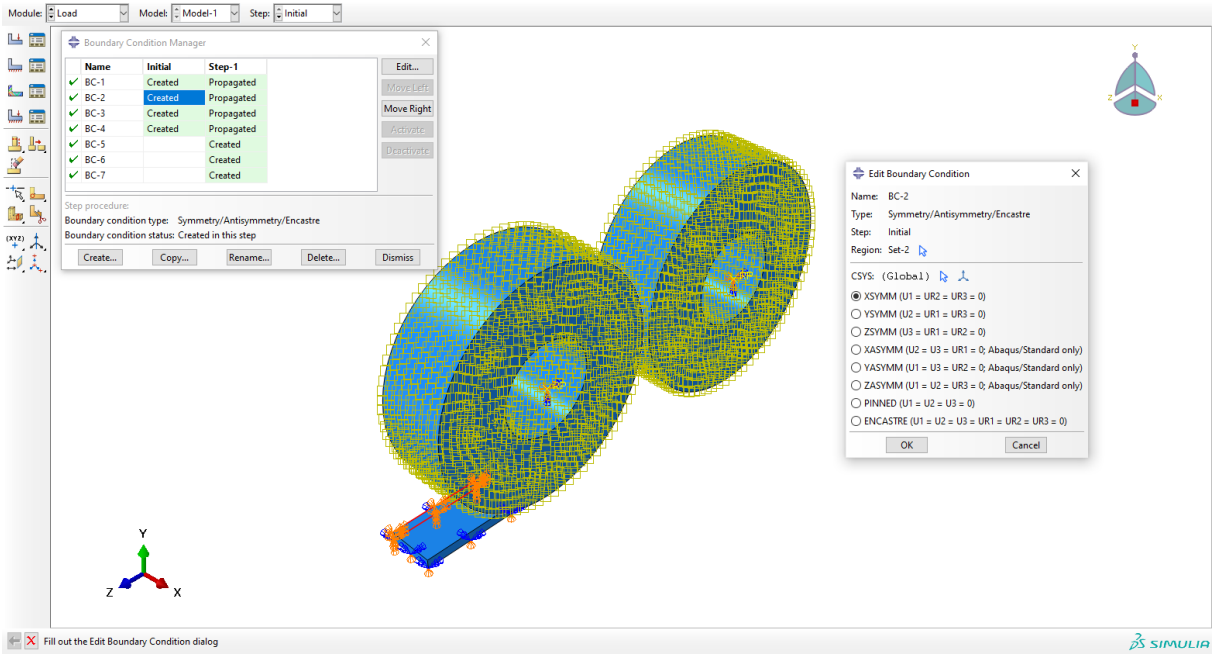

Figure 102. Boundary conditions

Rollers are provided only one degree of freedom which is rotation on the X axis.

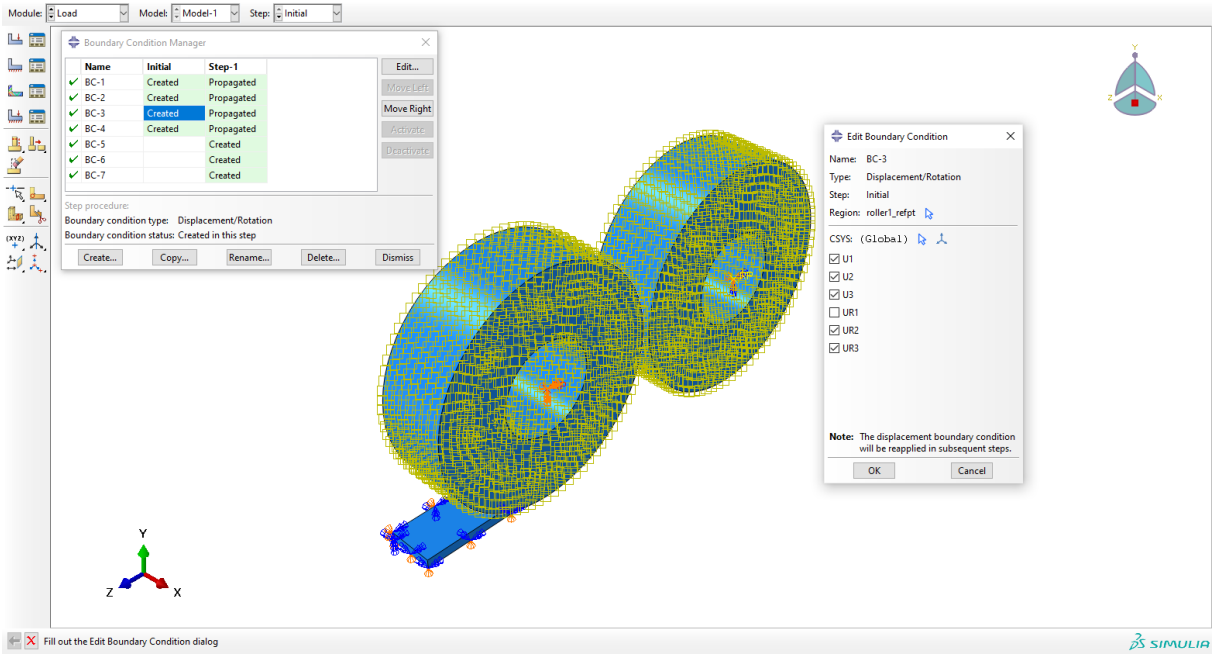

Figure 103. Boundary conditions

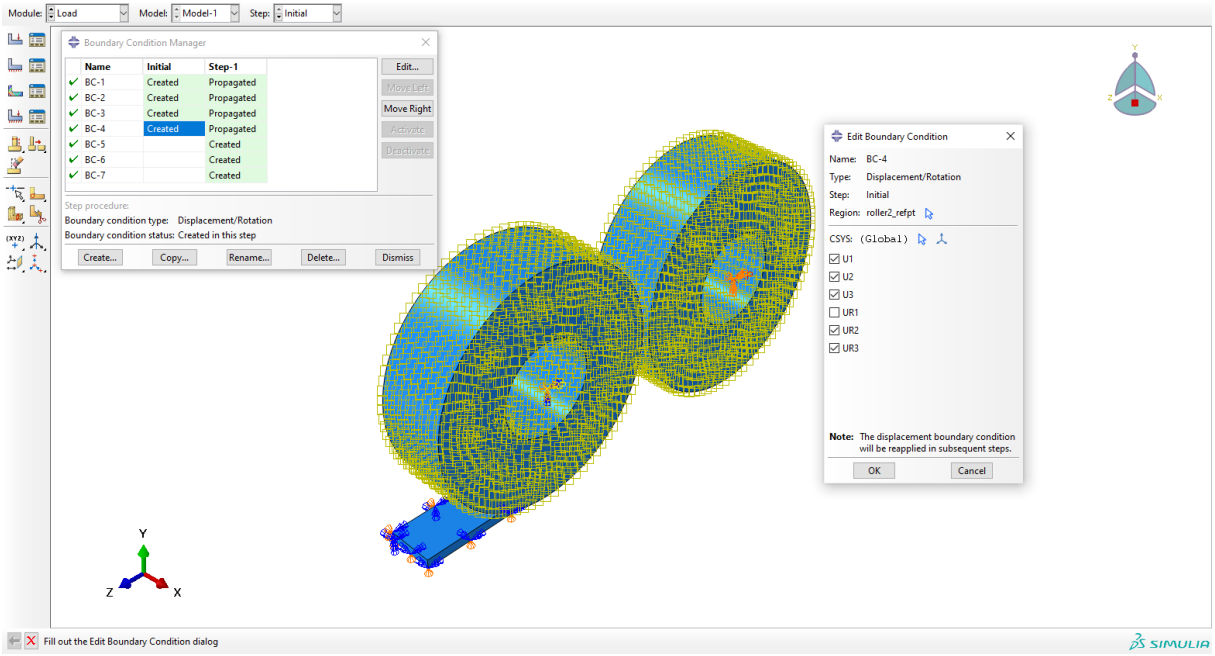

Figure 104. Boundary conditions

Rotation velocity is applied to the rollers:

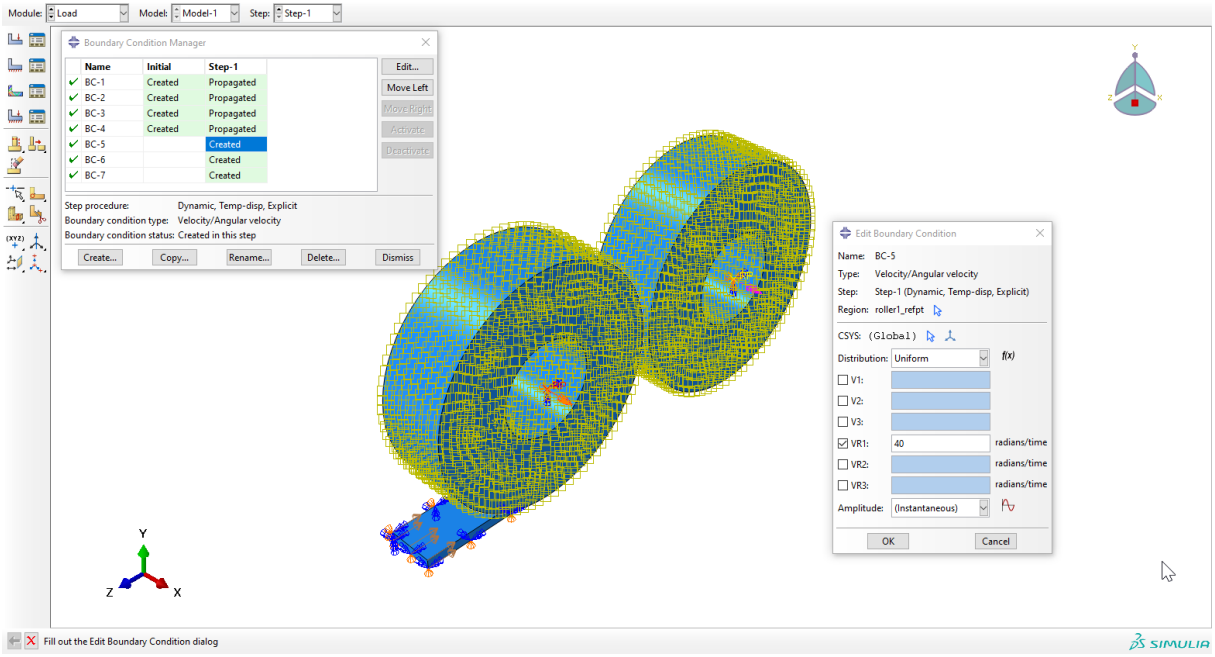

Figure 105. Boundary conditions

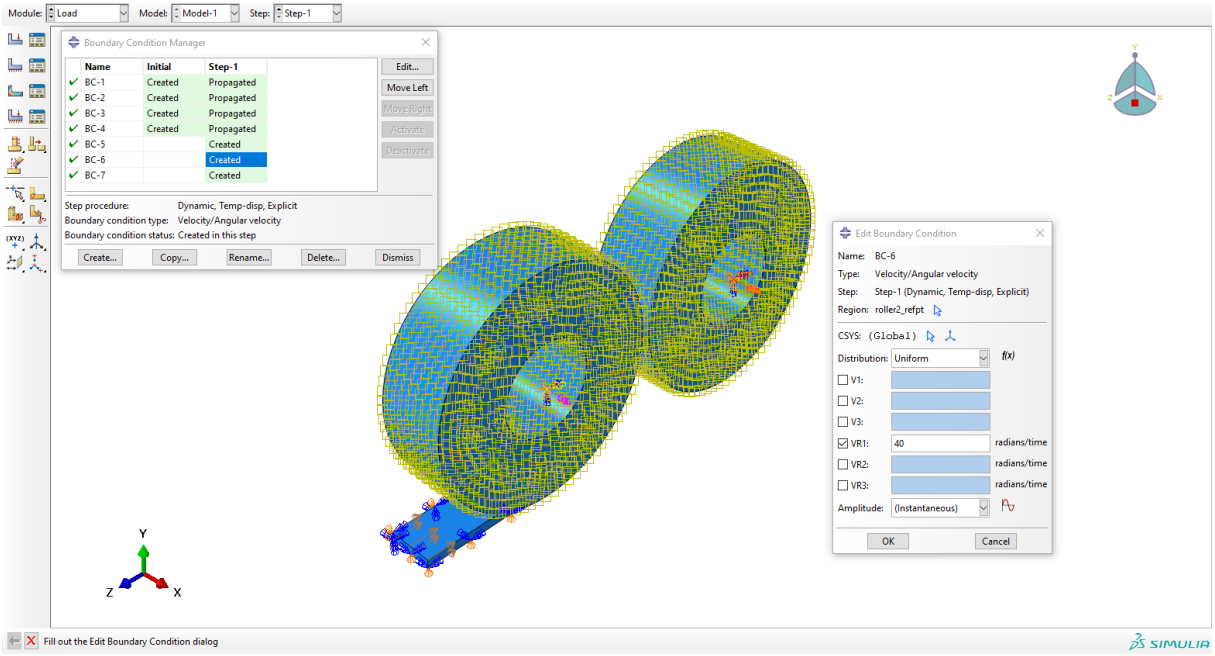

Figure 106. Boundary conditions

Lineal velocity is applied to the plate in negative Z direction:

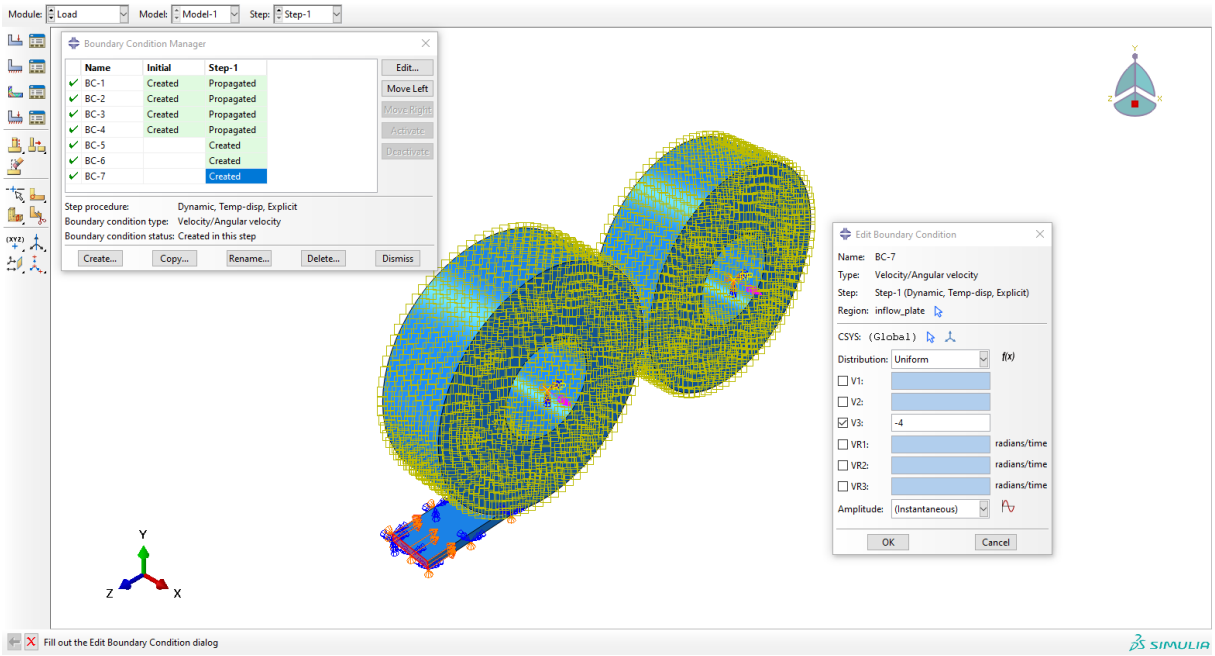

Figure 107. Boundary conditions

To provide the whole model an initial temperature, a new set with all nodes is created.

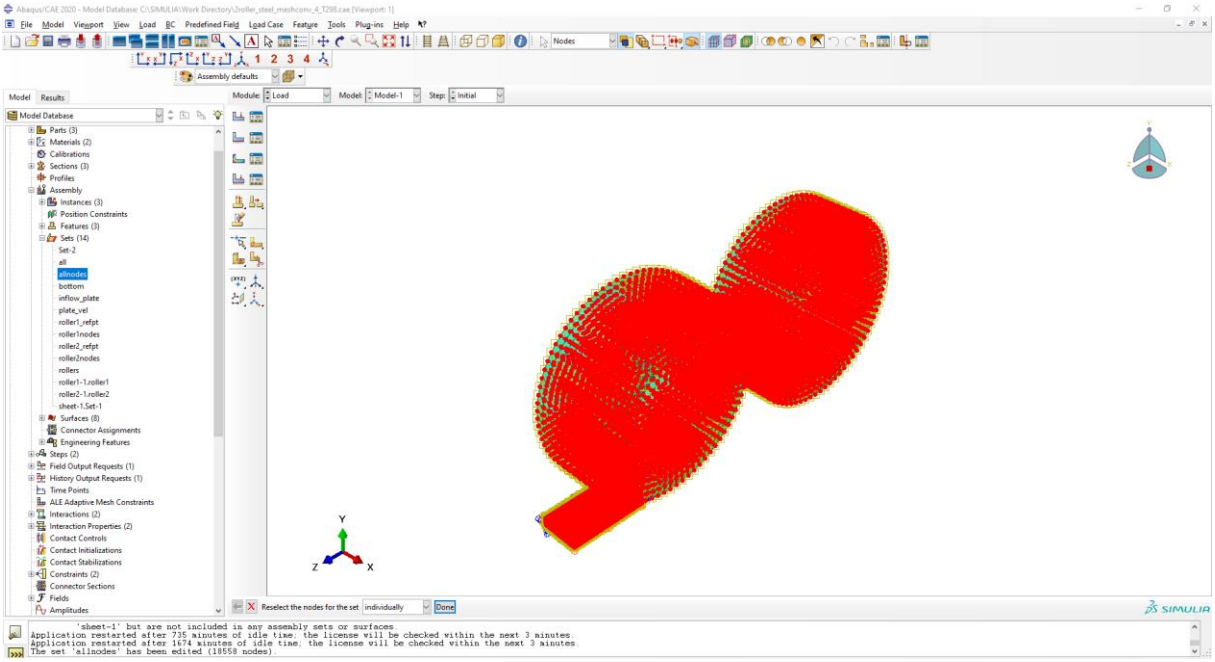

Figure 108. All nodes set creation

Temperature field for initial temperature is set up.

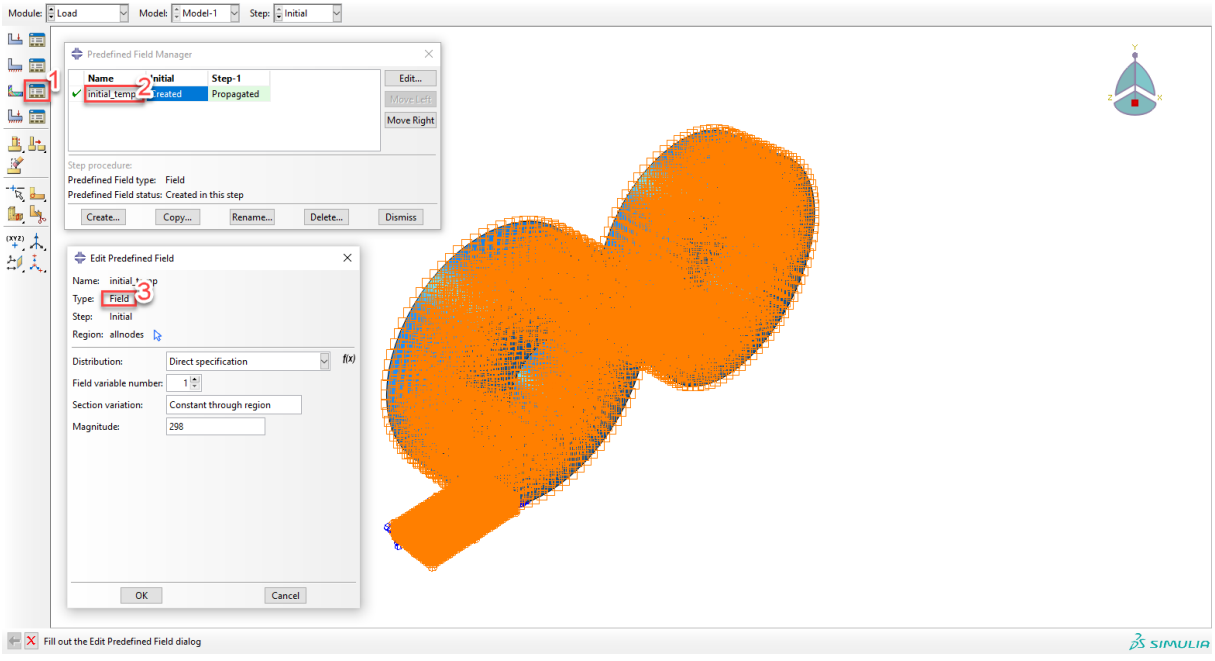

Figure 109. Initial temperature definition

Job

New job is created:

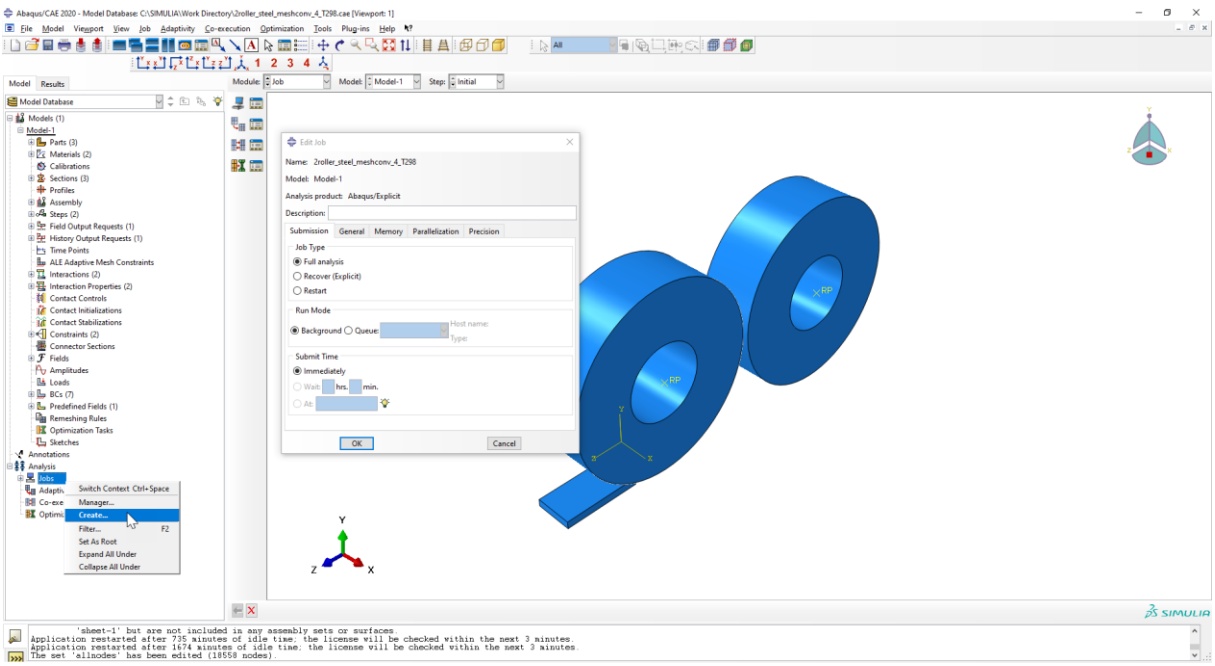

Figure 110. Job definition

It is important to use multiple processors with the objective of reducing computing time.

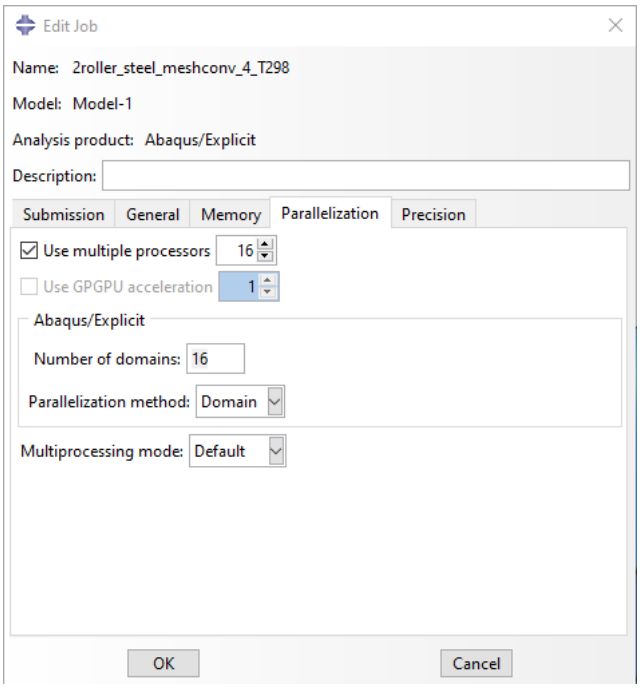

Figure 111. Job definition

Visualization of results

It is checked that the movement that is intended to be performed in the simulation is correct.

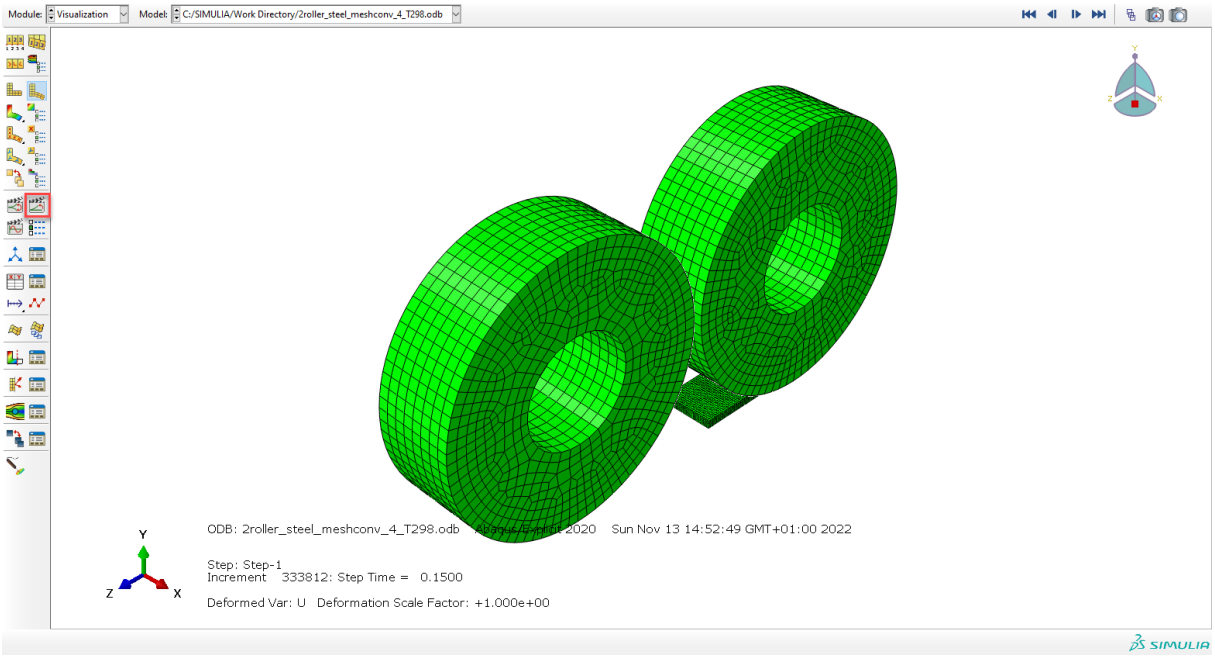

Figure 112. Visualization of results

Using visualization module, results are extracted from each model.

ANNEX 2. Mesh convergence analysis results

Annex 2.1 Model 1

- **Max PEEQ in timeframe 3**

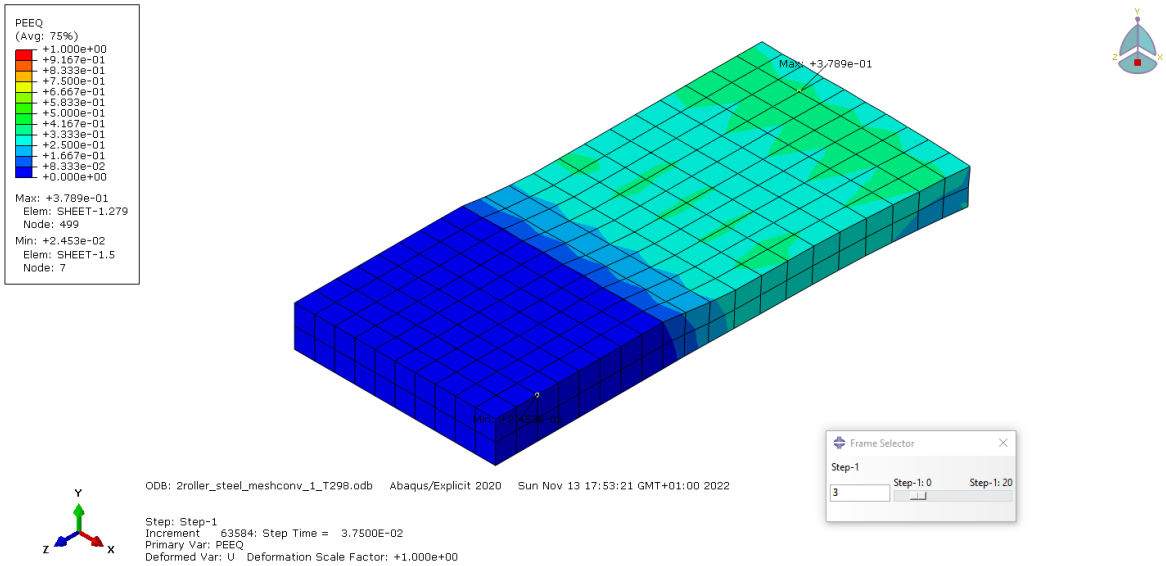

Figure 113. Model 1 PEEQ

- **Min RF2 in timeframe 3**

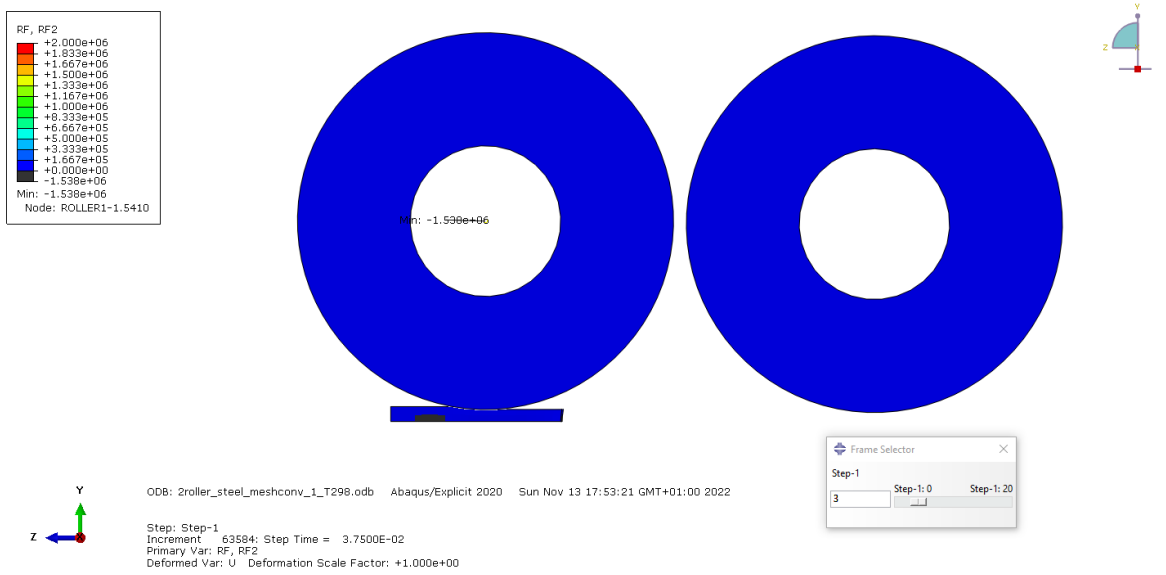

Figure 114. Model 1 RF2

- **Max NT11 in timeframe 3**

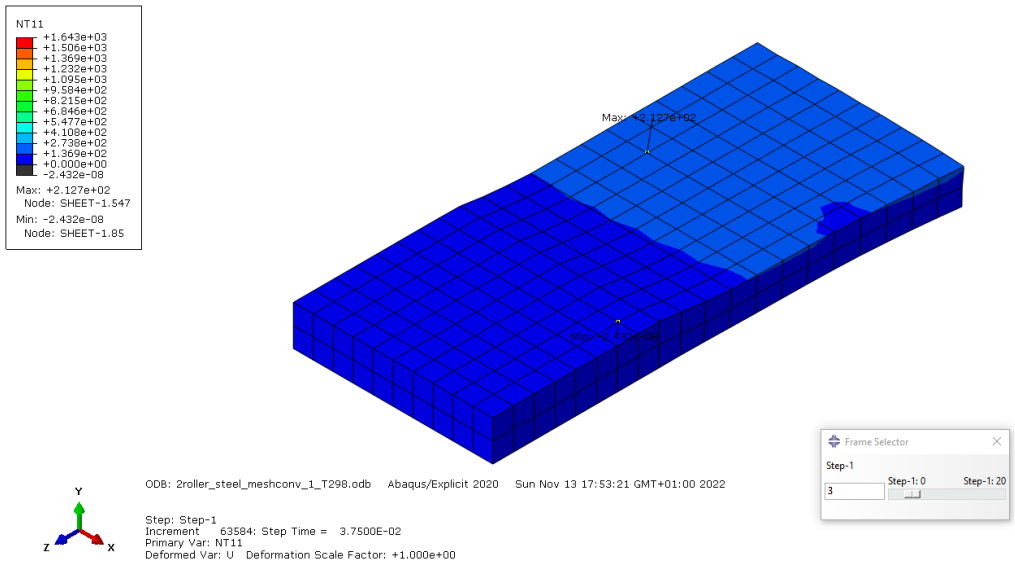

Figure 115. Model 1 NT11

Annex 2.2 Model 2

- **Max PEEQ in timeframe 3**

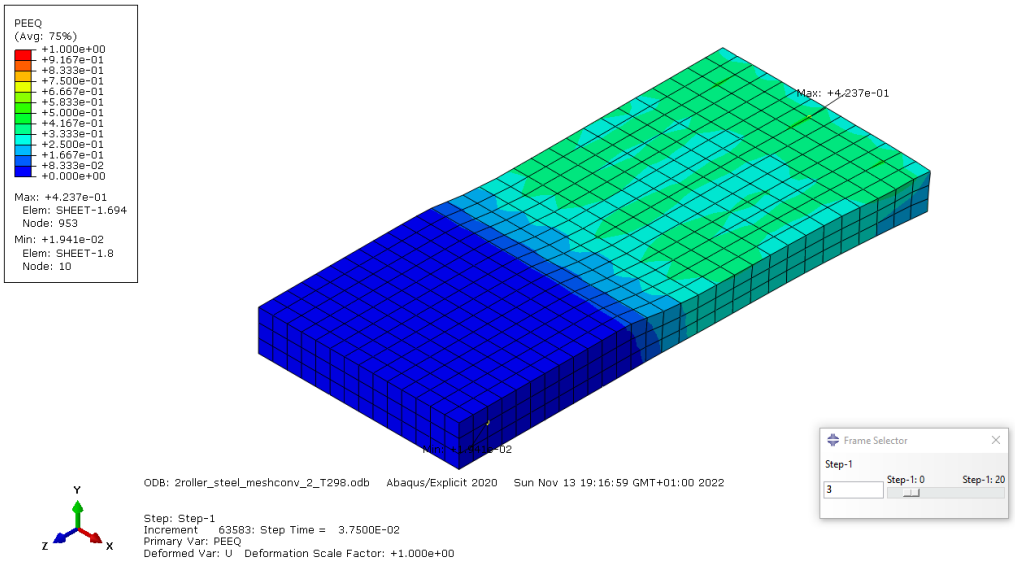

Figure 116. Model 2 PEEQ

- **Min RF2 in timeframe 3**

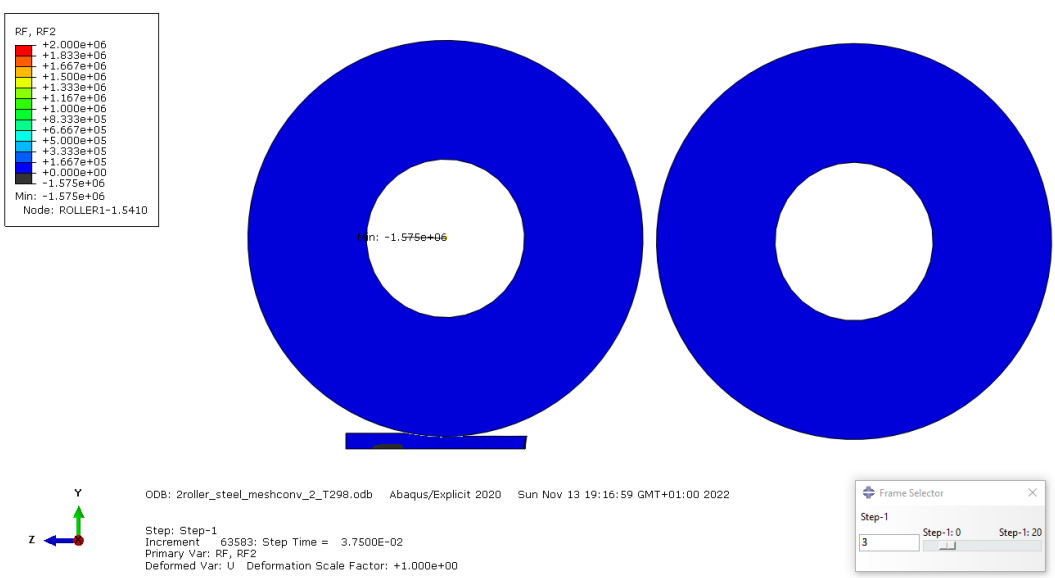

Figure 117. Model 2 RF2

- **Max NT11 in timeframe 3**

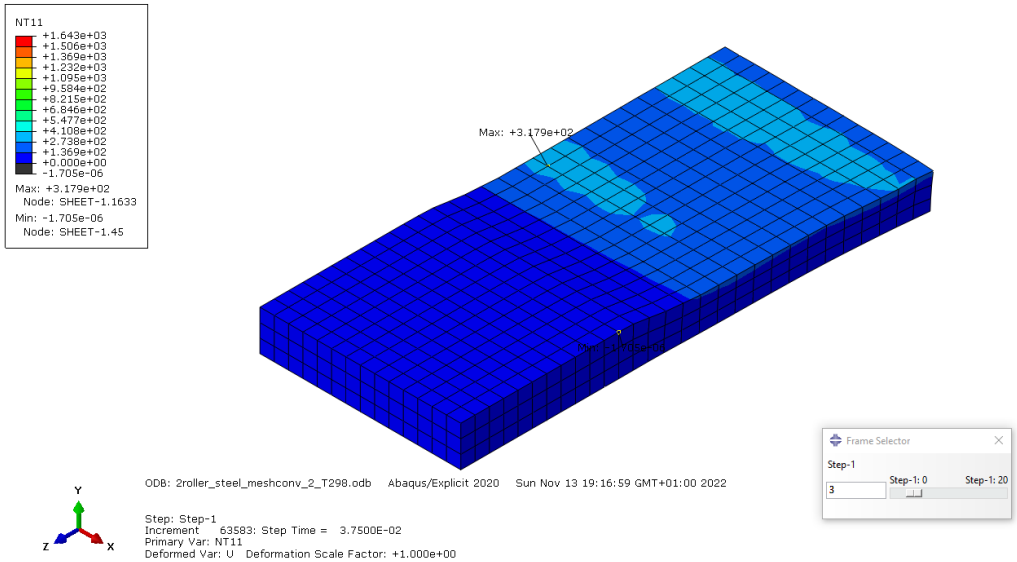

Figure 118. Model 2 NT11

Annex 2.3 Model 3

- **Max PEEQ in timeframe 3**

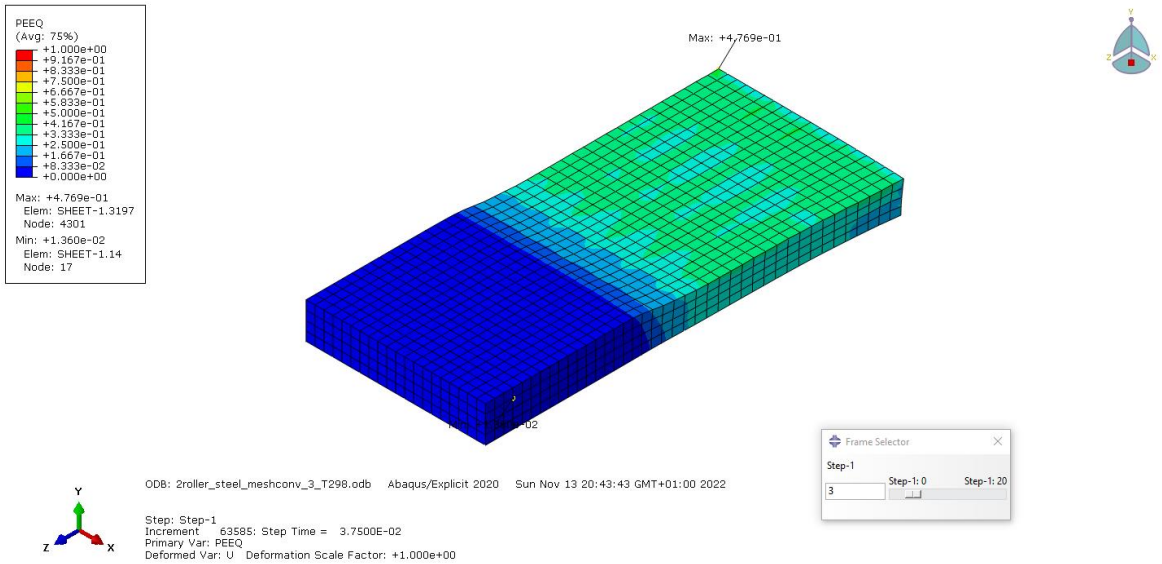

Figure 119. Model 3 PEEQ

- **Min RF2 in timeframe 3**

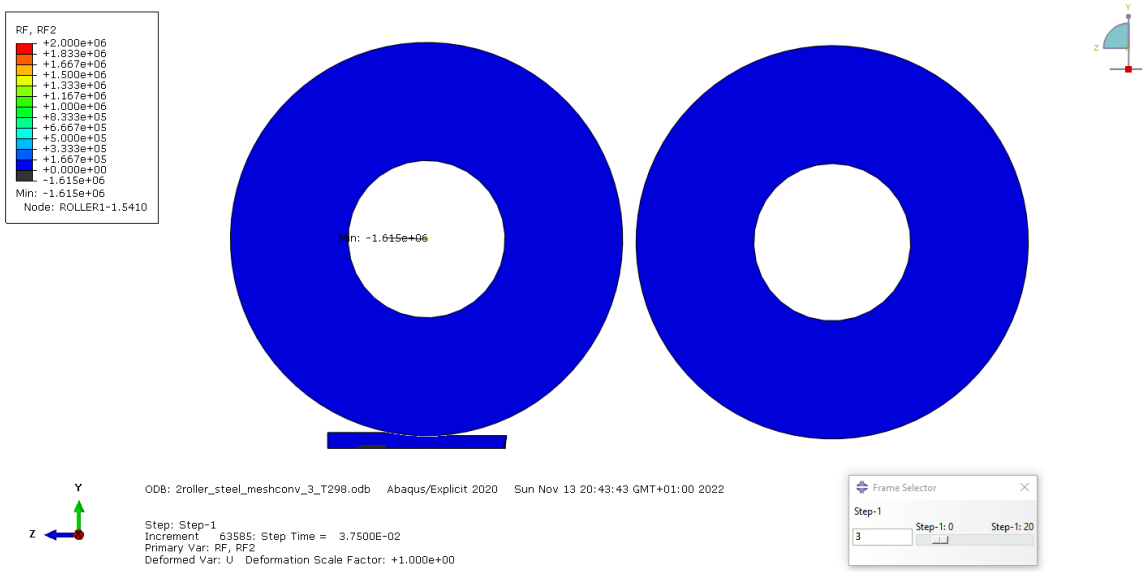

Figure 120. Model 3 RF2

- **Max NT11 in timeframe 3**

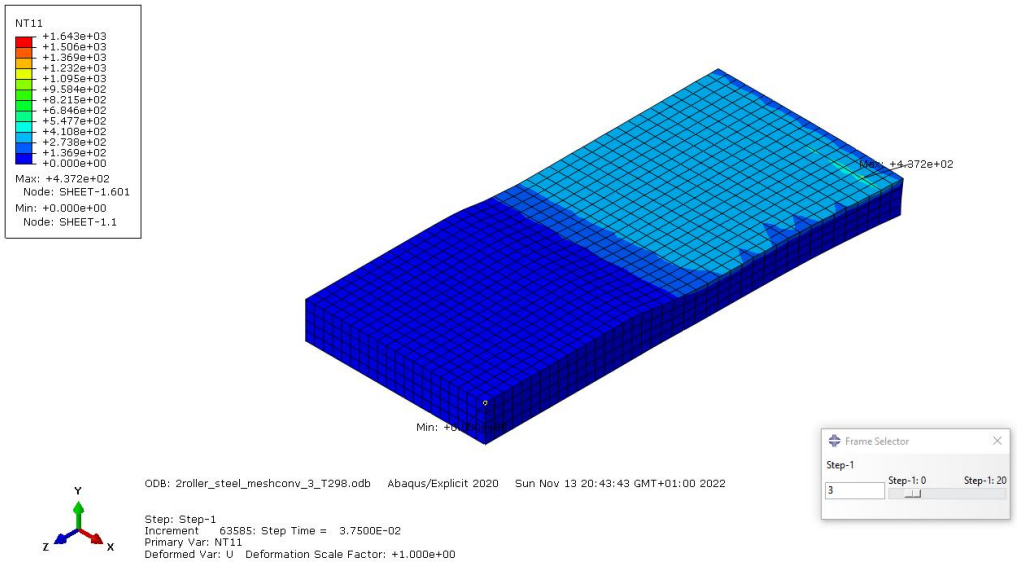

Figure 121. Model 3 NT11

Annex 2.4 Model 4

- **Max PEEQ in timeframe 3**

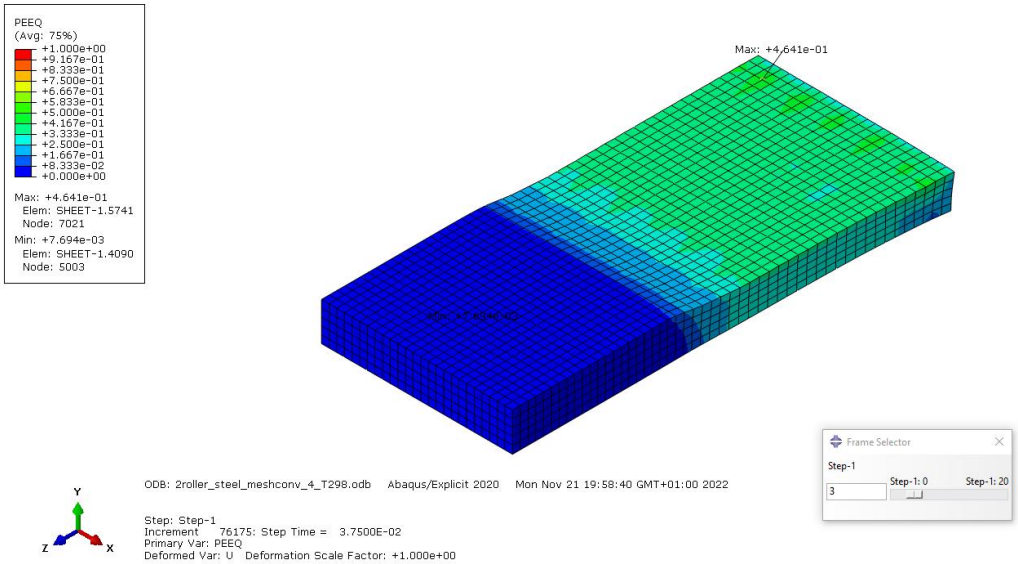

Figure 122. Model 4 PEEQ

- **Min RF2 in timeframe 3**

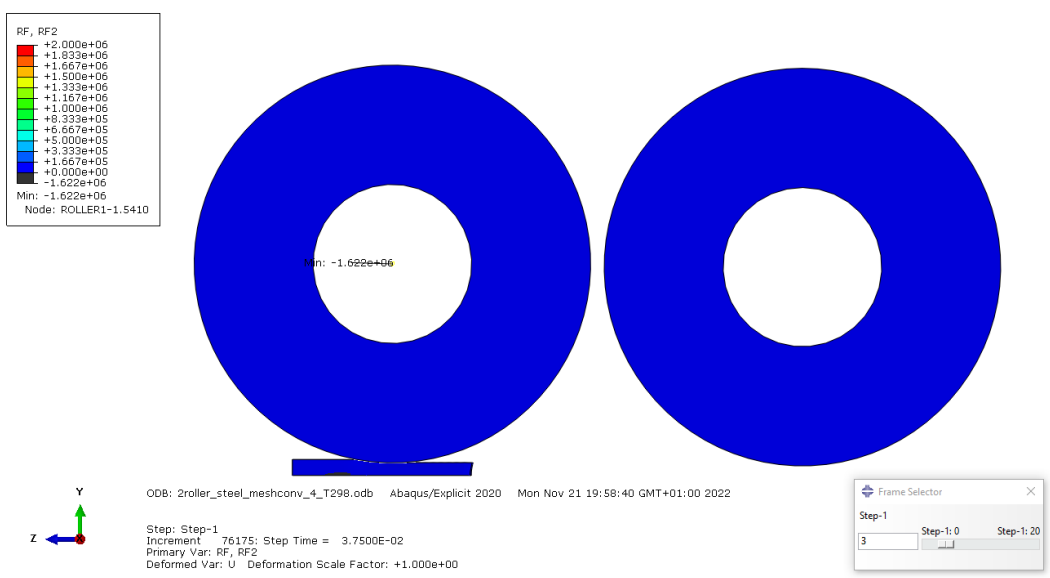

Figure 123. Model 4 RF2

- **Max NT11 in timeframe 3**

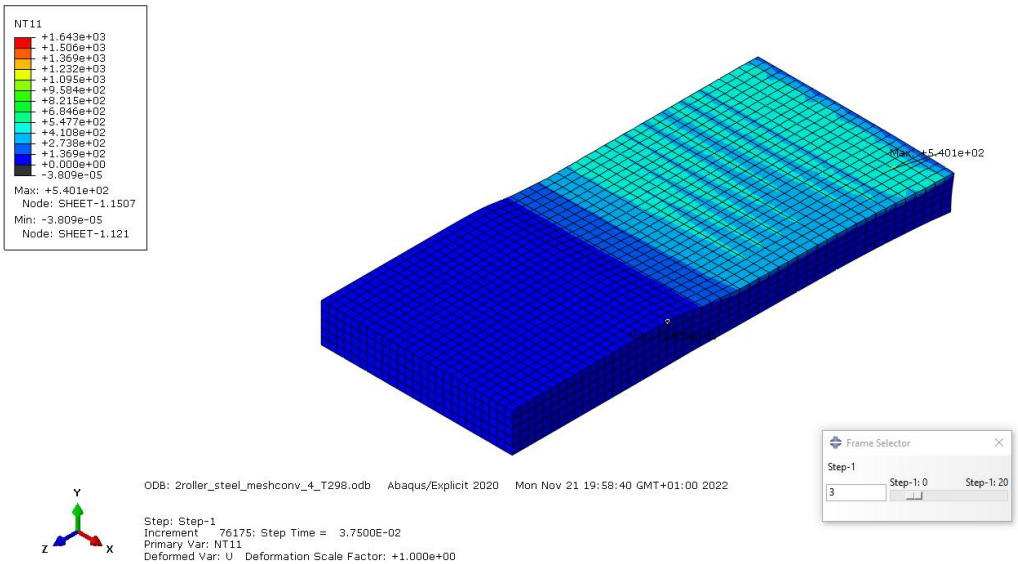

Figure 124. Model 4 NT11

Annex 2.5 Model 5

- **Max PEEQ in timeframe 3**

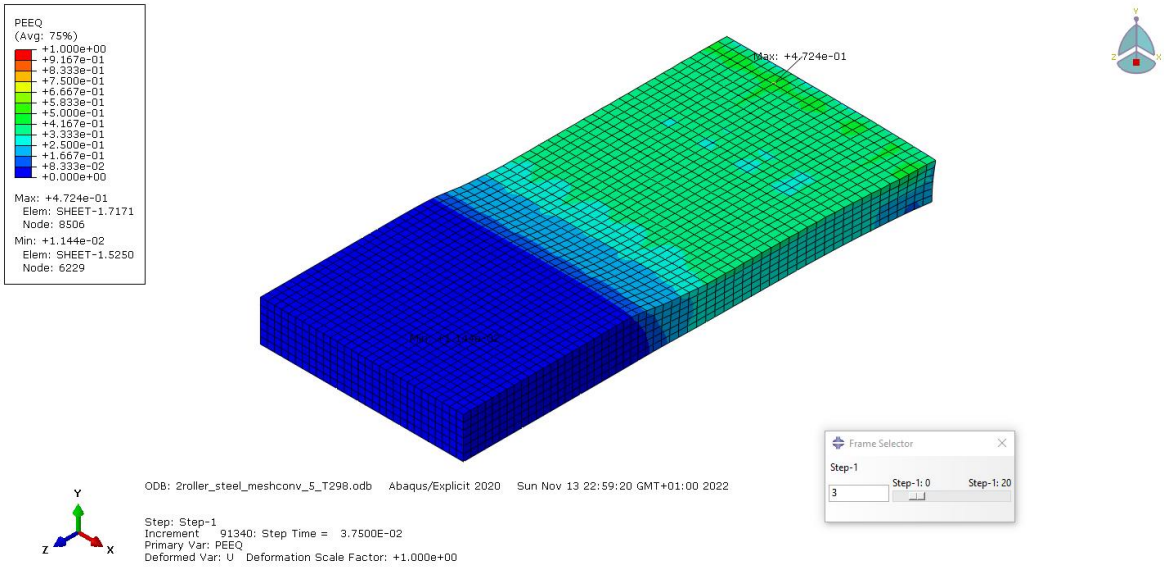

Figure 125. Model 5 PEEQ

- **Min RF2 in timeframe 3**

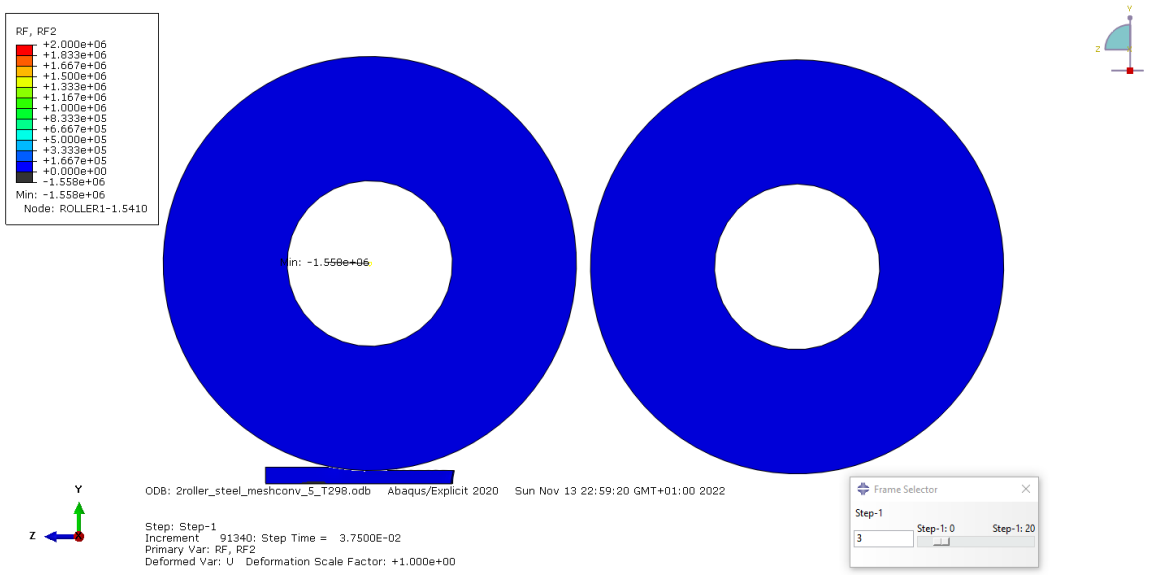

Figure 126. Model 5 RF2

- **Max NT11 in timeframe 3**

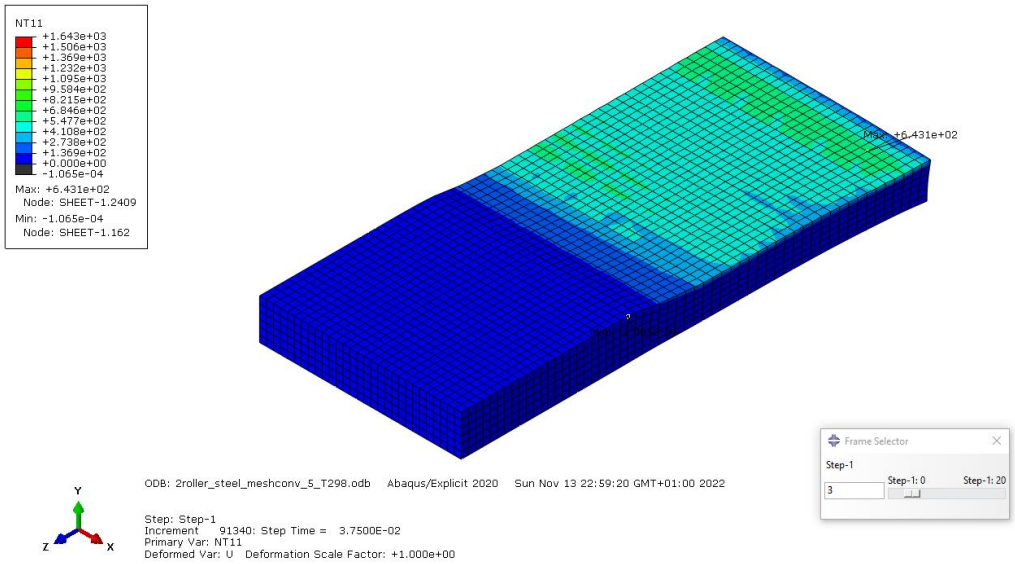

Figure 127. Model 5 NT11

Annex 2.6 Model 6

- **Max PEEQ in timeframe 3**

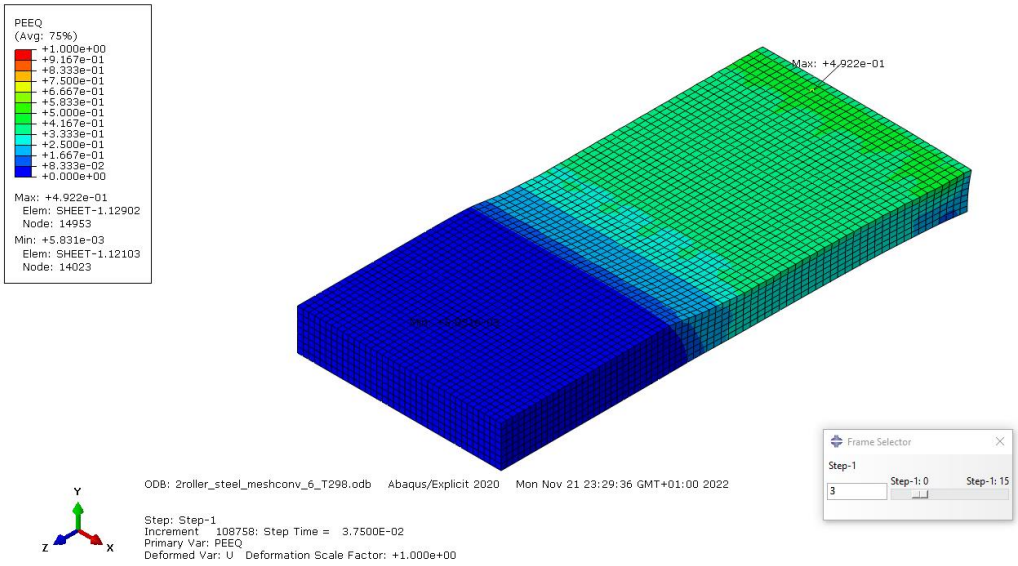

Figure 128. Model 6 PEEQ

- **Min RF2 in timeframe 3**

Figure 129. Model 6 RF2

- **Max NT11 in timeframe 3**

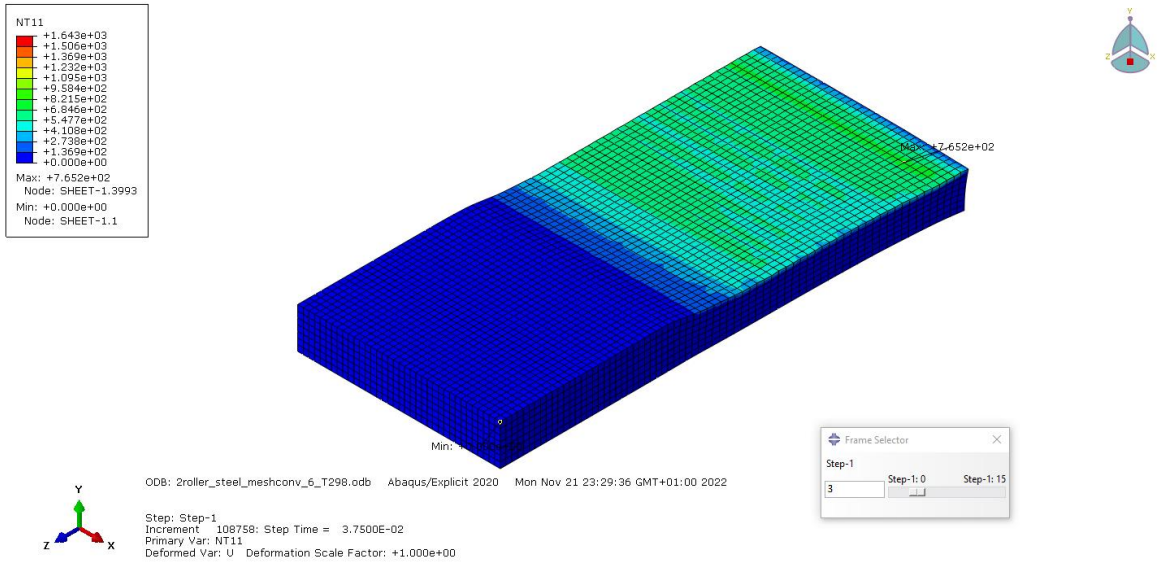

Figure 130. Model 6 NT11

Annex 2.7 Model 7

- **Max PEEQ in timeframe 3**

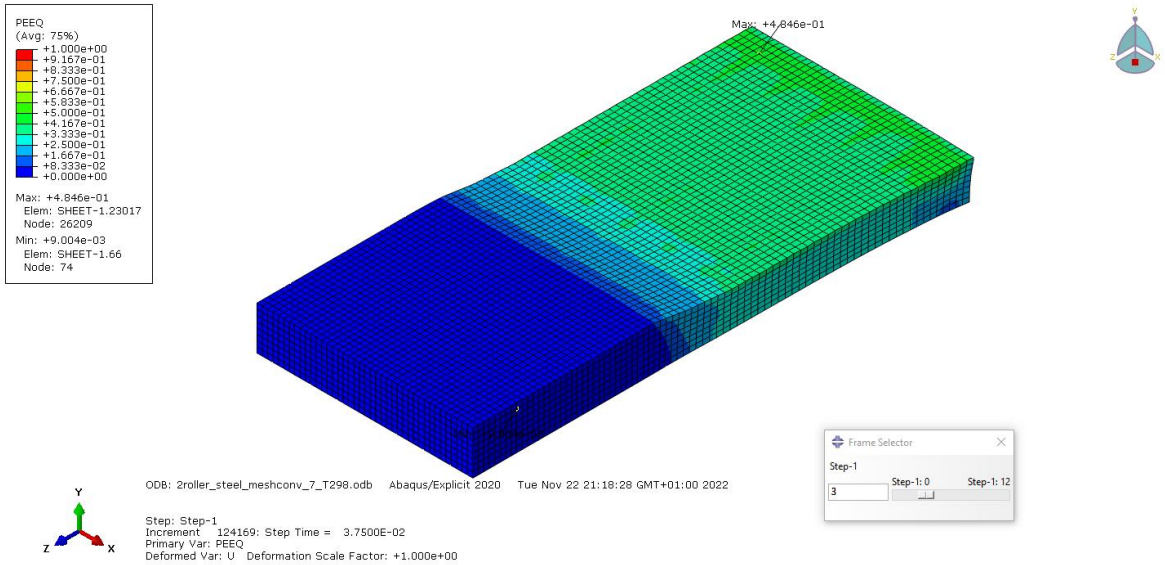

Figure 131. Model 7 PEEQ

- **Min RF2 in timeframe 3**

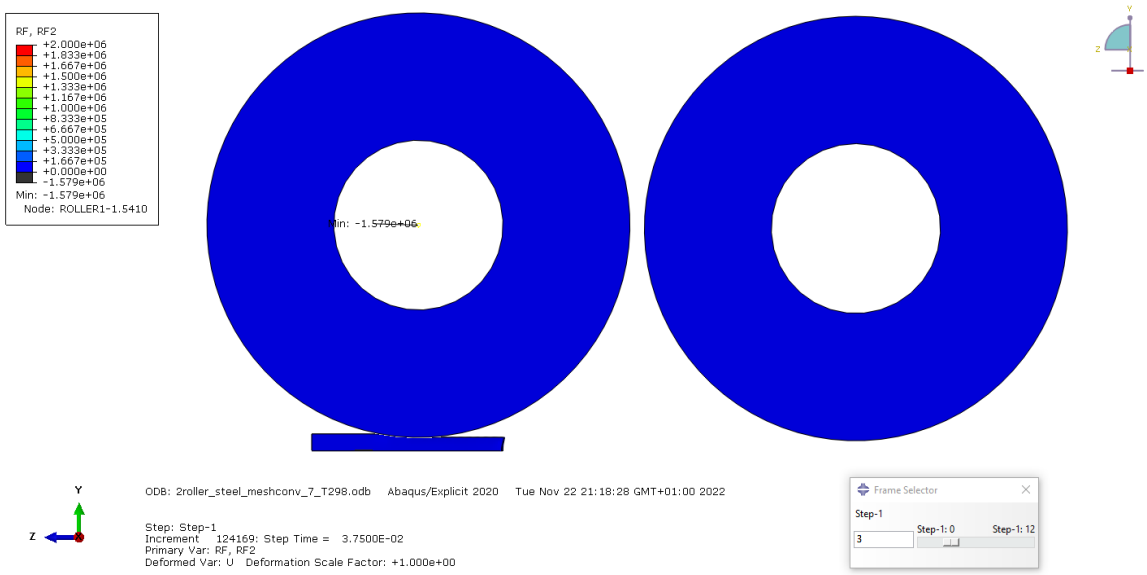

Figure 132. Model 7 RF2

- **Max NT11 in timeframe 3**

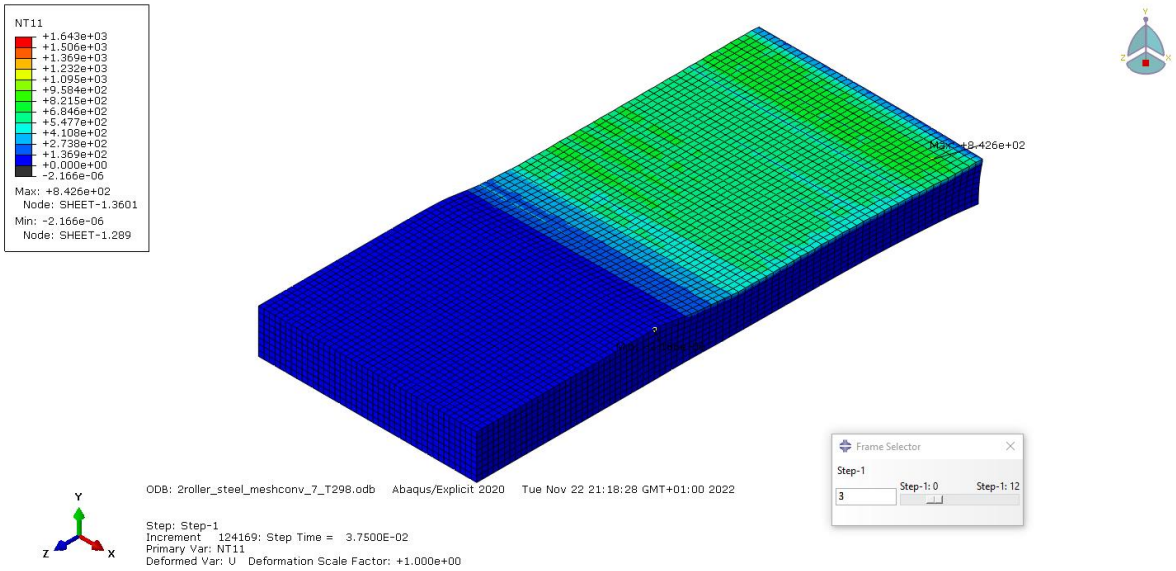

Figure 133. Model 7 NT11

Annex 3 Temperature for mesh convergence analysis

With the purpose of having comparable results and avoiding to select nodes with temperature peaks due to model imperfections, it is selected a node with a location similar to the maximum nodal temperature location for model 1 and model 2. Following the screenshots with the node selected, the temperature corresponding to that node and the distance from the selected node to a corner of the plate to prove that the position of the selected node is similar. Please note that, as the mesh is changed for each analysis, it is not possible to take a point exactly with the same location.

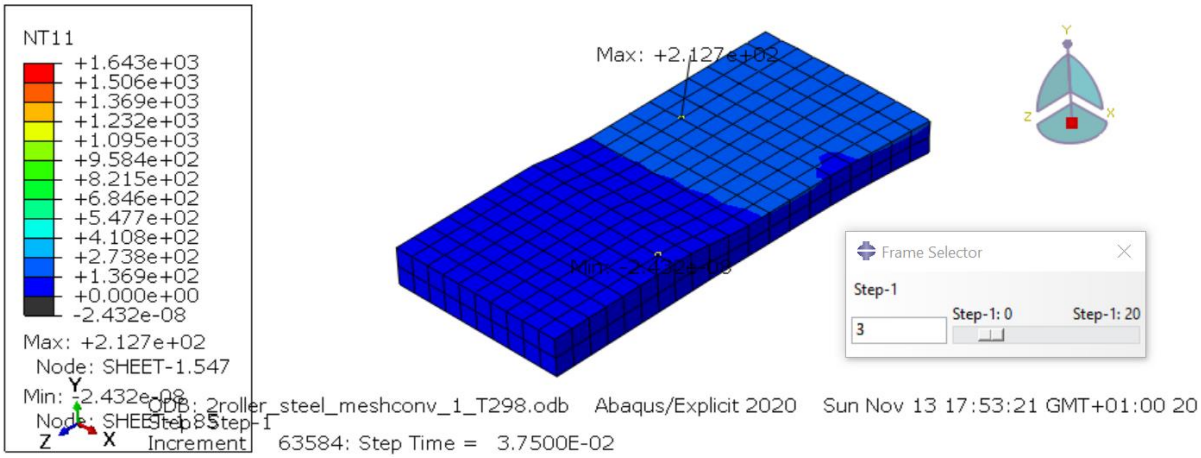

Figure 134. Maximum nodal temperature location for model 1

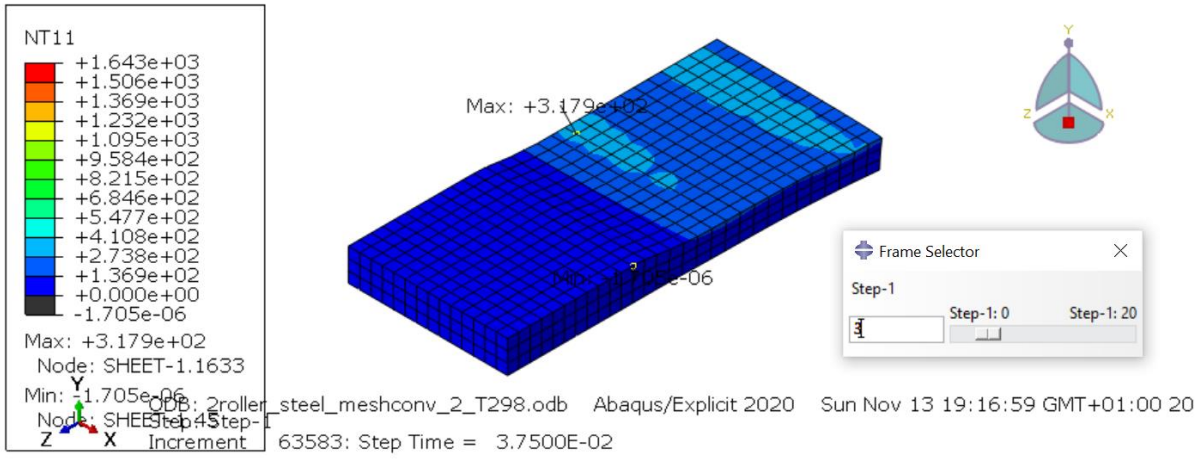

Figure 135. Maximum nodal temperature location for model 2

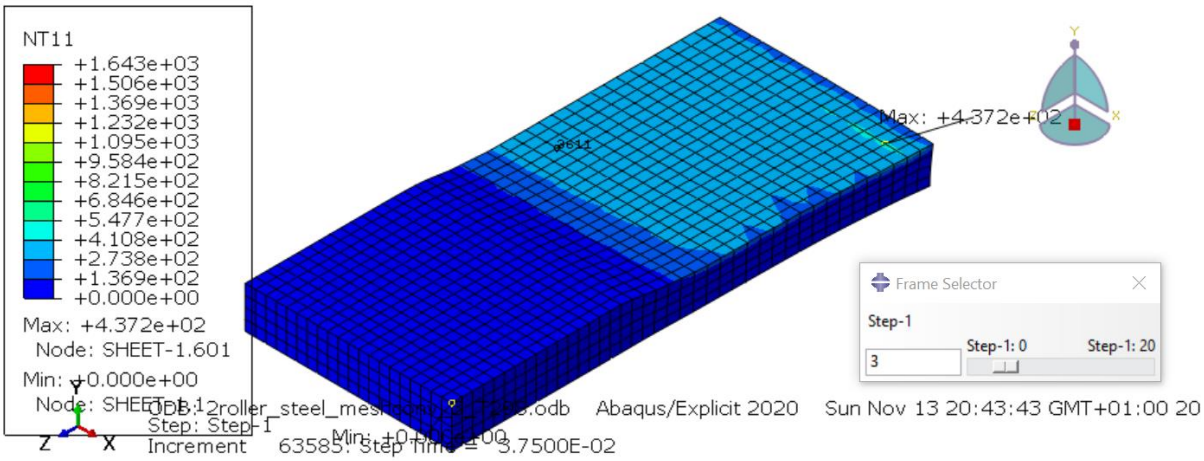

Figure 136. Model 3

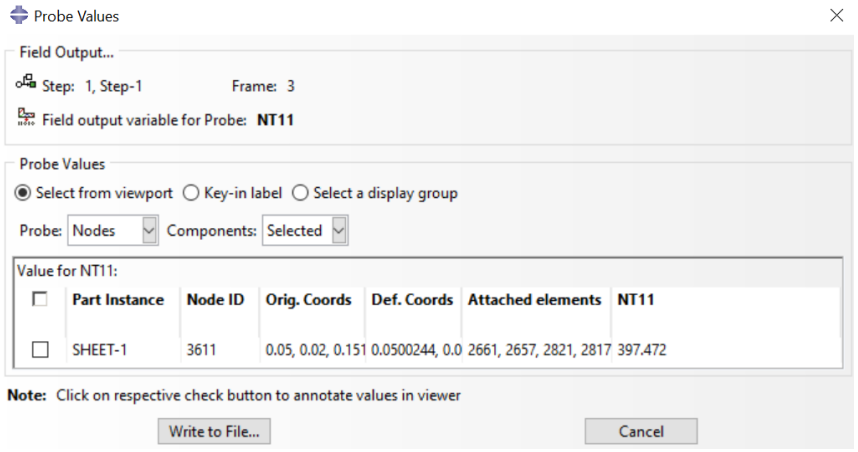

Figure 137. Model 3

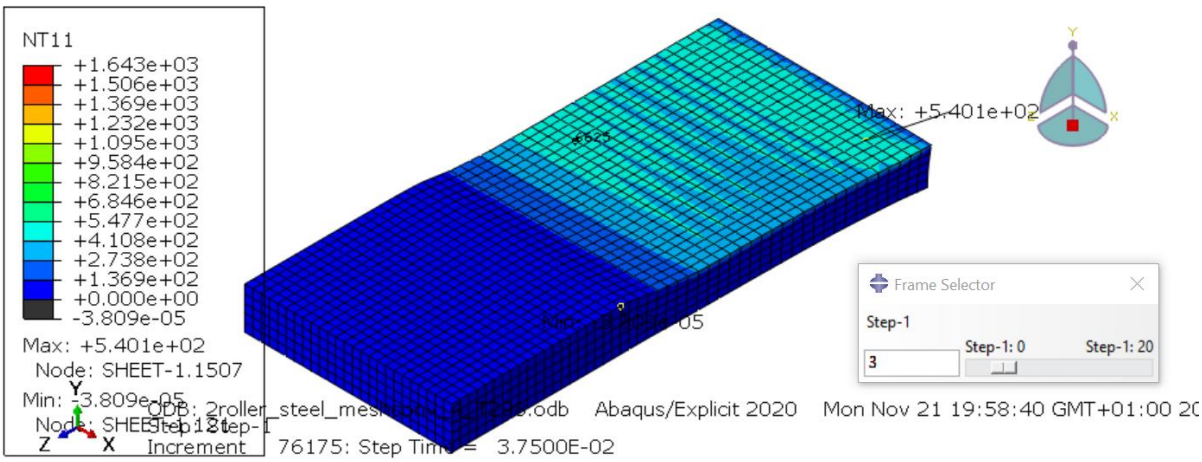

Figure 138. Model 4

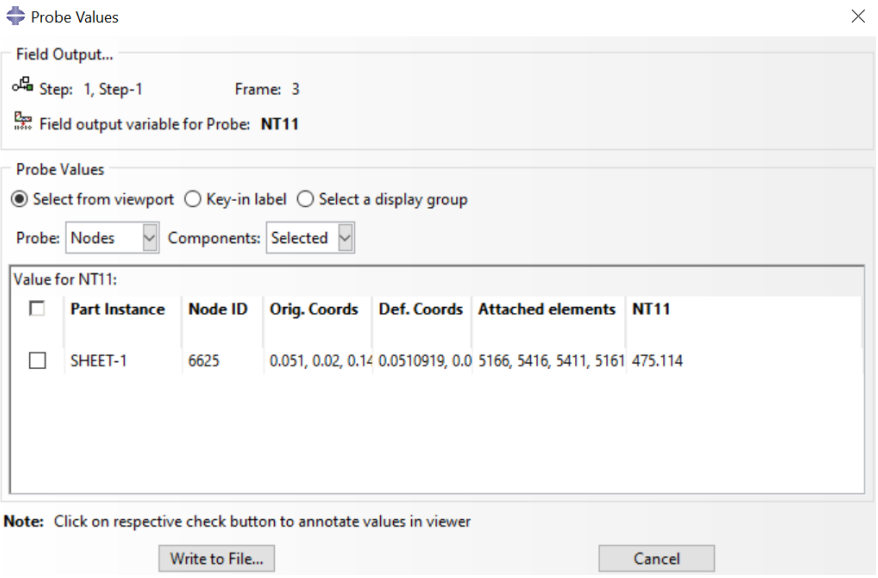

Figure 139. Temperature in model 4

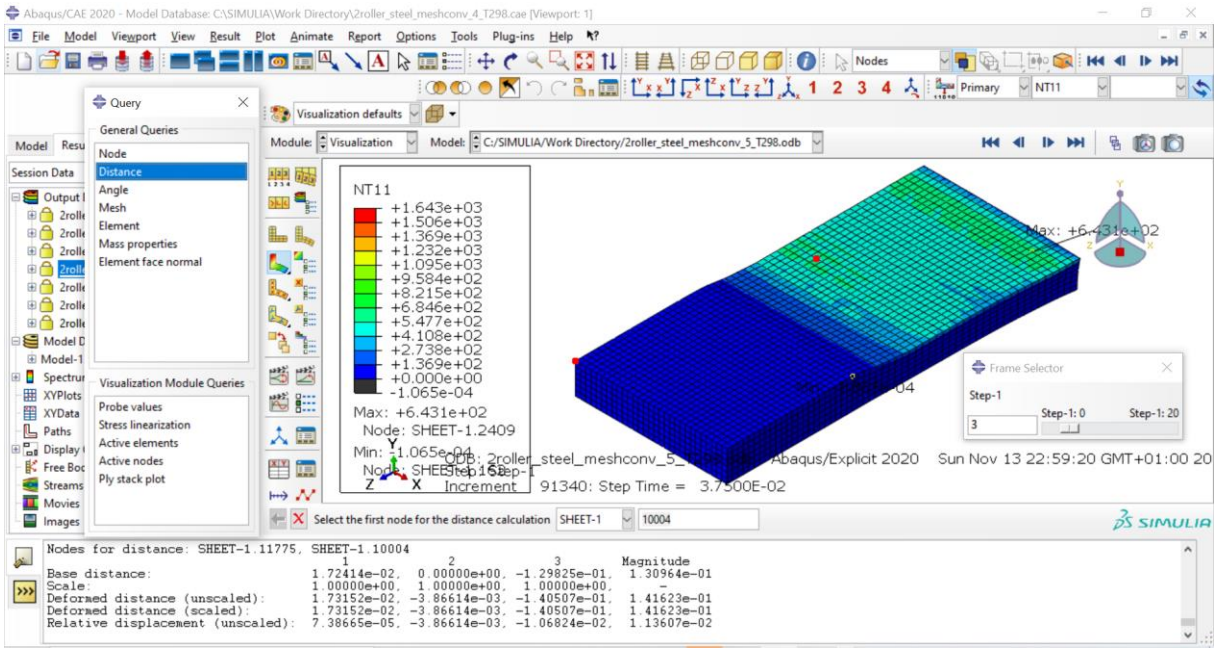

Figure 140. Model 5

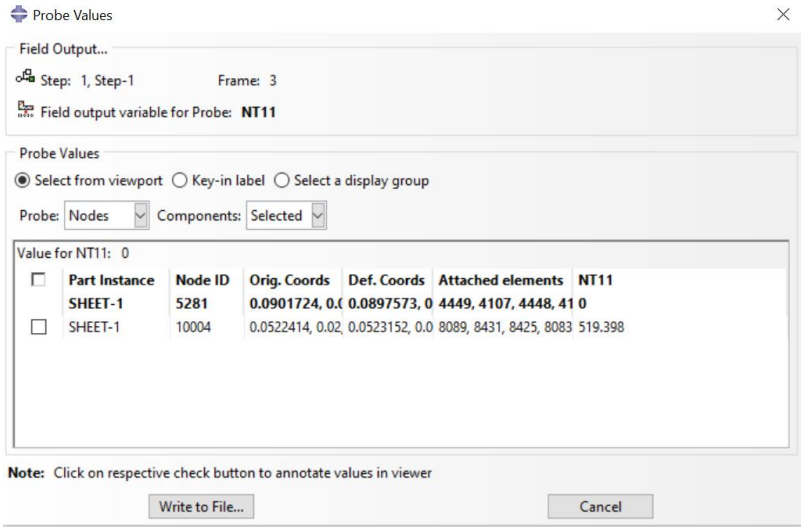

Figure 141. Model 5

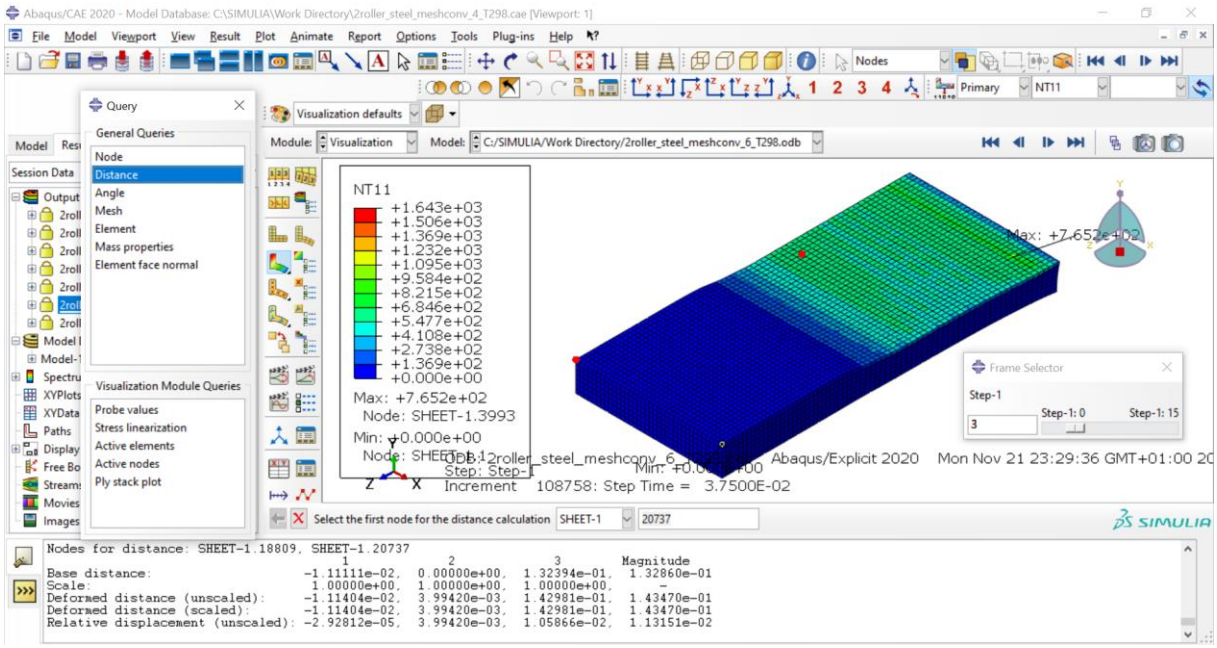

Figure 142. Model 6

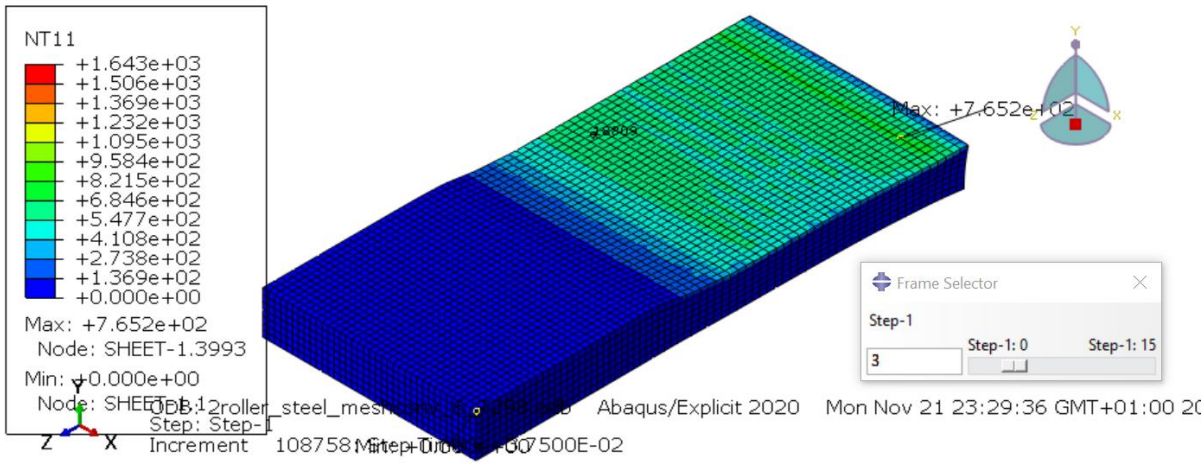

Figure 143. Model 6

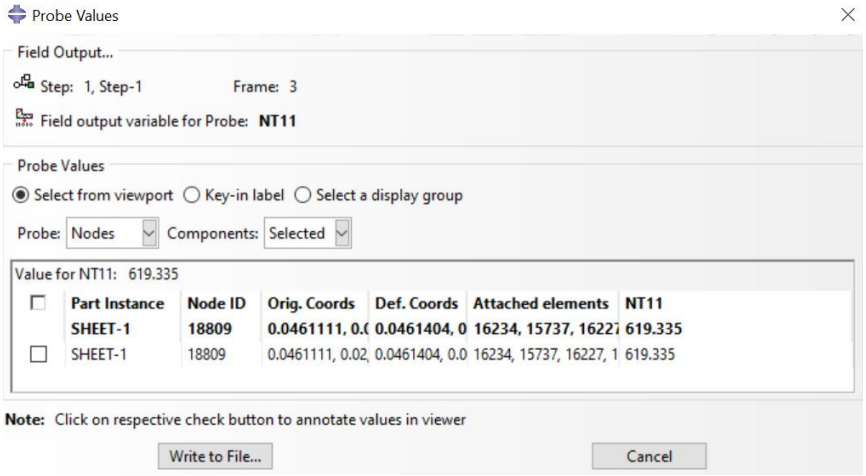

Figure 144. Model 6

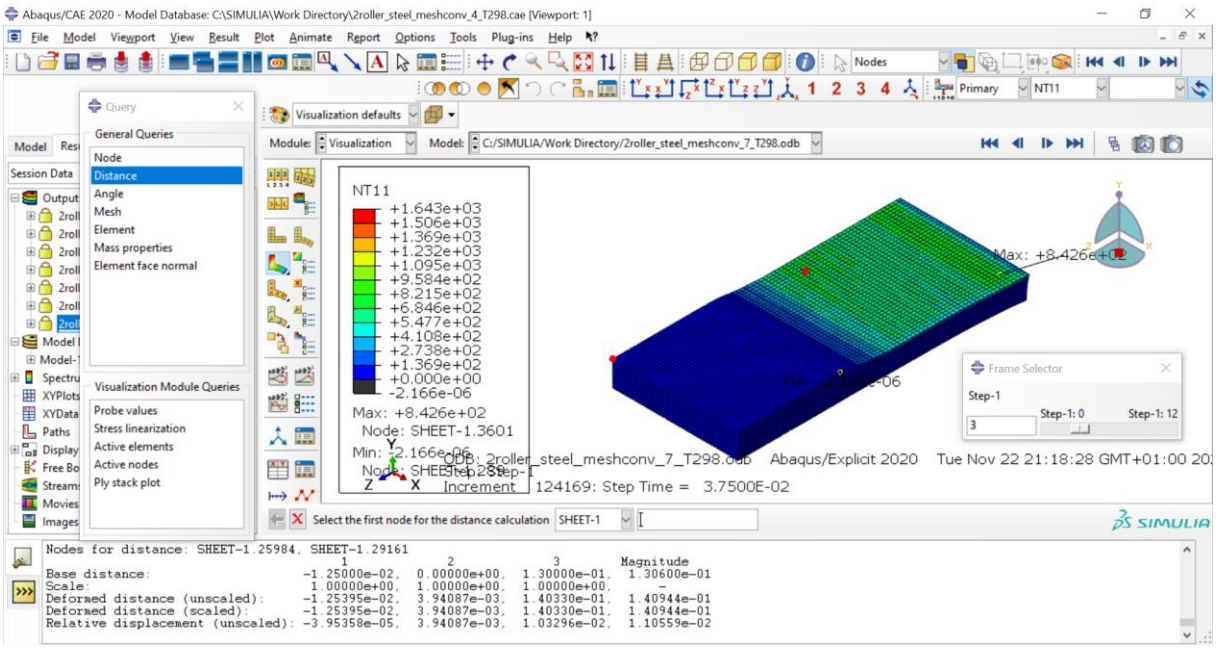

Figure 145. Model 7

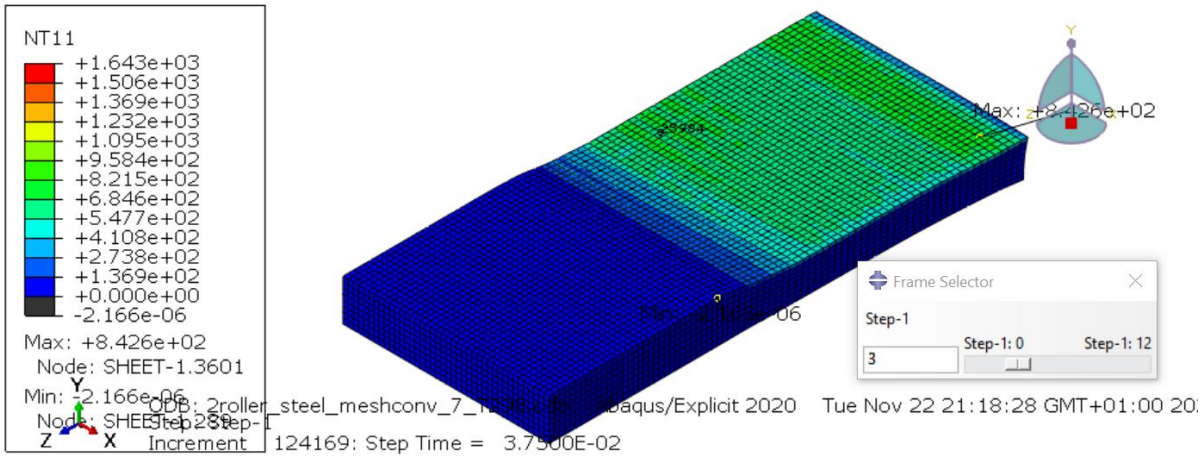

Figure 146. Model 7

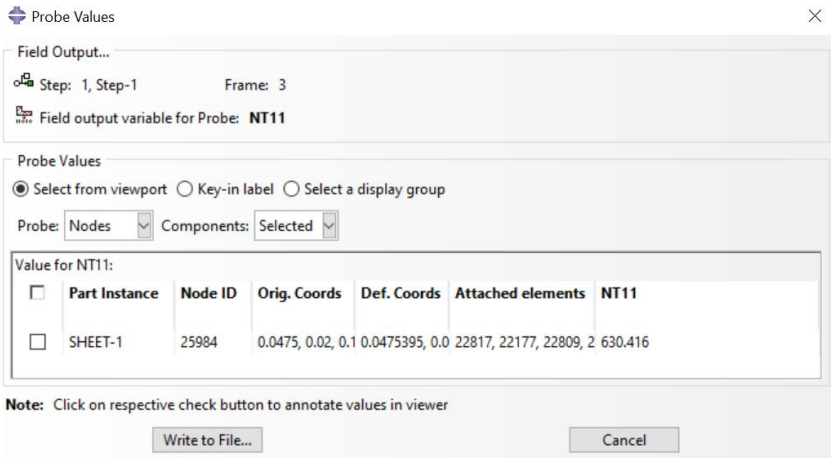

Figure 147. Model 7

Annex 4 Rigid solid roller model creation

Roller part is created as 3D discrete rigid:

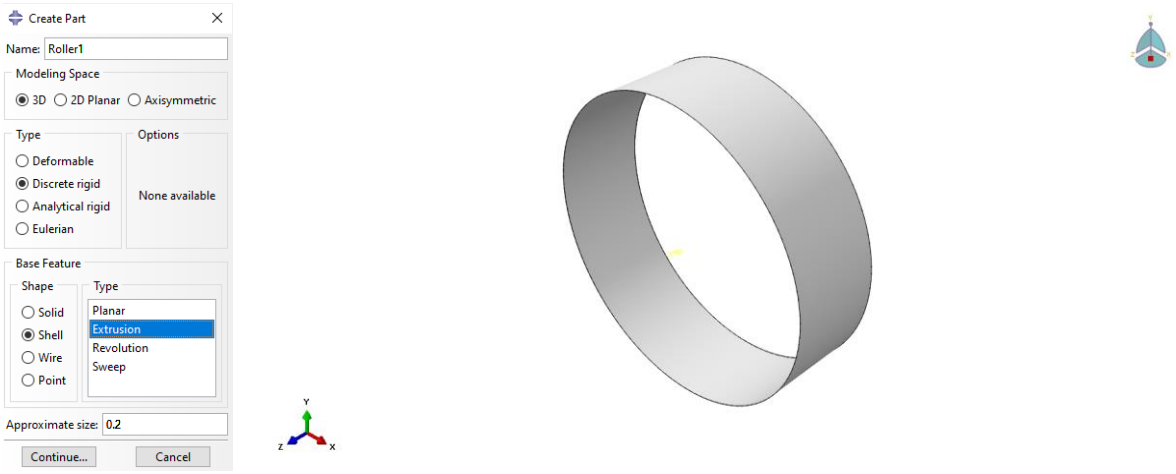

Figure 148. Roller part

Sketch created is a circumference of 0.25 m radious and 0.15 m extrusion to create a roller comparable to the one of the deformable model.

Second roller is created similarly as the first one. Then, parts are translated to obtain the following assembly:

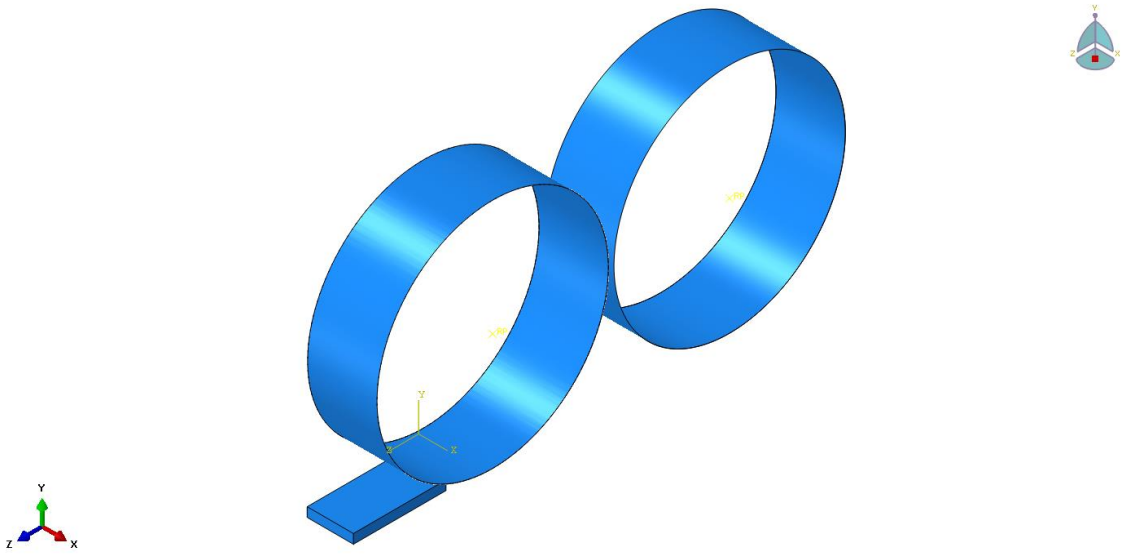

Figure 149. Assembly

Roller is meshed with discrete rigid elements R3D4:

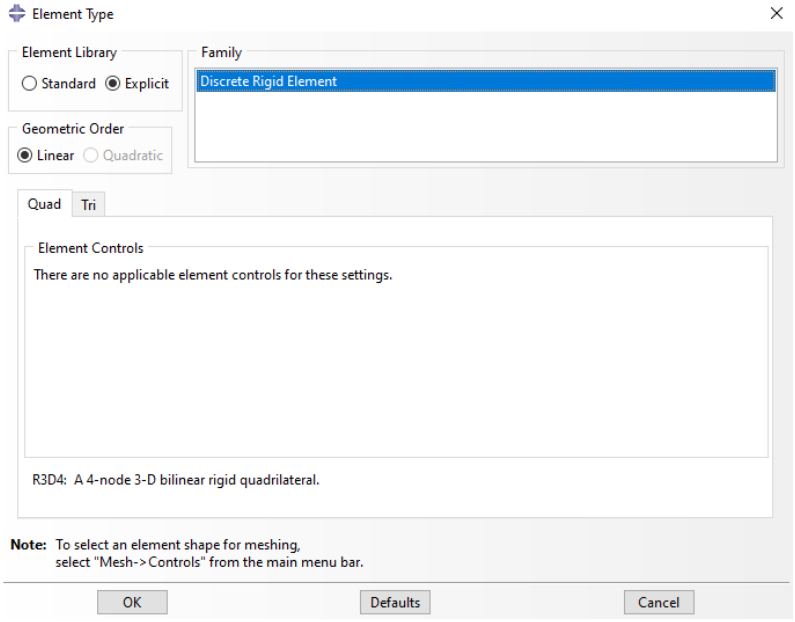

Figure 150. Roller mesh element type

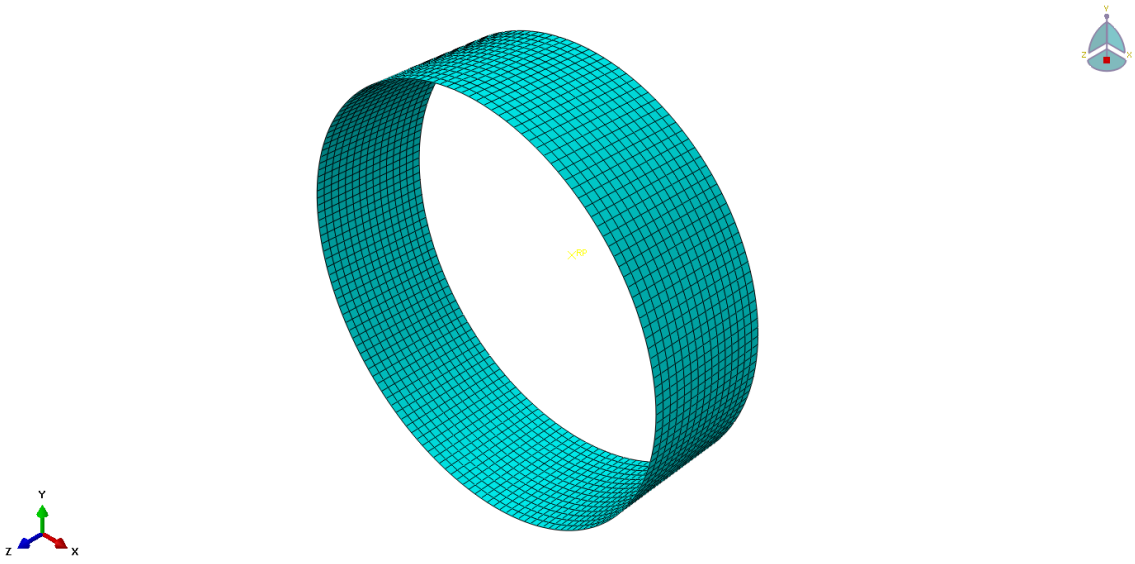

Figure 151. Roller mesh

Plate is meshed with explicit 3D stress deformable elements:

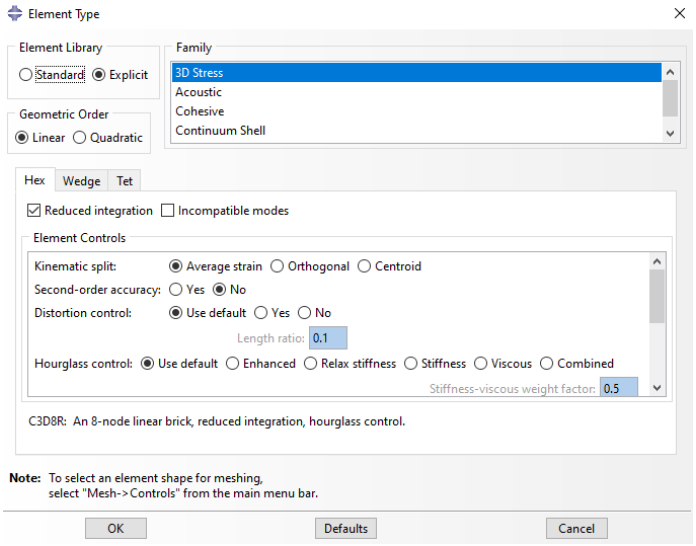

Figure 152. Plate mesh element type

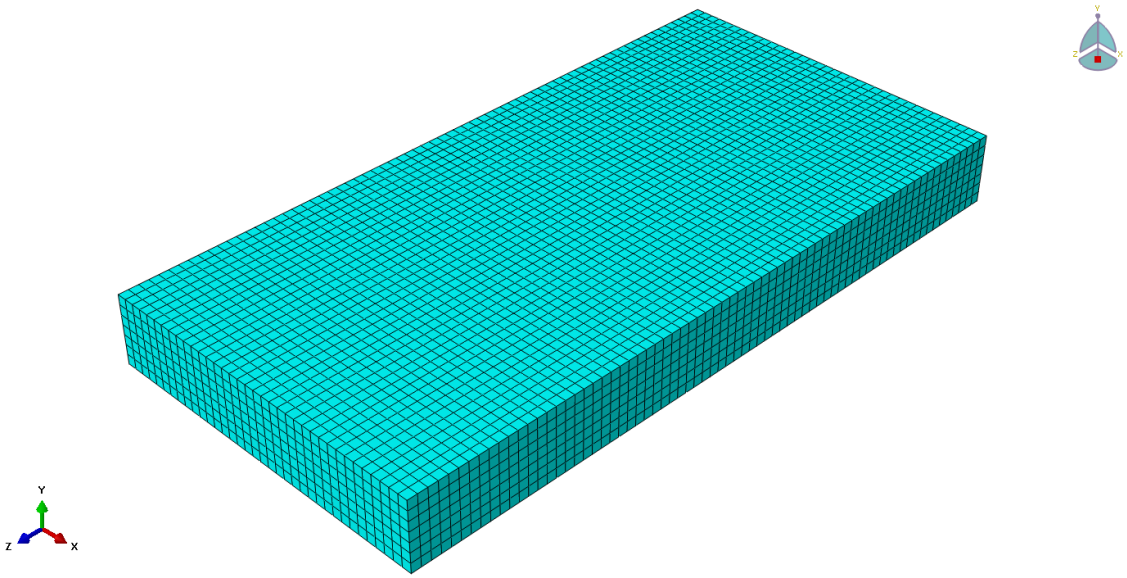

Figure 153. Plate mesh

Annex 5

Measeure of the plate thickness after the first pass.

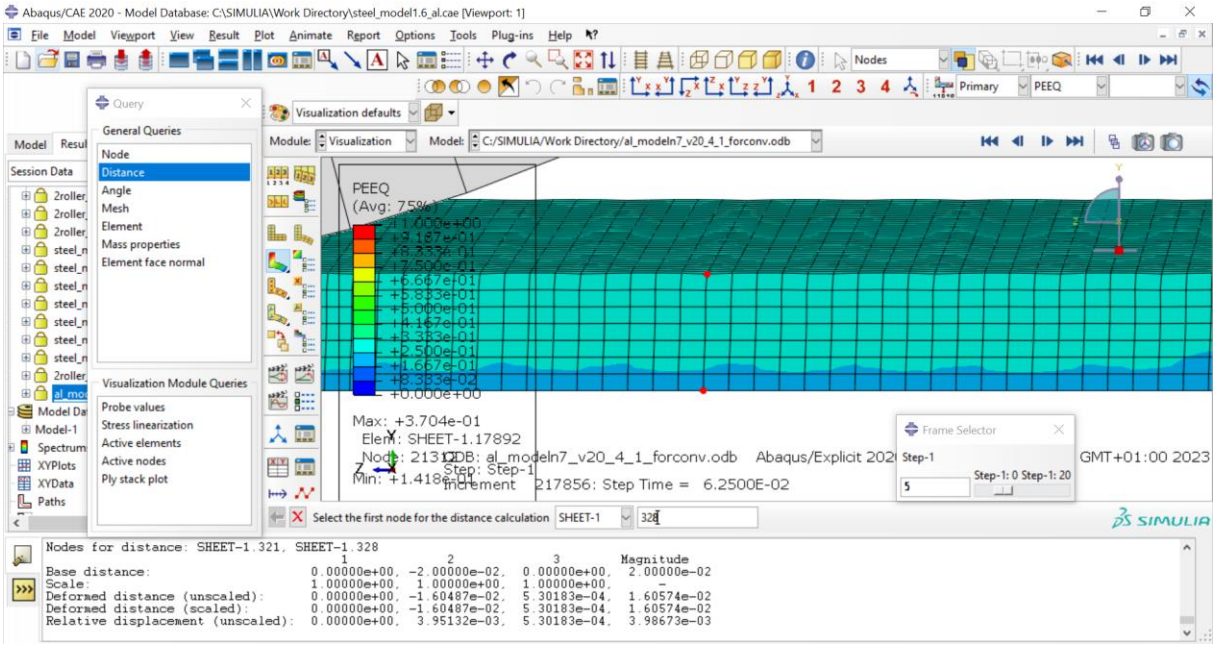

Figure 154. Plate thickness after the first pass

Measeure of the plate thickness after the second pass.

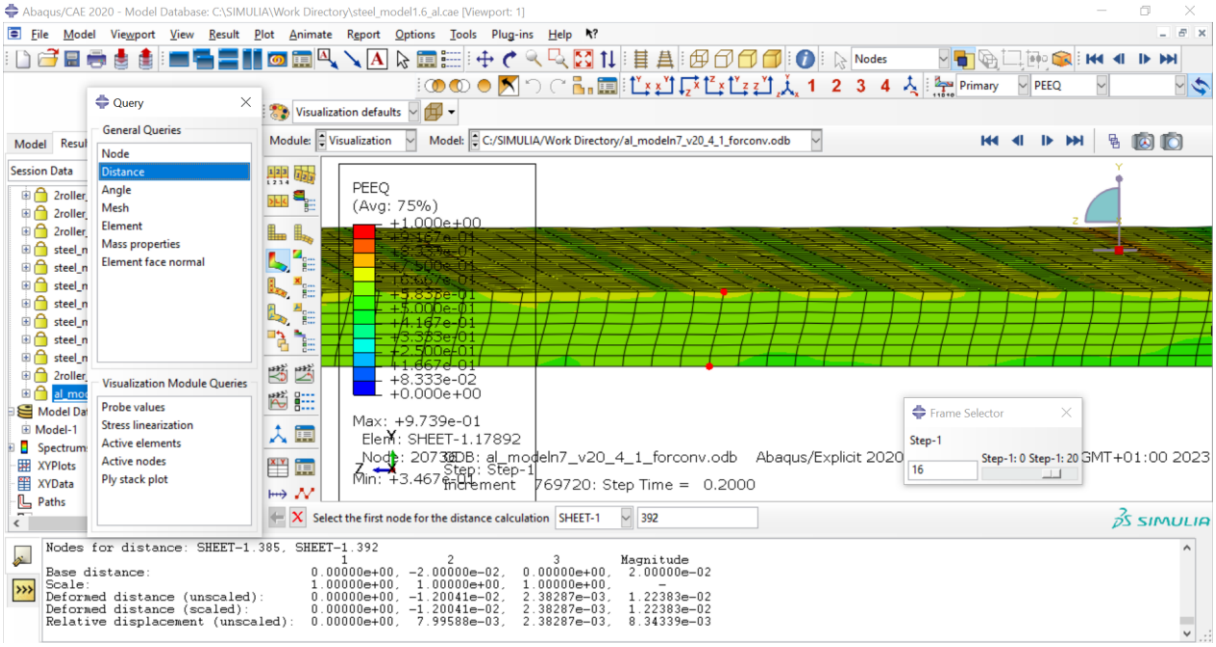

Figure 155. Plate thickness after the second pass

Length measure after the second pass:

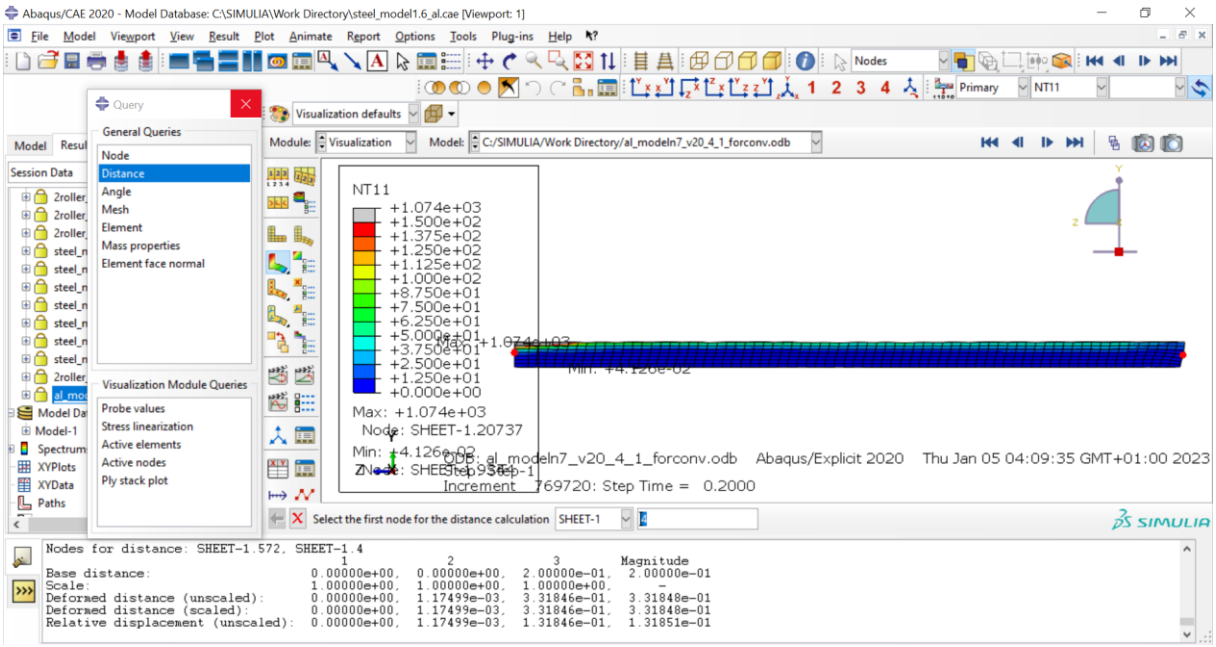

Figure 156. Plate length after the second pass

APPENDIX

R^2 definition

In statistics, the coefficient of determination, called R^2 and pronounced R squared, is a statistical coefficient used in the context of a statistical model whose main purpose is to predict future results or test a hypothesis. The coefficient determines the quality of the model to replicate the results, and the proportion of variation of the results that can be explained by the model. [35]

There are several different definitions for R^2 that are sometimes equivalent. The most common refer to linear regression. In this case, the R^2 is simply the square of the Pearson correlation coefficient. The closer the value of R^2 gets to 1, the better the trend line fit would be.

To calculate the pearson coefficient, the covariance would first have to be obtained. Covariance is a measure of the tendency of two variables to vary together. If we have two series, X and Y, their deviations from the mean are: [36]

$$dx_i = x_i - \mu x$$

$$dy_i = y_i - \mu y$$

Where μX is the mean of X and μY is the mean of Y. If X and Y vary together, their deviations tend to have the same sign. If we multiply them together, the product is positive when the deviations have the same sign and negative when they have the opposite sign. So adding up the products gives a measure of the tendency to vary together. Covariance is the mean of these products:

$$Cov(X,Y) = \frac{1}{n}\sum dx_i dy_i$$

Where n is the length of the two series (they have to be the same length). Covariance is useful in some computations, but it is seldom reported as a summary statistic because it is hard to interpret. Among other problems, its units are the product of the units of X and Y. So the covariance of weight and height might be in units of kilogram-meters, which doesn't mean much.

One solution to this problem is to divide the deviations by σ, which yields normal scores, and compute the product of normal scores:

$$\rho_i = \frac{(x_i - \mu x)}{\sigma_x}\frac{(y_i - \mu y)}{\sigma_y}$$

This value is called Pearson's correlation after Karl Pearson, an influential early statistician. It is easy to compute and easy to interpret. Because normal scores are dimensionless, so is ρ. Also, the result is necessarily between -1 and +1. To see why, we can rewrite ρ by factoring out σX and σY:

$$\rho = \frac{Cov(X,Y)}{\sigma_x \sigma_y}$$

R2 is the square of the Pearson coefficient:

$$R^2 = \frac{Cov^2(X,Y)}{\sigma_x^2 \sigma_y^2}$$

REFERENCES

[1] https://knordslearning.com/manufacturing-process-types/.

[2] J. P. Davim, Finite Element Method in Manufacturing Processes.

[3] «https://www.freepik.com/premium-photo/passenger-aircraft-flying-isolated-white-background_29285273.htm».

[4] https://www.sciencedirect.com/topics/engineering/boeing-787-dreamliner.

[5] Advanced composite materials of the future in aerospace industry.

[6] Y. C. J. H. Xuesong Zhang, «Recent advances in the development of aerospace materials».

[7] F. Campbell, Manufacturing Technology for Aerospace Structural Materials.

[8] J. Cutler, Understanding Aircraft Structures, 1981.

[9] https://www.pngitem.com/middle/TbmxhT_airplane-wing-png-plane-wing-transparent-background-png/.

[10] «https://www.swat-aircraft.com/service/aircraft-structural-repairs/#lg=1&slide=0».

[11] «https://www.outono.net/elentir/2019/10/13/asi-funcionan-las-alas-de-un-airbus-a-320-neo-durante-las-fases-de-aproximacion-y-aterrizaje/».

[12] https://www.godrej.com/p/aerospace-and-defence/Aerospace-Engineering/Sheet-Metal-Brackets.

[13] D. D. I. MECÁNICA, UMSS – Facultad de Ciencias y Tecnología Ing. Mecánica – Tecnología Mecánica II.

[14] https://www.mech4study.com/2017/05/rolling-process-types-working-terminology-application.html.

[15] Universidad del País Vasco – Euskal Herriko Unibertsitatea.

[16] V. L. N. O. V. Mazur, Theory and technology of sheet rolling_ numerical analysis and applications (2019, CRC Press).

[17] G. H. &. H. L. &. J. Z. &. N. K. &. Y. L. &. X. Y. &. Y. X. &. F. Shang3, Prediction and analysis of rolling process temperature field for silicon steel in tandem cold rolling.

[18] Z. B. Peter Kucsera, «Hot Rolling Mill Hydraulic Gap Control (HGC) thickness control improvement».

[19] R. B. Hetnarski, «Encyclopedia of Thermal Stresses,» 2013.

[20] R. J. Boulbes, «Troubleshooting Finite-Element Modeling with Abaqus_ With Application in Structural Engineering Analysis,» 2020.

[21] «https://classes.engineering.wustl.edu/2009/spring/mase5513/abaqus/docs/v6.6/books/usb/default.htm?startat=pt03ch06s03at07.html».

[22] D. Systèmes, «Abaqus Theory Guide,» 2014.

[23] D. I. N. Patrick Doelfs, «Using MSC.Nastran for Explicit FEM Simulations».

[24] T. S. P. D. B. E. Haug, «FEM-Crash, Berechnung eines Fahrzeugfrontalaufpralls,» 1986.

[25] R. L. Eric Mestreau, «Airbag Simulation Using Fluid/Structure Coupling.,» 34th Aerospace Sciences Meeting & Exhibit, Reno, NV, January 15–18, 1996.

[26] D. J. B. D. o. M. &. A. Eng., «The History of LS-DYNA,» LSTC (Livermore Software Technology Corp).

[27] «https://2022.help.altair.com/2022.1/hwsolvers/rad/topics/solvers/rad/ls_dyna_keywords_r.htm».

[28] «https://matmatch.com/es/materials/minfc6403-din-5512-2-grade-st-37-2-g-cold-rolled».

[29] «https://wiam.de/en/».

[30] «https://abaqus-docs.mit.edu/2017/English/SIMACAEGSARefMap/simagsa-c-matdefining.htm#simagsa-c-matdefining__simagsa-c-mat-stress-table».

[31] «https://spanish.globalsources.com/Placa-de/Placas-de-acero-de-carbono-1190885757p.htm».

[32] «https://classes.engineering.wustl.edu/2009/spring/mase5513/abaqus/docs/v6.6/books/usb/default.htm».

[33] «https://aerocommetals.co.uk/featured-inventory/aluminium-alloy-2024/».

[34] «https://asm.matweb.com/search/SpecificMaterial.asp?bassnum=MA2024T3».

[35] R. a. T. J. H. Steel, Principles and Procedures of Statistics with Special Reference to the Biological Sciences.

[36] A. B. Downey, Think Stats - Probablity and Statistics for Programmers-lulu.com, 2011.